# Sulfated Multivalent Polymers for inhibition of L-selectin and LOX-1 Receptors

Dissertation

to obtain the academic degree

Doctor rerum naturalium (Dr. rer. nat.)

submitted by

Shalini Kumari

Department of Biology, Chemistry, Pharmacy
Institute of Chemistry and Biochemistry
Freie Universität Berlin

December 2018

The work presented in this PhD thesis was supervised by Dr. Jens Dernedde and carried out in collaboration with the research group of Prof. Dr. Rainer Haag from September 2014 until December 2018 at the Institute of Chemistry and Biochemistry of the Freie Universität Berlin.

1. Reviewer. Dr. Jens Dernedde, Charité-Universitätsmedizin Berlin
2. Reviewer. Prof. Dr. Rainer Haag, Freie Universität Berlin

Day of Defence: 20.12.2018

Dedicated to my Family

**Acknowledgements**

First of all, I want to express my sincere gratitude to my doctoral supervisor Dr. Jens Dernedde for giving me the opportunity to work in his group and on such interesting projects. I thank him for the academic and scientific support he extended to me during last four years.

Secondly, but by no means less importantly, I would like to thank Prof. Dr. Rainer Haag for allowing me to be a member of his outstanding, international research group and significantly increase my scientific and research skills. His financial and scientific support for my projects as well as his encouragement were very much appreciated.

I would like to thank all the co-operation partners I have been working with during my PhD. I am thankful to Prof. Dr. Bart Jan Ravoo (University of Münster), Prof. Dr. Ir. Luc Brunsveld (Technical University of Eindhoven) for fruitful collaboration and allowing me to work in their labs.

I acknowledge the Marie Curie MULTI-APP ITN scholarship not only for the funding for last three years but also for the opportunity to work with the networking team including outstanding PIs and motivated PhD students. I want to specially thank PhD students from MULTI-APP ITN Wilber, Eva, Maria, Daniele and Peter for their friendship and support.

This interdisciplinary thesis would not be possible without support of all involved PhD students and post docs from Haag and Dernedde group. I would like to thanks all the present and past group members of Haag group for providing me nice working environment. I thank Jutta Hass and Eike Ziegler for taking care of my official documentation. I thank Dr. Wiebke Fischer for helping at various occasion. I thank Katharina Goltsche, Cathleen Schlesener, Anja Stöshel, and Elisa Quaas for taking care of ordering of chemicals, synthesis of glycerol based dendron, GPC measurements and support in bio lab. I thank Daniel Stöbener for MALDI TOF measurements. I thank Christian Kühne for the instrumental instruction to the BIACORE device and detailed discussion over SPR measurements. I would like to acknowledge the research facilities and the analytical department of FU Berlin for support and would like to thank specially to Dr. Andreas Schäfer, Dr. Andreas Springer and their colleagues for NMR and mass measurements.

I thank Dr. Pradip Dey for helping me to start my lab work, valuable suggestions and proof reading of my manuscript and this thesis. I specially thank Dr. Sumati Bhatia for her

constant scientific input, unconditional help and guidance. I thank my office and lab mates Dr. Christoph Schlaich, Mohammad Suman Chowdhury, Abbas Fahani, Dr. Sabine Reimann, Dr. Abhisekh Singh, Dr. Lei-Xiao Yu for friendly environment and discussion over scientific and non-scientific topics.

I specially thank Serena Rossi and Kim Silberreis not only for their warm and friendly behaviour but also for their support and help extended in the bio-lab without that it would not be easy to learn biological experiments.

I acknowledge our multivalency subgroup and would like to thank Dr. Katharina Achazi, Dr. Luis Cuellar Camacho, Dr. Manoj Muthlaya, Dr. Badri Prasad, Dr. Nadine Rades, Dr. Virginia Wycisk, Antara Sharma, for fruitful discussions and friendly behaviour.

I thank the group of friends in Berlin outside university, Sreekant Debnath, Swati Kiran, Abhishek Jha, Sirisha, Dr. Manoj Krishna, Dr. Vineeta, Dr. Vivek for their friendship and help.

I specially thank Pallavi Kiran for being with me in both personal and professional platform like a family member.

I feel lucky to have friends like Vandana, Beena, Alka, Simaranjeet who supported and encouraged me at different stages of my life.

I am grateful to my parents for their affection, blessings and understanding without that it would not be possible to get success in my life. I acknowledge my elder brothers Shantanu, Sambuddha, and Samrendra for their constant support and encouragements. I acknowledge Rikeshwer not only for his love and support but also for his critics on my projects which encouraged me to improve them.

# Table of Contents

# 1 Introduction

In recent years, nanomaterials have received great attention in the areas of diagnostic and therapeutic healthcare.[1, 2] Nanomaterials are defined as materials with a dimension in the range of 1-100 nanometers.[3] These materials have been widely investigated for medical applications including diagnostic, drug delivery and tissue engineering.[1, 4] In the last decades diverse nanostructured materials have been vastly explored including quantum dots, superparamagnetic nanoparticles, liposomes, polymer based fibers and others.[5] These nanomaterials have not only been applied for the development of new diagnostic tools such as nanobiosensors, but also for therapeutic applications.[6], [7] Some of the materials have been discovered for various application at different time point (**Figure 1**) and many of them approved by the FDA such as Copaxone® (glatiramer acetate) used as an immunomodulator for the treatment of multiple sclerosis and Neulasta® a PEGylated granulocyte colony stimulating factor approved for chemotherapy induced neutropenia, but more are emerging in the clinical trials, such as CYT-6091 (PEGylated rh tumor necrosis factor (TNF) bound to colloidal gold) for solid tumor treatment.[1, 8, 9]

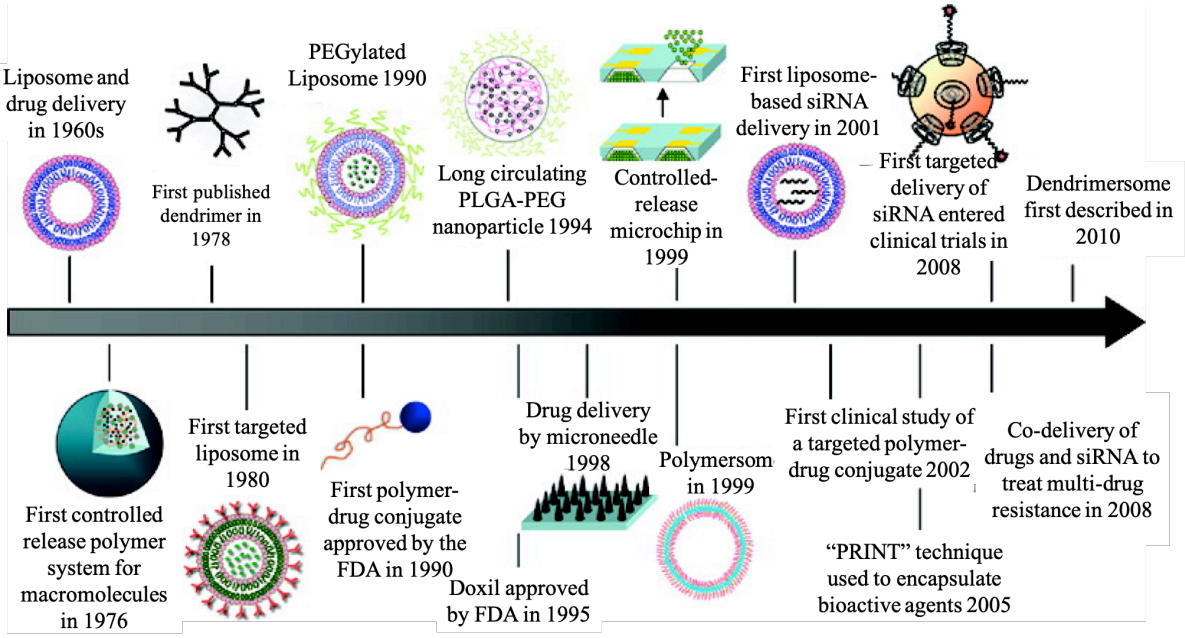


**Figure 1.** Timeline for the discovery of the nanotechnology-based drug delivery. Reprinted with permission from Shi et al., *Nano lett.* **2010**, *10*, 3223-3230.[9] Copyright (2010) American Chemical Society.

Currently, there is a rise in concern for its safety and biocompatibility that has to be addressed. From the material science point of view therapeutic efficacy, pharmacokinetics can be tuned by controlling several factors such as size, surface area, functional group composition and concentration.[10, 11] Biocompatibility of individual materials is dependent on the complex interaction with the extrinsic biological environment.[12] Size and nature of the materials determine the specificity of the interaction with plasma protein and play an important role for targeting and their clearance.[13, 14]

It is obvious that the intrinsic properties of a target structure always determine the design of a synthetic ligand. The choice of an appropriate scaffold e.g. flexible vs. rigid architecture, branched vs. linear shape have to be considered. Apart from the scaffold architecture the number and type of functional groups of a nanomaterial have an impact on targeting and with respect to cytotoxicity and cellular uptake.[11, 15]

In this context multivalency plays a critical role for the interaction of nanomaterials and biological surfaces.

## 1.1 Multivalency

Multivalency is a design principle that is often used by nature to achieve strong binding using weak univalent receptor – ligand interactions. It provides a strategy to convert a system having multiple, identical binding site into well-defined oligovalent species.[16-18] The prospect of multivalent interaction can be used to understand the evolutionary benefit of combining multiple existing interactions to increase the final affinities. A de novo redesign instead of stronger interacting molecules is not necessary.[17, 19, 20] The multivalency concept plays also a significant role in the development of new architectures in the areas of supramolecular, medical and material chemistry.[18, 21, 22] In case of perfect fit of ligand and receptor the degree of multivalency can potentiate the binding affinity.[17]

A monovalent interaction affinity is calculated on basis of an association and dissociation constant. Multivalent interactions are often difficult to describe and therefore often mentioned as apparent affinities. Multivalency can be classified into bivalent (two binding partners), oligovalent (≤ 10) or polyvalent (> 10) interactions.[18]
Whiteside *et al.* defined the enhancement factor as a ratio of $K_d$ avidity and $K_d$ affinity.[18] The enhancement factor can be explained by the thermodynamics of multivalent systems and a monovalent interaction. Thermodynamics tells us that an ideal equilibrium system exist as a result of minimizing free energy that could be achieved by low enthalpy and high entropy.[19, 23] According to the thermodynamic principle of multivalency, enthalpy of binding is additive while the translational and rotational entropy of interaction is unfavorable of binding.[18, 24] In the case of a multivalent nanomaterial the local concentration of the ligands is increased after first ligand-receptor interaction as the ligands are interconnected, which leads to a reduction of unfavorable entropic penalty.[17, 18] An interaction that causes enhanced binding enthalpy for the next ligand to receptor interaction, this type of enhancement is known as enthalpically enhanced binding.[16] One example from nature showing this type of binding is the interaction of the pentavalent cholera toxin towards five ganglioside ($GM_1$) ligands displayed on a cell surface.[25] In other scenario the binding of one ligand to an oligovalent receptor might cause steric hindrance for the next interaction. In this case, the binding is known as enthalpically diminished. This type of binding is common when the binding entities are conformationally rigid but not synchronized.

### 1.1.1 Multivalency in biological system

Multivalency is strikingly common and a highly important factor seen in nature for achieving strong yet reversible interactions.[17] In many cases proteins arrayed on cells, bacteria, or viruses can bind strongly in a superselective fashion to their counterpart cell surface receptors.[16] As a consequence, these interactions trigger specific biological processes. To unravel the communication between biological systems is one of the miracles in molecular biochemistry and the principle of multivalency has been studied only for few decades.[16] Some of the examples of polyvalency, which are significant for human biology are – the adhesion of influenza virus to the cell surface via the interaction between multiple trimers of hemagglutinin and densely packed sialic acid on cell surfaces;[26, 27] the adhesion of *E. coli* pili proteins to host cell surface glycans (i.e. mannosylated structures);[28] and the adhesion of neutrophils to endothelial cells *via* interactions of multiple glycoproteins displaying the carbohydrate sialyl Lewis$^X$ and the lectins E-, L- and P-selectin.[29] Biological systems instruct polyvalent interactions in many different situations because of some functional advantages such as clearance of pathogens, mediated by attachment of multiple antibodies to macrophages; interaction involving different ligand - receptor pairs causing enhancement in strength and specificity of interactions; polyvalent interactions on a large cell surface promote intimate conformal contact leading to efficient cell-cell communication.[16] In principle, polyvalent inhibitors can be designed to suppress undesired biological processes and in the best case to promote desired ones. Among the multivalent approaches some examples are inhibiting the attachment of influenza virus to host cell using polymers by entropically enhanced binding or steric inhibition;[27, 30] polyvalent interactions inducing induction of signal causing promotion of desired interaction;[31] to facilitate the targeted imaging of tumor by utilizing the physiochemical parameters of the synthetic polymers.[14]

### 1.1.2 Different ways to achieve polyvalency

In order to harness the benefit of multivalency to rationally design new polyvalent ligands not only the intrinsic affinity of each ligand, but also their spatial orientation have to be considered. A common approach to achieve multivalent ligands is the choice of scaffolds, which could be flexible or rigid. A flexible scaffold provides wide conformational space to the system but thermodynamically speaking flexibility cause a huge loss in conformational

entropy during multivalent binding events.[16, 17, 32] Flexible backbones can be considered as a great choice to anchor ligand for multivalent binding. In the last few decades, linear or coiled structure having a certain degree of flexibility have been explored to attain the desired multivalent interaction.[17] Some of the examples of such scaffolds for polyvalent architectures and their uses are: polyacrylamides functionalized with sialic acid to inhibit the viral adhesion to the target cells by strong interaction and steric shielding of the virus,[27] ROMP (Ring Opening Metathesis Polymerisation) based linear polymers for signal transduction,[33] linear polyglycerols functionalized with sialic acid for inhibition of virus-cell interactions,[34] and semisynthetic polysaccharides consisting of α-1,6 linked D-glucose.[35] Another scaffold choice is the rigid one where the possibility for loss of entropy is reduced, but the ligands need to be precisely oriented to avoid loss of enthalpy of binding. Depending upon the rigidity of the backbone entropy gain and loss can happen during ligand-receptor interaction. By perfect fitting and rigid arrangement an enhancement in affinity can be expected (**Figure 2**).

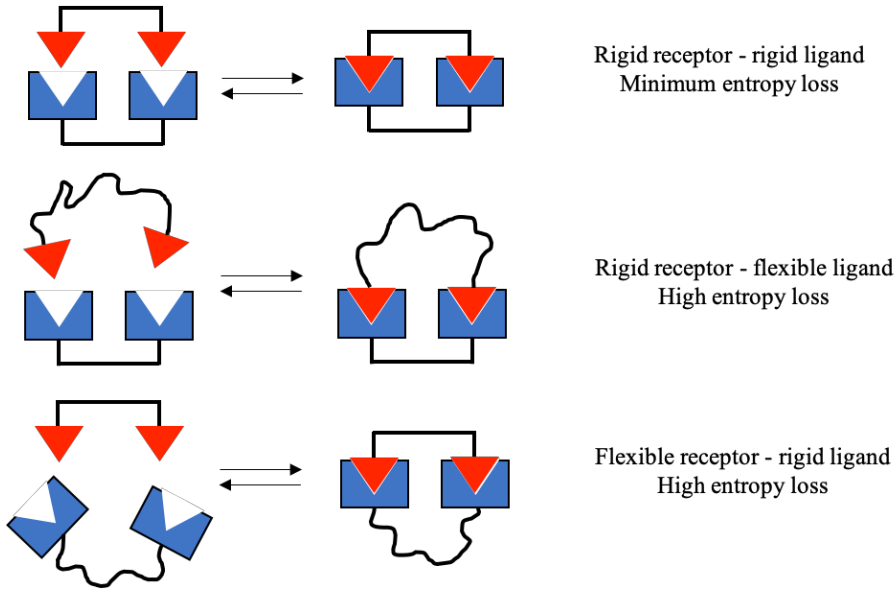


**Figure 2.** Entropy loss in ligand-receptor interaction due to rigidity of backbone. Modified with permission from Koschek et al.[36]

Limited flexibility in the backbone is achieved by radial arrangement of ligands e.g. dendrimers having almost defined architecture which could be functionalized on surface. Different chemical structure can be used to achieve dendritic architecture i.e. polyamidoamine dendrimers or hyperbranched polyglycerols. Some of the scaffolds used to design of polyvalent architectures are shown in **Figure 3**. In dendritic scaffolds to achieve

optimum special orientation, the ligands are attached to the periphery through a spacer of optimal length. The choice of a linker is crucial for design of inhibitors in terms of length and other physiochemical characteristics.

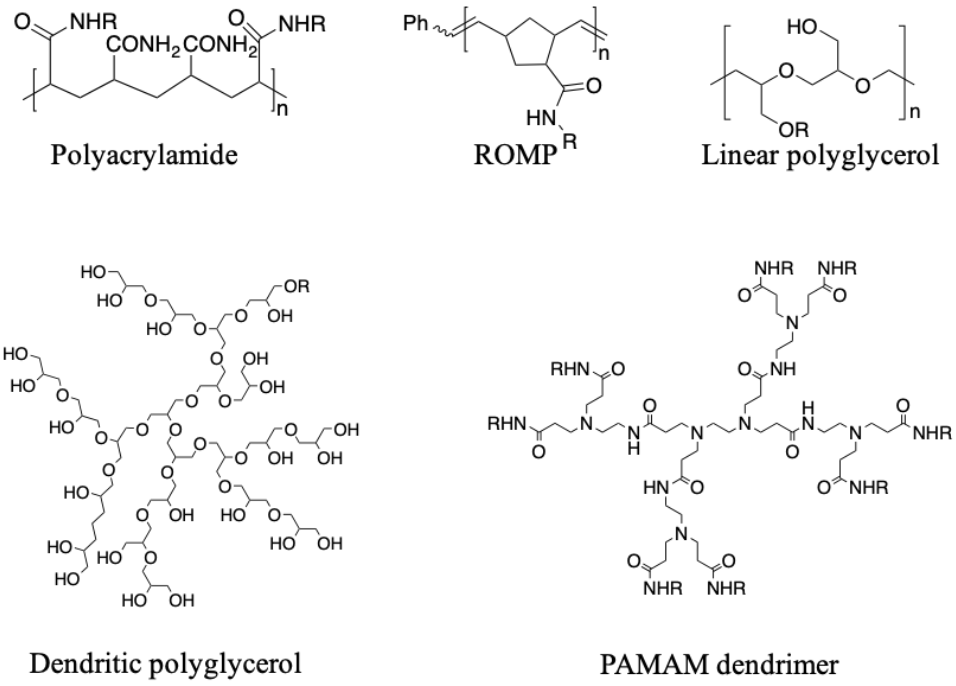


**Figure 3.** Examples of rigid and flexible scaffolds for polyvalent ligands: polyacrylamide ROMP, linear polyglycerol (lPG), dendritic polyglycerol (dPG), PAMAM dendrimer.

A wide range of linkers were summarized by Whitesides et al. (**Figure 4**). In some cases flexible spacers such as (polyethylene glycol) are of great importance to achieve high binding affinity,[17, 37] but in some cases well designed conformationally nonflexible spacers can also help to achieve high affinity.[21] To design a perfect fit spacer or scaffold the distance between the binding sites of the receptors can be measured by spatial screening using DNA rulers.[38] Apart from designing multivalent binders, polymers are also involved to improve the bioavailability of available drugs by enhancing the circulation time (attachment of PEG to therapeutic agent) or by reducing the systemic toxicity of the drug (polymer as a delivery system). Apart from covalent systems a number of interesting scaffold made up of a discrete number of assembled subunits, known as supramolecular assemblies have been developed. The spatial organization of supramolecular architectures are supported mostly by noncovalent interactions like hydrogen bonding, van der Waals forces, π–π interaction, hydrophobic/hydrophilic attraction and electrostatic interactions.[39]

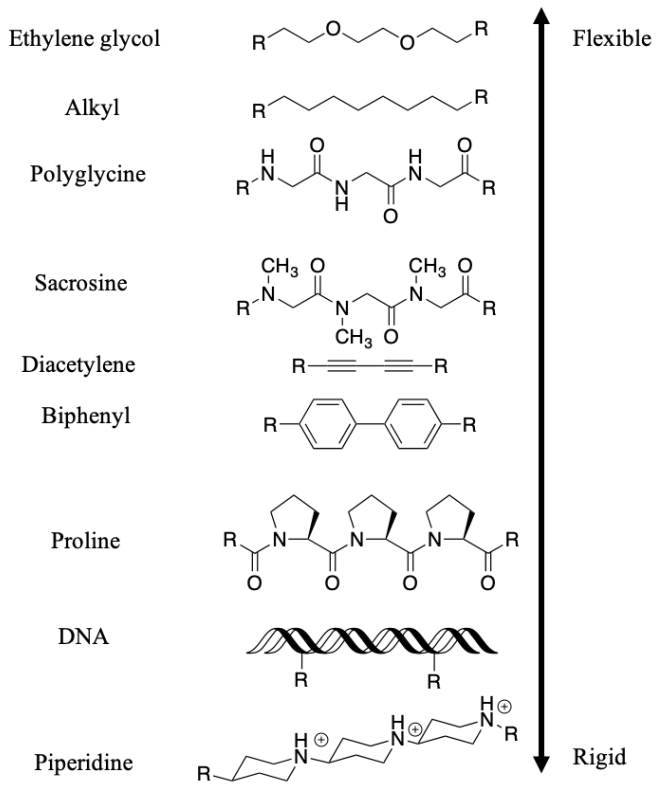


**Figure 4.** Examples of flexible and rigid linkers used in bivalent ligands: ethylene glycol,[40] alkyl,[41] polyglycine,[42] sacrosine,[43] diacetylene,[44] biphenyl,[45] proline,[46] DNA,[47] piperidine.[48]

Among various interactions in supramolecular chemistry, host-guest interaction is an important phenomenon giving rise to models integrated in a facile and reversible manner.[49] Molecules like amphiphilic cyclodextrins (CDs) yielding unilamellar bilayer vesicles in aqueous solution, calixarenes, pillarenes, and cucurbiturils, possessing cavities can be explored as hosts for host-guest interaction (**Figure 5**).[50] Considering all the above factors we can say that a multivalent system is of great significance to render customized interactions in biological systems.

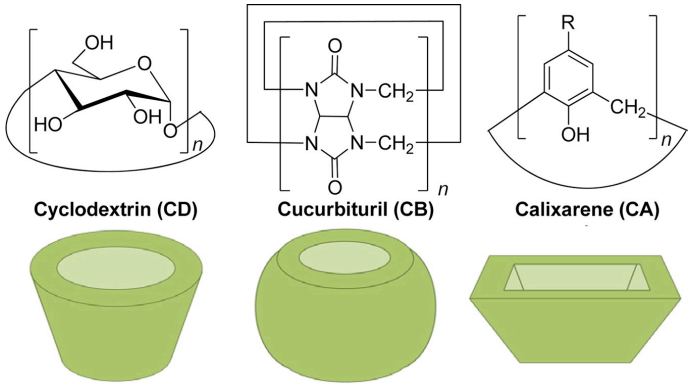


**Figure 5.** Chemical structure of cyclodextrin, cucurbituril, and calixarene and their schematic representation as host for supramolecular interactions. Reprinted with permission from Ma et al.[49] Copyright (2015) American Chemical Society.

## 1.2 Polyelectrolyte

Polyelectrolytes are polymers containing ionizable groups that dissociate in aqueous solution. The free or substituted ionizable groups behave as partial or full salts and could be acidic (containing carboxylate, sulfonate, sulfate, or phosphate groups) or basic (amine groups).[51] Examples of charged biological macromolecules are DNA, RNA, polypeptides and polysachharides (e. g. heparin), whereas the synthetic electrolytes include polystyrene sulfonate and polyacrylic acid.[52] Self-assembled artificial polyionic complexes can be employed in biomedical applications due to their properties to form various structure i. e. micelles, layer-by-layer membranes, capsules.[53] Low toxicity is an additional benefit for polyelectrolytes as the complex is stablized by electrostatic forces and there is no need to involve many cross-linkers. Polyelectrolytes play a vital role in biological systems for interaction causing gene expression, cell-cell communications and ligand-receptor binding.[54, 55] Due to carrying both positive and negative charges, proteins can interact with the oppositely charged polyelectrolytes leading to precipitation or phase separation. In the formation of polyion complexes the entropy is a driving force as a large number of counterions are released, but these mechanisms are also affected by the various physiochemical properties of these polyelectrolyte. The thermodynamic information of the protein – polyelectrolyte interaction is well understood by isothermal calorimetry.[56] Interaction of proteins with various polyelectrolyte is well studied and reviewed, both theoretically and experimentaly by Ballauf et al. and the release of counterions was found to be the major driving force for protein interaction including linear and dendritic polyelectrolytes.[57] They proved the similar fact that binding is dominated by counterion release in a detailed study on binding of highly charged sulfated dendritic polyglycerol with human serum albumin.[58] There are many other challenges for biological electrolytes e. g. hydration mediated interaction at a very low distance from the electrolyte is not well understood, different couterions can cause different behavior of polyelectrolytes even if the charges are similar.[52, 55]

### 1.2.1 Application of polyelectrolytes

Polyelectrolytes can be broadly classified as positively and negatively charged macromolecules. Synthetic positively charged electrolytes are employed in gene delivery system, cationic lipid or polymers can form complexes with DNA (polyplex) and enter the

cell after interaction with the negatively charged plasma membrane of the target cells.[55] Further, the polyplex loaded endosome/lysosome mediates buffering of $H^+$ and cause accumulation of chloride in lysosome leading to osmotic swelling and endosome lysis.[15] Via this route the content is delivered to the cytosol, compounds that needs to target the nucleus, must be further transported. Negatively charged polyelectrolyte are anionic macromolecules. One of the well-explored examples is sulfated dendritic polyglycerol used as an anti-inflammatory agent and other examples from natural origin are hyaluronic acid, heparin (highly sulfated glycosaminoglycan) and polysaccharides.[59, 60]

### 1.2.2 Role of polysulfates in protein interaction

Common anionic groups of charged polyelectrolyte are phosphate, carboxylate, sulfonate, and sulfate. Among these charged moieties, sulfates are widely explored for their function in biological systems. Sulfate can be defined as an oxidized form of sulfur and can be a source of sulfur containing metabolites.[61] The degree of sulfation and the linkage of sulfate to specific sugar residues of glucosaminoglycans (GAGs) defines their function. Sulfated GAGs of physiological significance are dermatan sulfate, chondroitin sulfate, heparin, heparan sulfate, and keratan sulfate. The only GAG, which is not sulfated, is hyaluronan. Chondroitin sulfates are glycosaminoglycans with a wide range of structure and show potential therapeutic properties.[62] Heparin is a polymer composed of highly sulfated polysaccharide. The molecular weight of unfractionated heparin ranges from 3 to 30 kDa.[63, 64] It is widely used as an anticoagulant by binding to serine protease inhibitor (antithrombin III), preventing the formation of clots.[65] Limitations for the use of heparin include – a short half-life, which causes frequent administration of heparin to achieve the desired effect,[65, 66] lack of adsorption in the gut so it needs to be administered intravenously or subcutaneously,[64] and common side effect like uncontrolled bleeding, pain, low platelet count.[64] Many unwanted side effects occur due to large number of heparin binding interactions. To solve this issue fractionation of low molecular weight heparin species has been developed by chemical or enzymatically controlled reactions.[67] Further, the synthetic analogue fondaparinux has been FDA approved.[68] Heparan sulfate structurally similar to heparin belongs to a family of linear sulfated, heterogenous polysaccharide.[69] Linked to protein, heparan sulfate proteoglycans play critical roles in various biological events due to their high degree of structural complexity. Heparan sulfate is located on the plasma membrane and is a part of the extracellular matrix and interacts

with a large number of different human proteins influencing the extracellular proteome and ultimately the cell function.[70] Heparin/heparan sulfate interacts with protein mostly via binding of negatively charge arising from carboxylate groups, O- and N- sulfates to positively charged amino acid e.g. lysine, arginine or protonated histidine.[71] Heparin and heparan sulfate are involved in binding and regulation of the activity of different proteins including enzyme, growth factors, and the cell surface proteins.[72] Heparin has also anti-inflammatory activity by regulating the inflammatory response or modulating the complement activity. The ability of heparin/heparan sulfate and chondroitin sulfate to bind many chemokines and cytokines in the extracellular matrix (ECM) regulates their bioavailability.

## 1.3 Inflammation

Inflammation is an early defense mechanism in response to microbial infection, disease and tissue damage that enables the removal of harmful stimuli.[73, 74] It is the body's vital part of the innate immune system to fight against injury and infection in order to finally heal damaged tissue. Acute inflammation shows the classical known symptoms including redness due to hyperthermia swelling due to enhanced permeability of microvasculature, followed by leakage of protein into interstitial space, pain because of changes in perivasculature, and heat associated with increased blood flow and metabolic activity.[73, 75] Regardless of the reason, inflammation is always involved as an adaptive response to restore health. Generally, a controlled inflammatory response is beneficial by providing defensive action against external injury or foreign invaders, but it can be adverse if not regulated properly.[74] The entire reaction is subdivided into different processes including initiation, regulation and resolution of the inflammatory response. An acute setting involves migration of leukocytes to the site of injury.[74] In case of microbial infections the immune response is activated by a set of pattern recognition receptors including Toll-like receptors and various scavenger receptors expressed on macrophages.[76] The major ligands to these receptors include lipopolysaccharides, surface phosphatidylserine or modified low-density lipoproteins. Ligation of particles presenting these ligands leads to endocytosis and lysosomal degradation via scavenger receptors. Recognition via Toll-like receptors leads to intracellular signaling and results in enhancement of phagocytosis, release of cytokines, autacoids, lipid mediators or reactive oxygen species production that ultimately cause the amplification of a local inflammatory response.[77] In order to understand the complex network of inflammatory response, these signals are distinguished as inducer and mediator. The signals that can initiate the inflammatory response are defined as inducers while the signals that can alter the functionality of tissue and organ are known as mediators. Inducers could be exogenous or endogenous.[74] Exogenous inducer could be certain conserved molecular pattern carried by microorganism or virulence factor also known as microbial inducer and allergens, irritants, foreign agents included in the sub-category of non-microbial inducers.[78] Endogenous inducer consists of signals due to stress and malfunction of tissues. These inducers trigger the production of inflammatory mediators, which can be further classified into seven categories including i) vasoactive amines (e.g. histamine), ii) vasoactive peptides (e.g. bradykinin), iii) complement fragments (e.g. anaphylatoxins: C3a, C4a, C5a), iv) lipid mediator (e.g. eicosanoids), v) pro-inflammatory cytokines (TNF-α, IL-

1, IL-6) vi) chemokines that control the leukocyte extravasation, vii) proteolytic enzymes (elastin, cathepsin).[74]

Acute inflammation results in the removal of infectious agents followed by a repair phase mediated by tissue residents and macrophages.[79] In case the trigger stimulus is not eliminated, the inflammation persists leading to a change in composition of infiltrating leukocytes from neutrophils to mononuclear phagocytes and T cells.[77]

In a chronic inflammation the signals orchestrate a repertoire of responses such as recruitment of leukocytes (will be discussed in the next section), extracellular matrix remodeling, cellular proliferation, and angiogenesis giving rise to various diseases like atherosclerosis, obesity, asthma, neurodegenerative disease, and cancer. [80]

### 1.3.1 Targeting inflammation via selectin

Early adhesion of white blood cells through cell-surface glycoprotein interaction is one of the critical events for the recruitment of leukocytes into sites of inflammation. Extravasation of leukocytes is a multistep process initiated by the attachment and rolling of leukocytes over vessel walls mediated by various signaling and adhesion molecules like selectins (**Figure 6**), Ig-CAMs, integrins and chemokines.[81] The selectin family consists of three members: E-, P-, and L- selectin, which initiate and sustain the rolling of leukocyte on the endothelial cells. Selectins are the C-type lectins and are named according to their appearance. All three selectins are type-1 transmembrane glycoproteins consisting of a N-terminal, calcium-dependent lectin domain, an epidermal growth factor domain, a variable number of complement regulatory units, a transmembrane domain, and a C-terminal intracellular domain.[82, 83] P-selectin and E-selectin are expressed on the vascular endothelial surface due to inflammatory stimuli with different expression kinetics.[83] E-selectin expression is transcriptionally regulated. P-selectin is in addition also expressed on activated platelets and stored in intracellular vesicles.[83] L-selectin is constitutively expressed on leukocytes. All selectins promote the inflammation process by mediating leukocyte-endothelial interactions. Selectins show relatively weak, calcium dependent binding of the lectin domain to the tetrasaccharide sialyl Lewis x ($SiaLe^x$) and sialyl Lewis a ($SiaLe^a$). P-selectin glycoprotein ligand-1 (PSGL-1), which is a mucin like glycoprotein is expressed on leukocytes.[84] PSGL-1 is a well characterized ligand of all selectins and has a bi-ligand architecture. In addition to the $SiaLe^x$ carbohydrate epitope presented on an O-glycan three sulfated tyrosine residues at the N-terminus of PSGL-1 are required for high

affinity binding to L- and P-selectin.[85] In contrast, E-selectin mediates PSGL-1 binding in a tyrosine sulfate-independent manner. The difference in binding affinities of E- vs. L- and P- selectin to PSGL-1 can be explained with the composition of the binding interface. In all selectins the carbohydrate binding area looks similar. Basic residues adjacent to the carbohydrate binding interface are solely present in L- and P-selectin and contribute to high affinity recognition of tyrosine sulfates of PSGL-1.[86] Moreover, binding avidity of selectins can be enhanced by clustered arrangement of the receptors.[87]

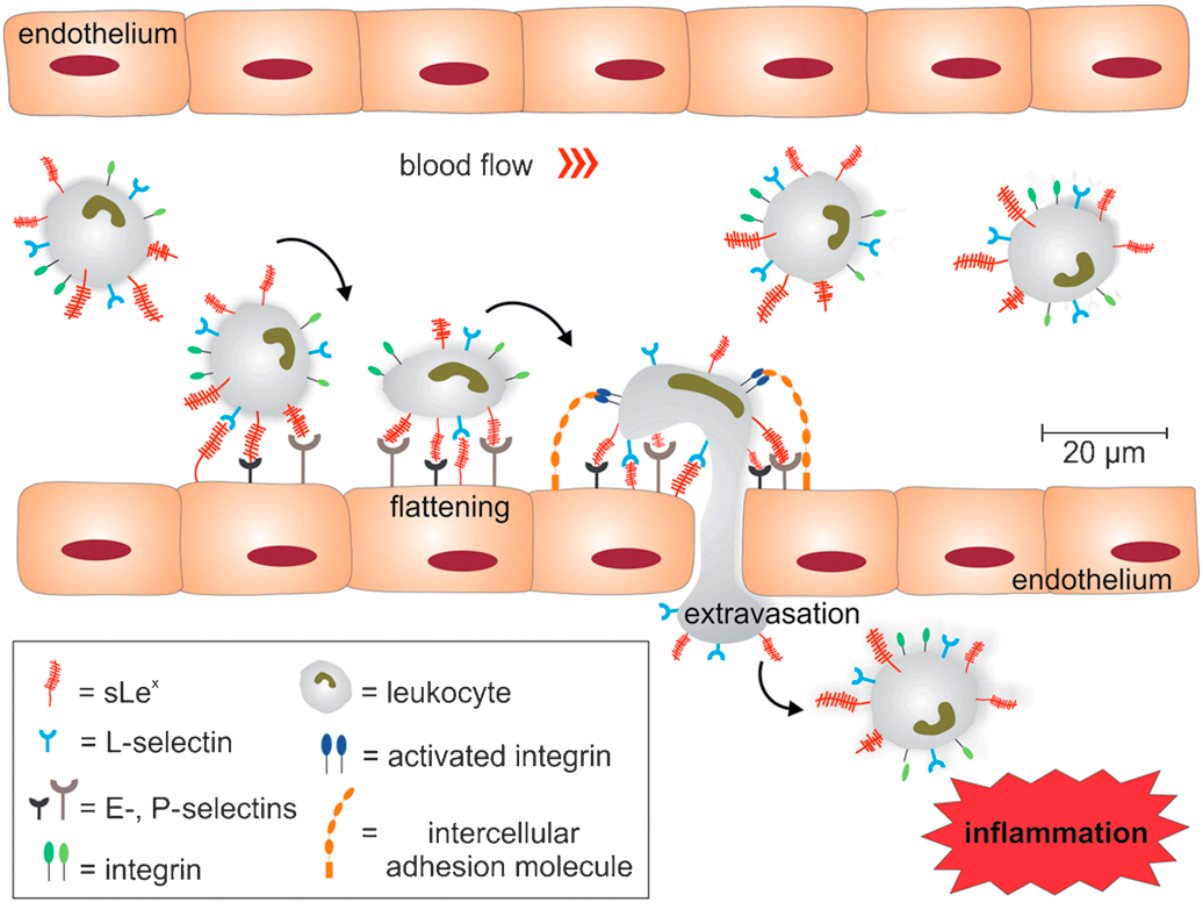


**Figure 6.** Recruitment of leukocytes to the vascular endothelium is initiated by selectin-ligand interactions and followed by transmigration of leukocytes from blood vessel to the site of inflammation. Adapted with permission from Wiley Materials: Fasting et al., *Angew. Chem. Int. Ed*. Copyright (2012).[17]

## 1.3.2 Inhibitors of selectins

A therapeutic approach to treat chronic diseases could be the specific inhibition of selectin-ligand recognition. Starting from the early days, monoclonal antibodies neutralizing E-, L-, and P-selectin were the first anti-selectin blocker.[88] After the finding that sialyl Lewis$^x$ the major ligand for selectins, Buerke et. al. developed sialyl Lewis$^x$ oligosaccharides as selectin inhibitors. Due to their short half-life time the sialyl Lewis$^x$ oligosaccharide was conjugated to liposomes and this formulation improved the potency by 25-fold.[89] Other multivalent SiaLe$^{x/a}$ based inhibitors were decorated on a polylactosamine backbone or polyacrylamide based scaffold and supplemented with sulfated tyrosine residues.[90]

Other than synthetic molecules natural glycosaminoglycans (GAGs) (**Figure 7**) has been known for years to be anti-inflammatory agents due to L- and P- selectin binding.[91] Rivipansel, a synthetic glycomimetic and a potential E-selectin inhibitor is an example for a small molecule, which is in clinical trial for the treatment of sickle cell anemia.[92] There is a demand for synthetic mimetics with desired properties and less side-effects.[93]

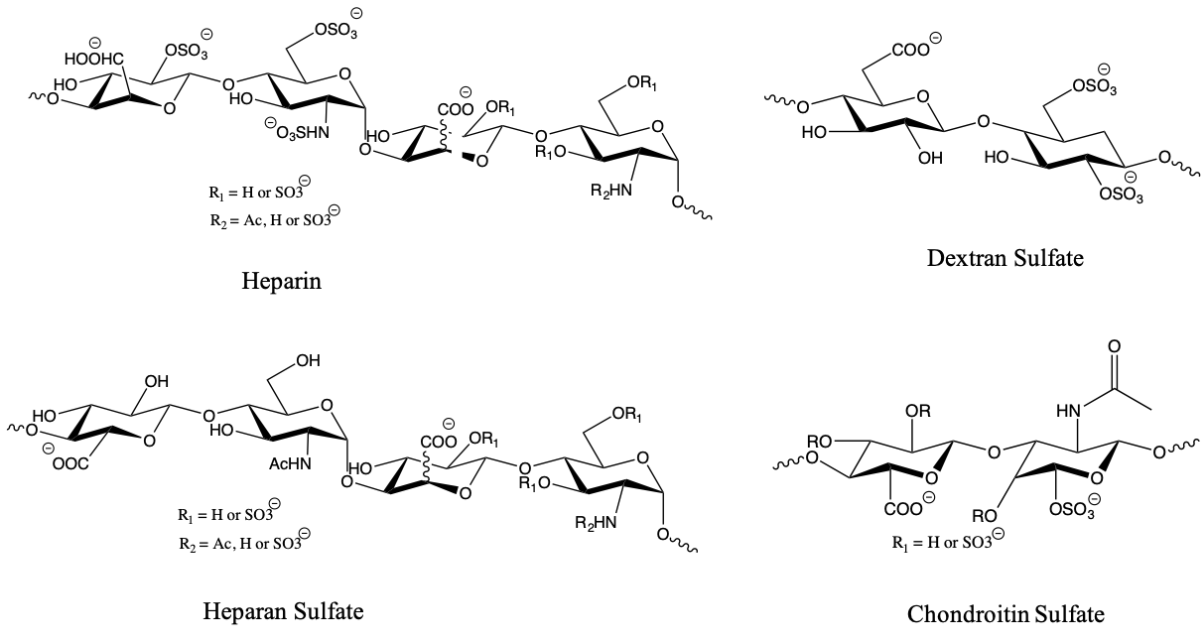


**Figure 7.** Examples of structurally related glycosaminoglycans, which bind to L- and P-selectin.

Inspired by interaction of PSGL-1 with all the three selectins, polysulfates were considered as potential anti-inflammatory compounds and a new class of molecules: sulfated polyglycerols was established. Dendritic polyglycerol sulfate proved to be a multivalent selectin binder and could inhibit the complement activation in vitro.[60]

Weinhart et al. proved that core size and degree of sulfation determine the binding affinity.[94]

## 1.4 Atherosclerosis

Atherosclerosis is defined as an age linked disease of large and medium sized arteries, characterized by hardening of the vessel wall and narrowing of the diameter, which can slowly block the arteries and can put blood flow at risk (**Figure 8**).[95]

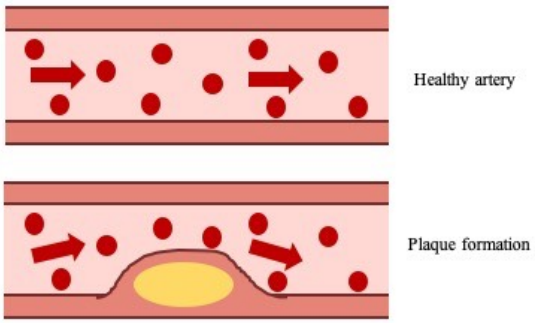


**Figure 8.** Healthy and diseased arteries showing plaque causing blockage of blood flow.

Atherosclerosis is a leading cause of cardiovascular disease and one of the major burden of death in our westernized societies.[96],[97] Although the exact cause of atherosclerosis is still unclear, however, initial factors contributing to this injury include hypertension, high blood pressure, diabetes, smoking, obesity or high level of cholesterol in the blood. Mild atherosclerosis with gradual narrowing usually does not show any symptom for decades as the arteries enlarge on plaque formation, until the arteries is severely narrowed affecting the blood flow.[98] Some of the initial symptoms of narrowed arteries are pain or cramps due to hindrance in blood flow leading to lack of oxygen supply to the tissues and in case of sudden blockage of arteries it could lead to heart attack or stroke in brain. At a later stage, blockages can be diagnosed by electrocardiography and detection of cardiac markers, cholesterol or triglycerides levels in the blood. Based on which artery is affected atherosclerosis can cause diseases including i) coronary artery disease – when coronary arteries are hardened and prevent the flow of blood to the heart[99] ii) carotid artery disease – when an occluded carotid artery blocks the blood flow to the brain[100] iii) peripheral artery disease – when hardening of arteries prevent the circulation of blood in legs, arms and lower body[101] iv) kidney disease – when the blood flow in renal artery is reduced.[102] Mechanism of atherosclerosis can be explained as a series of events correlated to the

expression of adhesion molecules,[103] mononuclear cell recruitment to endothelium,[104] and activation of leukocytes leading to inflammation.[105] Apart from these findings the major characteristic feature of atherosclerosis is sub-endothelial accumulation of apolipoprotein B (apoB)–containing lipoproteins (LPs).[106] Recent studies suggest that atherosclerotic vascular plaque formation is significantly affected by the increase of oxidized low density lipoprotein (OxLDL) rather than native low density lipoprotein (LDL).[107] OxLDL uptake by macrophages causes the foam cell formation, which leads to the release of certain proinflammatory cytokines (**Figure 9.**).[108, 109] Inflammation and attack of leukocytes to the artery lumen of endothelium leads to formation of plaques in arterial tunica intima.[98, 107] Inflammation and other physiological factors could trigger the rupture of plaque and cause immediate occlusion or other cardiovascular disease.[110]

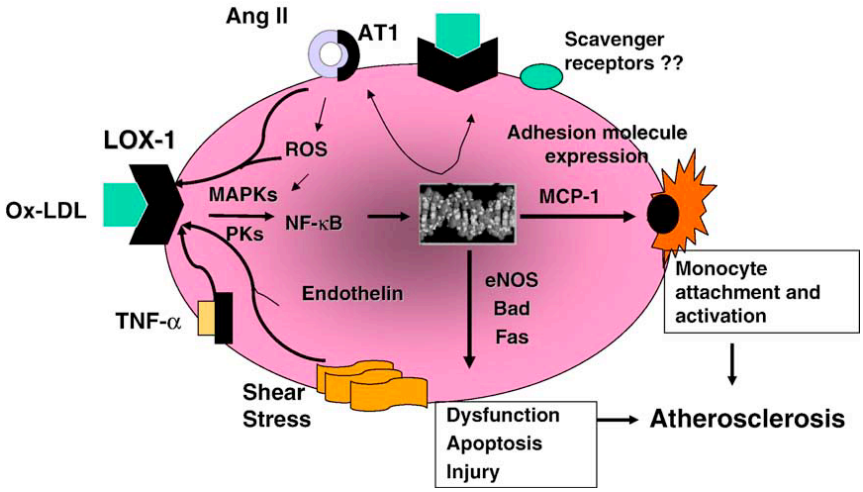


**Figure 9.** Mechanism showing activation of AT1 and LOX-1 followed by cell dysfunction, apoptosis, monocyte activation and eventually atherosclerosis. Mehta et al. by permission from Oxford University Press.

### 1.4.1 Scavenger receptor

In 1979 scavenger receptors (SR) were first described by Goldstein and Brown.[111] SR constitute a superfamily of membrane bound receptors and are involved in a wide range of biological functions. These receptors were initially thought to participate in binding and internalisation of modified low density lipoprotein but later on the studies revealed that SR are involved in binding to endogenous proteins, lipid transport, pathogen clearance, cargo transport within cell and even as taste receptor.[112, 113] SR are integral membrane proteins expressing isoforms of soluble receptors. The common feature of all the scavenger receptors is their binding ability to common negatively charged ligands like phospholipids,

apoptotic cells, cholesterol ester, carbohydrates, lipoprotein. Binding of the scavenger receptor to lipid particles, subsequent uptake and intracellular storage leads the macrophage differentiation into foam causing enhancement of atherosclerotic condition.[113, 114] Based on the structure and biological activity, scavenger receptors are classified into ten classes A to J (**Figure 10**). Zani et al. have well summarized the classification of the scavenger receptors based on structure and biological functions.[115]

Among all the classes of scavenger receptors Class E SRs are well studied and explored for their critical role in the initiation of atherosclerosis. Class E SR are type II membrane protein and consists of four domains: N- terminal cytoplasmic domain, transmembrane domain, neck region, and C-terminal carbohydrate recognition domain. They are expressed mainly on endothelial cells but also found on vascular smooth muscle cells and macrophages. Major ligand for class E SRs are OxLDL, phosphatilydserine and bacteria.[116, 117]

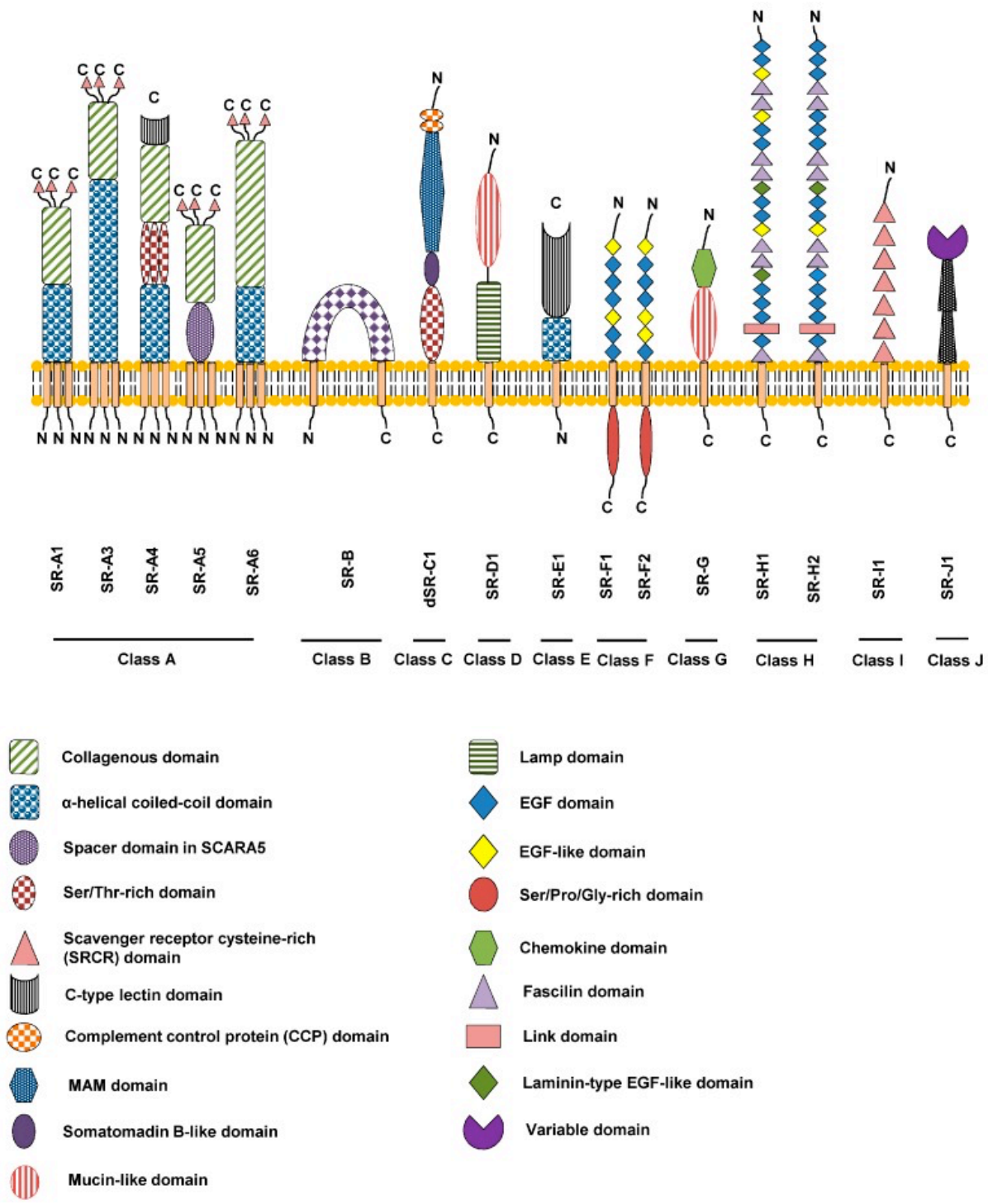


**Figure 10.** Overview of the classification and structural characteristics of SR. Adapted from Zani et al..[115] under the Creative Commons Attribution 4.0 International Licence.

## 1.4.2 LOX-1

In 1997, a class E scavenger receptor for oxidised low density lipoprotein was discovered in endothelial cells[118] and defined as LOX-1. It is a membrane bound type II glycoprotein and belongs to C-type lectin superfamily. Structurally speaking, LOX-1 consists of four domains: N-terminal cytoplasmic domain, single transmembrane domain, NECK domain and a C-type lectin like domain (CTLD) (**Figure 11**.).[119, 120]

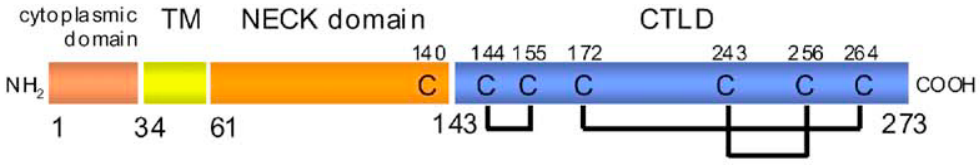


**Figure 11.** Primary structure of human LOX-1 showing four domains: cytoplasmic domain, transmembrane (TM), NECK domain and CTLD domain with intrachain disulfide bonds. Reprinted from Ohki et al.[120] Copyright (2005), with permission from Elsevier.

Special structural feature of the CTLD domain is its sequence homology to C-type lectin, which can recognize and bind to specific carbohydrate ligands. Another structural features are the three conserved intrachain disulfide bonds stabilizing the CTLD fold and a interchain disulfide bond between monomers via cysteine at 140 position.[121] In the cellular environment LOX-1 is expressed as a noncovalent oligomer of homodimers connected via disulfide bond at C140. A threshold expression level is necessary to mediate a significant binding of ligands.[122] Based on the crystal structure analysis the length of the dimeric CTLD surface is approximately 7 nm. The formation of oligomeric dimers is described (**Figure 12.**).[119-121] The C-terminal lectin like domain plays a critical function for ligand recognition, binding, and cargo internalisation.[120] In the absence of the lectin domain LOX-1 loses the function of recognition and binding to the negatively charged ligands. Over the dimer surface there is a linear arrangement of arginine residues, which is defined as “basic spine”. Due to basic spine, the CTLD domain is positively charged and cooperatively recognizes negatively charged molecules including oxLDL, apoptotic cells, and poly-anions.[123] The arginine residue of basic spine plays a very important role in ligand binding and the replacement of each arginine residues leads to a reduction in binding affinity.[120]

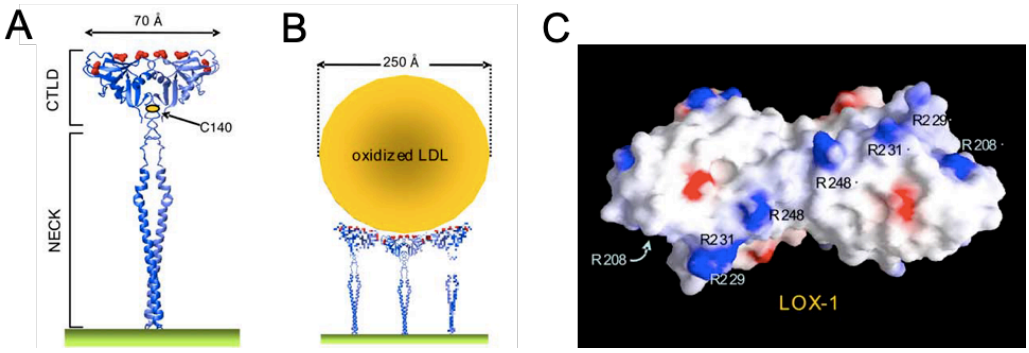


**Figure 12.** Dimer of LOX-1 expressed on the cell surface (A) Dimer of LOX-1 showing 7 nm of CTLD dimer length based on the crystal structure. (B) Comparison between size of 3 clustered LOX-1 dimers and an oxLDL particle. (C) Top-view of the dimer consists of linearly aligned arginine residues (in blue). Reprinted from Ohki et al.[120] Copyright (2005), with permission from Elsevier.

The Neck region connecting the CTLD to the transmembrane domain is important for the formation of homodimers via an interchain disulfide bond and contributes to further oligomerization. The extracellular domain of LOX-1 is a heart shaped homodimer, is modified by N-linked glycosylation, and constitutes a central hydrophobic tunnel to accommodate hydrophobic ligand structures. The N-terminal cytoplasmic domain is involved in intracellular signal transduction.[108] LOX-1 was first detected on endothelial cells but it is also expressed on macrophages, smooth muscle cells, and platelets.[124] The basal cellular expression of LOX-1 is quite low but the expression can be induced by various signals including pro-oxidative, pro-inflammatory and mechanical stimuli. Angiotensin II is an important factor for upregulation of LOX-1 via ATI receptor activation and enhances the uptake of oxLDL.[125] Oxidant species like $H_2O_2$ leads to an upregulation of LOX-1 expression in endothelial cells, smooth muscles cells, and fibroblasts. In vitro many pro-atherogenic factors like oxLDL, tumor necrosis factor, high glucose and C-reactive protein cause the upregulation of LOX-1.[126] In vivo, LOX-1 upregulation could be due to the presence of pathological conditions like hypertension, diabetes and atherosclerosis.[127]

### 1.4.3 Role of LOX-1 in pathological states

Binding of oxLDL to LOX-1 induces endothelial cell activation followed by dysfunction of endothelial. Additionally, oxLDL stimulates the expression of chemokines and adhesion molecules, which facilitates the initiation of atherosclerosis.[128] LOX-1 expression causes induction of hypertension via participating in the genesis of diminished endothelium-dependent vasorelaxation.[129] LOX-1 expressed on platelets could lead to internalisation of oxLDL followed by reduced eNOS activity and enhanced platelet aggregation. In this way LOX-1 can play an important role in oxLDL mediated platelet activation leading to thrombosis.[130] LOX-1 also supports the adhesion of Gram-positive and Gram-negative bacteria to vascular endothelial cells leading to bacterial inflammation.[131] LOX-1 also plays a role in oxLDL induced smooth muscle cell proliferation, apoptosis and foam cell formation.[132] Pathogenesis of myocardial ischemia after a short coronary artery occlusion followed by reperfusion involves the role of LOX-1.[133, 134] LOX-1 contributes to inflammation in a bi-functional way by overexpression of pro-inflammatory cytokines and utilization of oxLDL.[135] Additionally, LOX-1 interaction with oxLDL leads to expression of cytokines like interleukin-1β and tumor necrosis factor α which further expresses adhesion molecules including VCAM 1, ICAM 1.[136] Taking into account all the above mentioned effects the involvement of LOX-1 for initiation and progression of atherosclerosis is obvious. A blockade of the LOX-1 receptor leads to an improvement in cellular function, suggesting LOX-1 as a potential therapeutic target for prevention of atherosclerosis and other cardiovascular diseases (**Figure 13**).[137] LOX-1 exhibit a broad ligand specificity.[138] The protein was identified as a receptor for oxLDL but later, *in vitro* studies showed that LOX-1 can also binds to other chemically modified lipoprotein such as acetylated LDL, hypochlorite-modified high-density lipoproteins, carbamylated LDL and remnant-like lipoprotein particles.[116, 138, 139] Further, LOX-1 also recognizes ligands, which does not share any similarities with lipoproteins such as polyanionic moieties including heparin, dextran sulfate, polyinosinic acid.[138] Anionic phospholipids like phosphatidylserine, phosphatidylinositol and phosphatidylglycerol seems to work as a ligand for LOX-1.[116, 138] Cellular ligands such as activated platelets, aged/apoptotic cells, bacteria have been explored as a ligand for LOX-1.[131, 140] According to the recent findings C-reactive protein (CRP) an acute-phase protein expressed in response to inflammation and tissue damage shows selective binding towards LOX-1 in comparison to other SRs.[141]

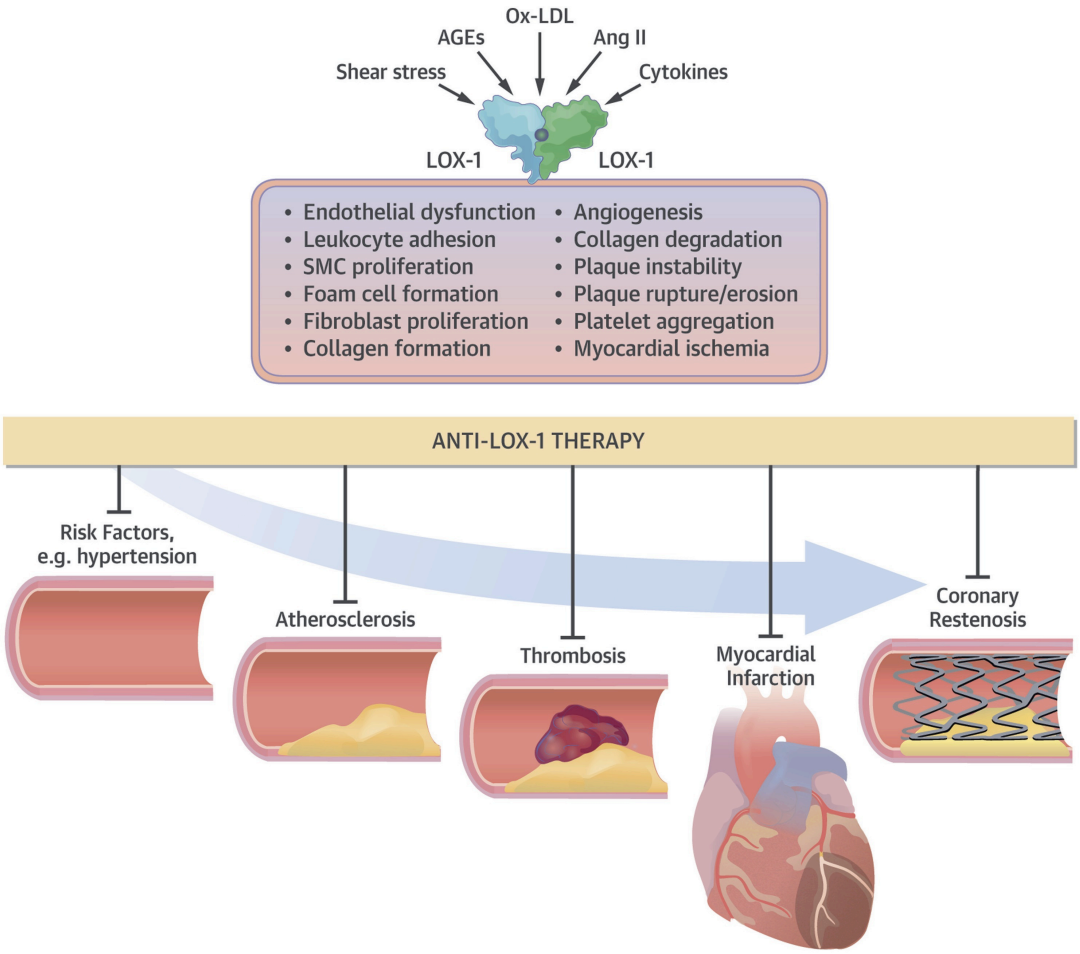


**Figure 13.** Illustration of potential disease states where an anti-LOX-1 therapy can be of potential therapeutic benefit. Reprinted from Pothineni et al., *J. Am. Coll. Cardiol.*, **2017**, *69*, 2759-2768,[134] Copyright (2017), with permission from Elsevier.

### 1.4.4 LOX-1 modulators

In the last few decades LOX-1 is explored as a novel therapeutic target in cardiovascular disease and wide research is under process to identify and pharmacologically characterize compounds for modulation of LOX-1.

Various categories of ligands are studied as LOX-1 modulators such as

i) Naturally occurring compounds: tanshinone II-A an active derivative of herbal drug can inhibit LOX-1 and ox-LDL uptake, curcumin- an active ingredient of turmeric inhibits Ang-II mediated overexpression of LOX-1.[142, 143] Various other natural components like berberine, epigallocatechin gallate, resveratrol are involved in LOX-1 inhibition.[144]

ii) Synthetic modulators for LOX-1: Primary binding site for the interaction of phospholipid moieties of oxLDLD and LOX-1 is the hydrophobic tunnel in the dimer of the receptor, moieties that can fit properly in this hydrophobic tunnel can block LOX-1 and oxLDL binding. In this direction modified lipid were developed by Falconi et.al. and small chemical inhibitors were screened by structure based drug design techniques and the selected molecules were evaluated for their efficiency to reduce oxLDL uptake and LOX-1 mRNA expression.[145, 146]

iii) Other cardiovascular drugs: In addition to specific LOX-1 inhibitors other compounds including antihypertensive agents like calcium channel blockers (amlodipine, statins), anti-inflammatory drug like aspirin or NF-kβ inhibitor (pyrrolidine dithiocarbamate), antihyperglycemic agents like metformin or gliclazide demonstrate modulatory effects and a reduction in oxLDL mediated expression of LOX-1.[127, 147-149]

iv) Various food stuffs rich in procynidins including grape seed or apple could potentially inhibit the uptake of oxLDL.[150]

v) A specific inhibition of LOX-1 can also be done by monoclonal antibodies, use of these antibodies has shown to cause a reduction in oxLDL uptake but due to the adverse effect from immune response these antibodies are challenging to use in humans.[151]

Understanding the complex mode of action of LOX-1, its contribution towards cardiovascular disease development including atherosclerosis, the wide range of ligand binding, and modulation of LOX-1 activity is challenging, but can be addressed by the design and development of potent synthetic inhibitors.

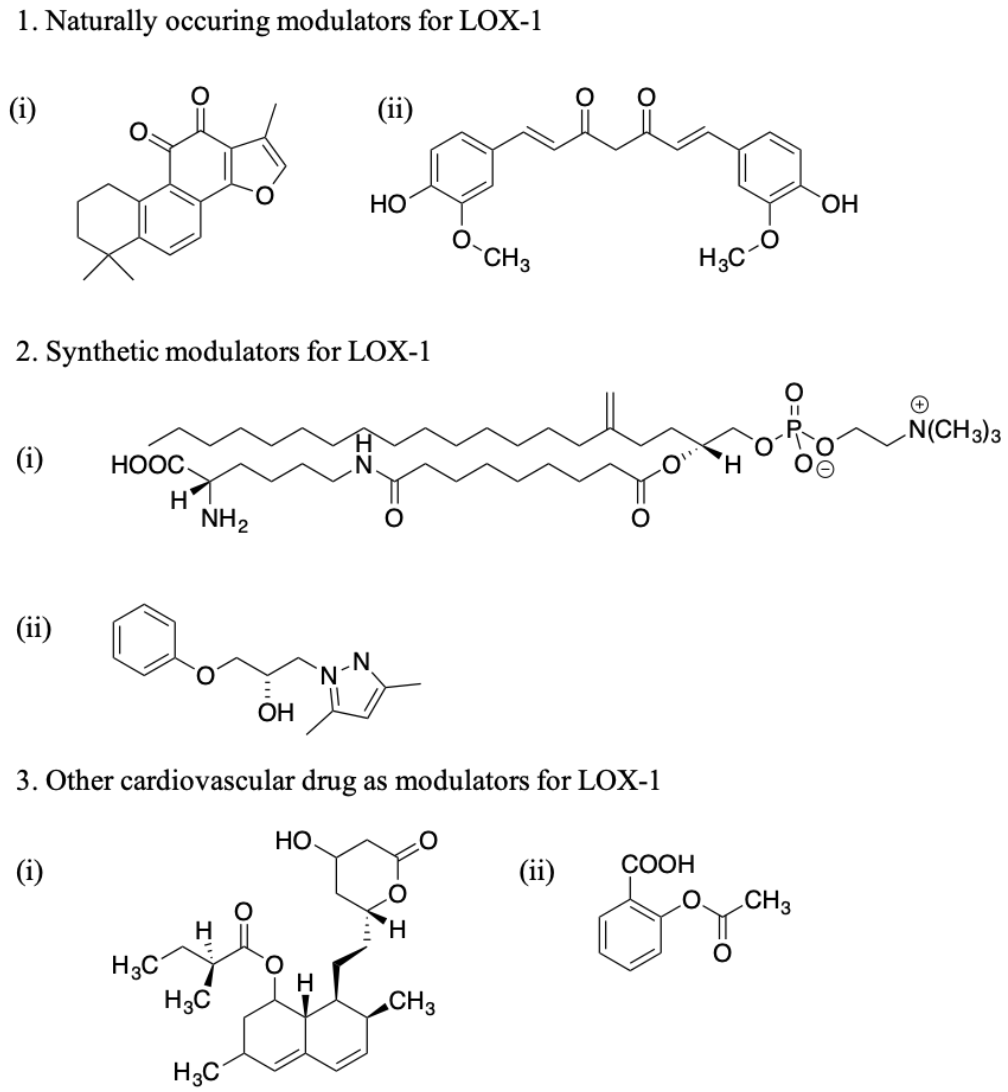


**Figure 14.** Examples of LOX-1 modulators 1. Natural modulator (i) Tanshinone II-A,[142] (ii) curcumin.[143] 2. Synthetic modulators (i) PLAzPC (modified oxidised phospholipid),[146] (ii) small molecule discovered by virtual screening.[152] 3. Other cardiovascular drug as LOX-1 modulators (i) statins,[148] (ii) aspirin.[149]

# 2 Scientific Goal

The concept of multivalency is widely spread in biological systems and it is utilized to enhance single interactions of low affinity. The Haag group has well explored dendritic polyglycerols as a scaffold for further functionalization. Polyglycerol based dendritic structures are of high interest due to their tunable chemical properties. Another multivalent scaffold is supramolecular vesicle of β-cyclodextrin, a cyclic oligosaccharide consisting of D-glucopyranose as repeating unit. The special orientation of the repeating units creates a conical shaped hydrophobic cavity. This host system can bind guest molecules like adamantane. Assembled into a spherical architecture a multivalent scaffold is generated. Sulfate is used as a targeting moiety to further functionalize both scaffolds.

It was the aim of this thesis to develop, characterize and evaluate multivalent sulfated dendrons targeting the basic, positively charged surface of two proteins: L-selectin and LOX-1.

In the first part of the thesis cyclodextrin vesicles shall be functionalized with sulfated oligoglycerol dendron conjugated to adamantane, and all the host-guest complex will be analysed regarding their physiochemical properties by ITC (isothermal calorimetry) and the binding study with L-selectin will be conducted.

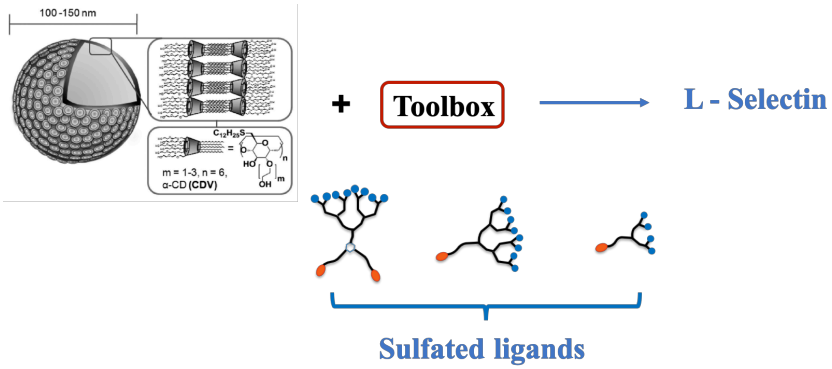


**Figure 15.** Overview for the main objective of first part of thesis

In the second part of thesis polyethylene glycol bifunctionalised with sulphated dendrons shall be synthesised and evaluated for the binding behaviour with LOX-1. Cell based in vitro studies will also be conducted to gain more information about potential binding molecules. Additionally, the synthesized molecules will also be analyzed for toxic behaviour in cellular environment.

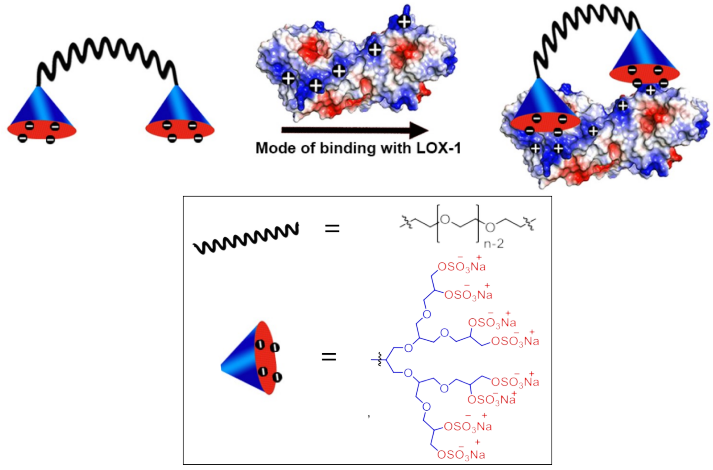


**Figure 16.** Overview for the main objective of the second part of the thesis

# 3 Publication and Manuscript

This chapter lists the published article as well as submitted manuscripts and specifies the contribution of author.

## 3.1 A toolbox approach for multivalent presentation of ligand–receptor recognition on a supramolecular scaffold

Svenja Ehrmann[1], C.-W. Chu[1], **Shalini Kumari**[1], K. Silberreis, C. Böttcher, J. Dernedde, B. J. Ravoo[*], and R. Haag[*] *Journal of Material Chemistry B* **2018**, 6, 4216-4222.
[1] Authors contributed equally
http://dx.doi.org/10.1039/C8TB00922H

A supramolecular toolbox approach for multivalent ligand–receptor recognition was established based on β-cyclodextrin vesicles (CDVs). A series of bifunctional ligands for CDVs was synthesised. These ligands comprise on one side adamantane, enabling the functionalisation of CDVs with these ligands, and either mannose or sulphate group moieties on the other side for biological receptor recognition.

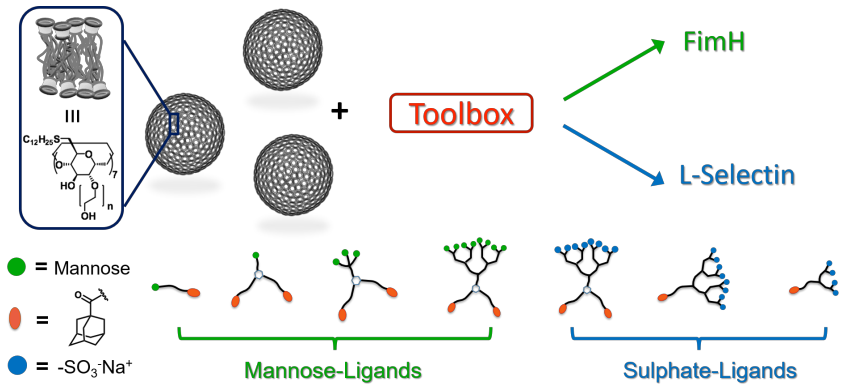


**Figure 17.** Adapted with permission from The Royal Society of Chemistry: Ehrmann et al. *J. Mat. Chem. B*. Copyright 2018.

In this publication the author contributed in the parts of concept, synthesis and characterization of sulfated glycerol based dendron conjugated to adamantane ligand and binding analysis of the sulfated architecture with L-selectin by MST and the preparation of manuscript.

## 3.2 Design and Synthesis of PEG-Oligoglycerol Sulfates as Multivalent Inhibitors for the Scavenger Receptor LOX-1

**Shalini Kumari**, Katharina Achazi, Pradip Dey, Rainer Haag, Jens Dernedde* *Submitted* Manuscript ID: bm-2018-014162.



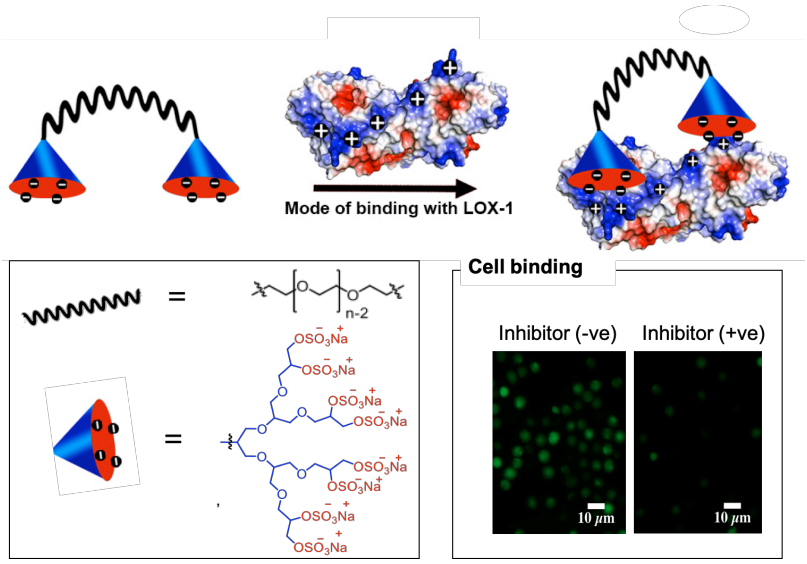


**Figure 18.** Graphical abstract for the above manuscript.

In this publication the author contributed with the concept, synthesis and characterization of PEG conjugated sulfated glycerol based dendron, binding analysis of the sulfated polymers with LOX-1 by SPR, proving the concept by cell-based assay and the preparation of manuscript

# Design and Synthesis of PEG-Oligoglycerol Sulfates as Multivalent Inhibitors for the Scavenger Receptor LOX-1

*Shalini Kumari,*[a] *Katharina Achazi,*[a] *Pradip Dey,*[a] *Rainer Haag,*[a] *Jens Dernedde*[b*]

[a]Institute for Chemistry and Biochemistry, Freie Universität Berlin, Takustr. 3, 14195 Berlin, Germany.

[b]Charité-Universitätsmedizin Berlin, Institute of Laboratory Medicine, Clinical Chemistry and Pathobiochemistry, CVK, Augustenburger Platz 1, 13353 Berlin, Germany

**KEYWORDS**: scavenger receptor, LOX-1 inhibitor, cardiovascular disease, PEG, polyglycerol sulfate.

**ABSTRACT**

Lectin-like oxidized low-density lipoprotein receptor-1 (LOX-1) is a cell surface scavenger receptor. The protein is involved in binding and internalization of oxidized low-density lipoprotein (oxLDL), which leads under pathophysiological circumstances to plaque formation in arteries and initiation of atherosclerosis. A structural feature of LOX-1 relevant to oxLDL binding is the "basic spine" motif consisting of linearly aligned arginine residues stretched over the dimer surface. Inhibition of LOX-1 can be done by blocking these positively charged motif. Here we report on the design, synthesis, and evaluation of a series of novel LOX-1 inhibitors having different number of sulfates and PEG spacer. Two molecules, compound **6b** and **6d** showed binding affinity in the low nM range i. e. 45.8 and 47.4 nM, respectively. The *in vitro* biological studies reveal that these molecules were also

able to block the interaction of LOX-1 with its cognate ligands oxLDL, aged RBC, and bacteria.

## INTRODUCTION

Scavenger receptors (SR) were first identified by Goldstein and Brown as membrane receptors that bind and internalize modified low density lipoproteins.[1] According to recent findings, these receptors belong to a large family of membrane-bound receptor and recognize a variety of ligands such as lipoproteins, apoptotic cells, cholesterol ester, and bacterial lipopolysaccharide.[2] Based on their structure and function SR proteins are classified into various classes (class A-J).[3] In 1997, Sawamura *et al.* discovered a class E scavenger receptor, designated as lectin-like oxidized low density lipoprotein receptor-1 (LOX-1), which is mainly expressed on endothelial cells.[4] Besides endothelial cells, LOX-1 is also present on macrophages, platelets and smooth muscle cells and is responsible for binding and internalization of oxLDL.[5,6] Pathobiological studies revealed that LOX-1 is involved in oxLDL internalization through receptor-mediated pathways.[7,8] Recent studies indicate that the focal accumulation of lipid-laden foam cells, derived from macrophages due to oxLDL uptake, is a critical event in the early stages of atherosclerosis. The disease is defined by hardening and narrowing of arteries and can put blood flow at risk.[9] Pro-inflammatory stimuli originate from damaged endothelial cells and sub-endothelial remodeling processes and induce a cascade of events at the early step in atherogenesis.[10,11] Ongoing vascular occlusion and finally plaque rupture therefore lead to cardiovascular problems and are the major cause of death in western societies.[12,13,14] Among other risk factors including hypertension, diabetes, smoking, and obesity the sub-endothelial accumulation of lipoprotein particles is of prime interest, calling for the development of an efficient strategy to block oxLDL uptake.[15]

LOX-1 is a 52-kDa type II membrane glycoprotein and consists of four domains - an N-terminal cytoplasmic domain, a transmembrane domain, a neck region, and the C-terminal

extracellular C-type lectin-like domain.[16] The basal complex contains two individual LOX-1 polypeptides linked via an intermolecular disulfide bond bridge in the neck domain (C140)[17]. The structural feature of LOX-1 known as "basic spine", consisting of linearly aligned positively charged arginine residues stretched over the dimer surface, is responsible for oxLDL particle recognition via interaction with negatively charged components of oxLDL.[17,18] In addition, a hydrophobic tunnel is important for lipid binding.[19]

With respect to a therapeutic approach, the design of specific inhibitors for LOX-1 that antagonize oxLDL uptake might be beneficial to treat cardiovascular disease and reduce the acute inflammatory response. Additionally, LOX-1 inhibitors might be applicable as bacteriostatic agents by avoiding bacterial adhesion. Natural substrate mimetics or structure-based design of LOX-1 inhibitors have been reported to inhibit LOX-1 activity by targeting the hydrophobic tunnel.[20,21] The known LOX-1 inhibitors are mainly based on small molecular drugs and hydrophobic moiety. Therefore, bioavailability is very less and until now, there is no multivalent inhibitor available, which can target LOX-1 specifically.

In recent years, we have shown how a rational design of multivalent entry inhibitors for pathogens such as viruses and bacteria can be applied to block and reduce infectivity. The effectiveness of the inhibitors not only depended on the nature of functional groups (specific interaction such as mannose - Concannavalin A,[22] hemagglutinin - sialic acid[23]) or charges (electrostatic interactions like sulfates with L-selectin[24]) but also the size and multivalency of the architectures e.g., dendritic versus linear polymers,[25] polymeric hydrogel particles,[26] 2D graphene sheet[27] *etc*. played an important role in increasing the affinity towards the target.[28]

In this work we present a novel class of multivalent inhibitors based on AB type diblock and ABA type triblock dendron polymer conjugates for the inhibitor of LOX-1. The inhibitor design is based on the given structure of the ligand binding site i.e., the linearly aligned arginine residues on the surface of the lectin-like domain. It has been previously reported that

mutations of arginine residues from the basic spine markedly reduce LOX-1 binding activity of oxLDL.[29] In LOX-1 the approximate distance between the basic patches of dimeric surfaces is 7 nm (Figure 1).[16, 17] To completely shield and effectively bind to LOX-1 a flexible handle/thread is needed which can stretch over the dimeric surface and span approximately 7 nm. In our design, the block (A) is composed of an anionic oligoglycerol dendron where the number of anionic sulfate groups can be varied based on the dendron generation while block (B) is a linear polyethylene glycol (PEG) polymer of 6 and 10 kDa (Figure 2). To support the inhibition of an acute inflammatory response, sulfates were chosen as anionic ligands inspired from dendritic polyglycerol sulfates (dPGS) which are known as multivalent inhibitors of inflammation, previously reported by our groups.[24] A PEG spacer was chosen due to its biocompatibility and convenience for functionalization at both ends.[30,31,32] The resulting macromolecules were analyzed for binding to recombinant LOX-1 by surface plasmon resonance (SPR). In addition, two lead molecules were evaluated for the ability to inhibit the interaction of LOX-1 with its other natural ligands: aged RBC, oxLDL and bacteria.

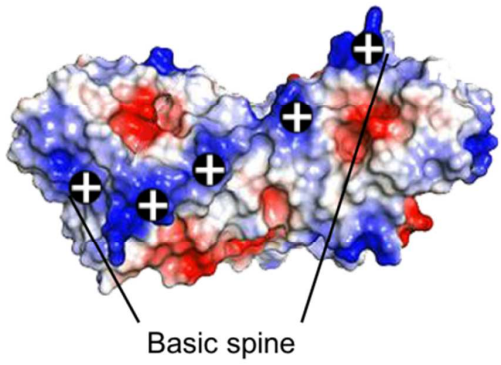


**Figure 1**. Top-view of LOX-1 showing positive patches of basic spine. Adapted from Thakkar *et al.*[33]

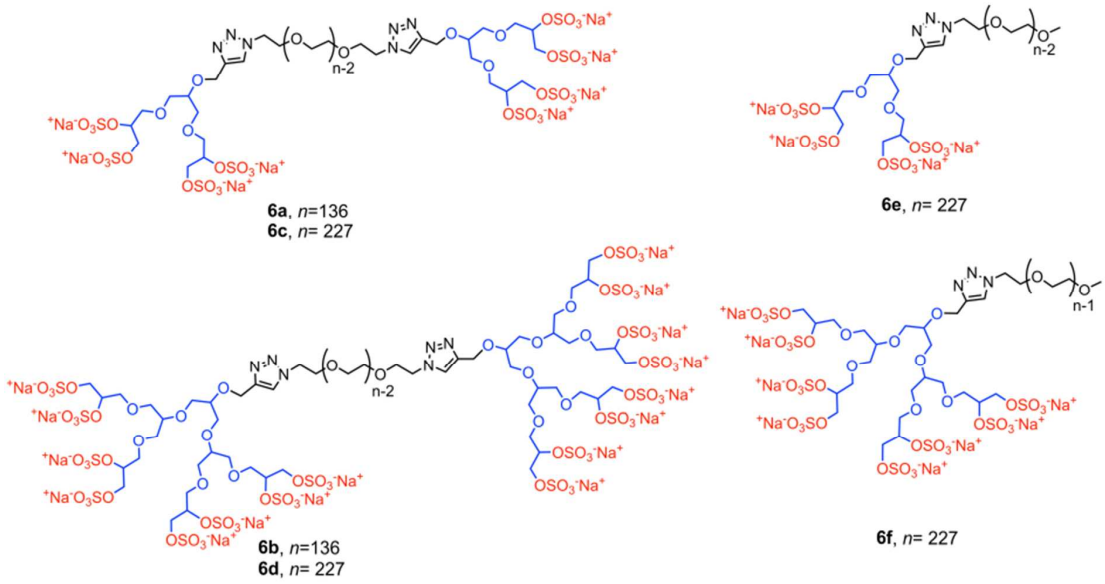


**Figure 2**. Structures of synthesized architectures

## EXPERIMENTAL SECTION

### Recombinant protein expression

In order to prepare the soluble protein, LOX-1 coding sequences were inserted into a derivative of the mammalian expression vector pFLAG-CMV-3 (Sigma-Aldrich). Expression of the full length membrane bound LOX-1 was realized from a pCDNA6/V5 His A derived (Thermo Fisher Scientific) recombinant expression plasmid. Detailed information is given in the Supporting information (SI). In brief, coding sequence was amplified via polymerase chain reaction (PCR) from a LOX-1 cDNA clone (Sinobiological, Gene Bank Ref. ID: NM_002543.3). To mimic essential oligomerization LOX-1 was expressed as fragment crystallizable (Fc) fusion protein carrying one or two aligned C-type lectin domains (CTLD) of LOX-1 fused to an IgG1 heavy chain.

Transient secreted protein expression was performed in the human embryonic kidney cell line in HEK293 cells after DNA transfection using Lipofectamine 3000 (Thermo Fisher Scientific) according to the manufacturer's protocol. Proteins 1CTLD-Fc and 2CTLD-Fc,

representing a divalent and tetravalent LOX-1 architecture, were purified from the supernatant on a Protein A sepharose (Thermo Fisher Scientific) column. After extensive washing with phosphate buffer saline (PBS) bound protein was eluted from the column with elution buffer (20 mM citrate, 150 mM NaCl, pH 2.5). The eluted protein was immediately neutralized by dropping into a prepared 1 M Tris solution, pH 8.0. Protein samples were further concentrated and equilibrated with washing buffer (PBS) by filtration (Amicon concentration device 10K). The protein samples were analysed by SDS-PAGE under non-reducing and reducing conditions. HEK293 cells were cultured in 10% DMEM supplemented with 10% fetal bovine serum and 1% penicillin/streptomycin at 37 $^{o}$C in 5% $CO_2$

**Binding assay - surface plasmon resonance measurements**

Binding analyses of the synthesized molecules was performed by surface plasmon resonance (SPR) on a BIACORE X100 (GE Healthcare) at 25 ℃. 2CTLD-Fc was immobilized on a protein A chip (BIAcore). Briefly, 2CTLD-Fc was dissolved in the HBS-Ca buffer solution (10 mM HEPES, pH 7.5, 150 mM NaCl, 1mM $CaCl_2$), and its concentration was adjusted to 60 μg/ml. The 2CTLD-Fc was injected at a flow rate of 10 μL/min for immobilization.

Ligand binding was recorded in HBS-Ca buffer at a flow rate of 30 μL/min with an association phase of 180 sec and a dissociation phase of 180 sec. Regeneration of the chip surface was performed by injection of 10 mM glycine-HCl, pH 1.5 at 100 μL/ min for 60 sec. Applying the single cycle kinetic approach five increasing ligand concentrations were passed over the LOX-1 functionalized surface without any regeneration procedure in between. Rate constants were calculated by using the BIAevaluation software 4.1.

**Inhibition assays - Red blood cells (RBC) and LOX-1 binding inhibition.**

Binding of aged RBC to LOX-1 was evaluated according to a previously reported protocol with slight modification.[34] Briefly, RBC isolated from fresh human blood and were washed three times with PBS. Thereafter, 20 % hematocrit was resuspended in PBS containing 0.1 % w/v of glucose and which was used as native RBC fraction. To produceaged RBC 20 % hematocrit was incubated at 37 °C for 4 days. To perform the assays RBC (aged or native) were fixed with 4 % formaldehyde and 0.2 % glutaraldehyde solution in PBS, and washed three times with PBS. Thereafter, 50 μL of 1 % hematocrit dissolved in Ham's F-12 medium containing 10 % fetal bovine serum were incubated for binding studies with 50 μg/mL of 2CTLD-Fc. In competition experiments the LOX-1 fusion protein was preincubated for 90 min at room temperature with compound **6d** or an inhibitory monoclonal antibody (mAB, R&D systems) at a concentration of 100 μg/mL. Treated RBC were then washed three times with medium and further incubated with FITC-labelled Protein-A (Invitrogen) for 30 min at room temperature and subjected to fluorescence microscopy and flow cytometry after three times washing with medium.

**LOX-1 mediated recognition of *E. coli***

LOX-1 plays an important role in recognition and binding of Gram positive and Gram negative bacteria. Here we analyzed *E. coli* (DH5α) recognition by LOX-1 transformed cells and monitored the inhibitory effect of compound **6d** according to the reported protocol with partial modification.[35] Briefly, HEK293 cells ($1x10^6$ cells) were seeded on slides (ibidi) and transiently transfected for full length LOX-1 expression using Lipofectamine 3000 (Thermo Fisher Scientific) according to the manufacturer's protocol. *E. coli* was labeled with fluorescein isothiocyanate (FITC) (Sigma) according to a reported protocol, [36] detailed information is provided in the SI. Transfected HEK293 cells and non-transfected control cells were incubated with FITC-labelled *E. coli* ($3x10^7$ cells/mL) in the cell culture medium at 37

°C for 1 h. For inhibition studies cells were pretreated with polyinosinic acid (Poly(I)) (100 μg/mL) and compound **6d** (100 μg/mL) for 15 min before FITC-labelled bacteria were added. During two washing steps with PBS unbound bacteria were removed. The adherence of bacteria was further visualized by fluorescence microscopy (Axiophoto 2; Zeiss). Cells were treated with trypsin for 5 min, and then detached cells harvested. Dilutions were plated on agar plates. After 18 h of incubation at 37 $^{o}$C the colony formation units (CFU) were counted.

**Dil-oxLDL binding study**

Dil-oxLDL uptake study was performed according to a published protocol with slight modification.[37] HEK293 cells ($1x10^6$ cells) were seeded on ibidi slides and cultured for 24 hours. Cells were transfected with plasmid for full length LOX-1 using Lipofectamine 3000 (Thermo Fisher Scientific) according to the manufacturer's protocol. HEK293 cells expressing LOX-1 and mock treated control were incubated with Dil-oxLDL (Sigma) 25 μL for 3 hours and washed three times with culture media and analyzed by confocal microscopy. To characterize an inhibitory potential cells were pre-treated for 30 minutes with either mAB anti LOX-1 or compound **6d** before labeled oxLDL was added. Cells were treated with trypsin and subjected to flow cytometry for quantification of the fluorescence signal.

**Cell viability assay**

The most active molecules were analyzed in a cytotoxicity assay using HEK293 cells with the lactate dehydrogenase (LDH) release assay. Briefly, HEK293 cells were seeded in a 96-wells plate at a concentration of $5\ x10^3$ cells/well and grown for 24 h. Cells were then treated with the compounds at concentrations ranging from 0.097-25 μM diluted in cell culture medium. To monitor 100% LDH release a detergent solution of 4% Triton-X-100 was used.

After 24 hrs of treatment the supernatant was collected for LDH activity measurements. The LDH assay kit (TaKaRa) was applied according to the manufacturer's protocol.

## RESULTS AND DISCUSSION

### Synthesis and characterization of sulfated dendron polymer conjugates

AB and ABA type dendron polymer conjugates (**6a-d**) were synthesized by coupling propargylated G1 and G2 oligoglycerol dendrons (3a and 3b) to monofunctional mPEG azide (10 kDa) and PEG bis azide (both 6 and 10 kDa, Table 1) via Cu catalyzed 1, 3 dipolar azide-alkyne cycloaddition reaction (Figure 2).[38] Oligoglycerol dendrons (G1, G2) were propargylated by propargyl bromide (Scheme 1) and purified via column chromatography following the procedure reported elsewhere.[39] Similarly PEG bis azide (6 and 10 kDa) and mPEG-azide (10 kDa) were synthesized in two steps by mesylation of hydroxy groups and substitution by azide as reported before.[40] A Cu assisted 1,3- dipolar cycloaddition reaction was monitored by FTIR (Figure S25) and continued until the disappearance of the azide peak at 2105 $cm^{-1}$. In addition, both side functionalization was confirmed using $^{1}$H-NMR comparing the peaks by the appearance of peak at 7.77 ppm to 4.23 ppm (Figure S7). Deprotection of protected dendron polymer conjugates (both AB and ABA type) lead to formation of hydroxy functionalized dendron polymer conjugates (Scheme 1). The disappearance of the peak at 1.39 ppm proved the successful deprotection of acetals (Figure S13). In addition, the formation of ABA dendron polymer conjugates were analyzed by MALDI–TOF MS (Figure 3A). The experimental peak molecular weights Mp (corresponding to the peak with the highest intensity in the MS distribution) are noted in Table S1 (column 2). Mp of PEG-6k_OH is found to be 6298 Da, which corresponds to the 142 oliogooxy repeating units. If single oligoglycerol dendrons of generation 1 and 2 were coupled to 2a the expected peaks should be observed at masses 6624 and 6920 Da respectively (Figure 3A,

Table S3). Obviously, there is no incidence of mono-functionalized oligoglycerol dendron conjugated to PEG. The complete shifts of Mp from 6298 Da to the maxima at 6955 (compound 5a) and 7417 Da (compound 5b) indicate the successful bi-functionalization (Figure 3a). The calculated molecular weights based on $^{1}$H NMR are reported in Table S1 (column 3) where the average molecular weight of PEG was considered 6000. Subsequent sulfation of the hydroxy groups using the sulfur trioxide pyridine complex led to the formation of desired macromolecules (6a-f). The polymers were characterized by $^{1}$H-NMR (Figure S1-24). S content was determined by elemental analysis and full conversion of the hydroxy groups to sulfates were confirmed by comparing the S content value for 100% conversion versus the obtained experimental value (Table 1). The results indicated full conversion of the hydroxy to sulfates. The detailed procedure and characterization for the synthesis of the above mentioned polymers is provided in SI.

Next, sizes of the polymers were measured in water by dynamic light scattering (DLS) (Table 1, Figure 3B). From the DLS measurements it could be seen that the hydrodynamic diameter of the polymers increased going from G1 to G2 dendrons in the same series (6a to 6b, Table 1). All polymers (6a-f) showed negative zeta-potentials (range -7 to -15 mV). In addition, the zeta-potential correlated with the dendron generation. The monovalent AB type polymers showed a comparatively low negative potential compared to ABA type copolymers when the dendron generations were the same due to less sulfate groups in the polymer.

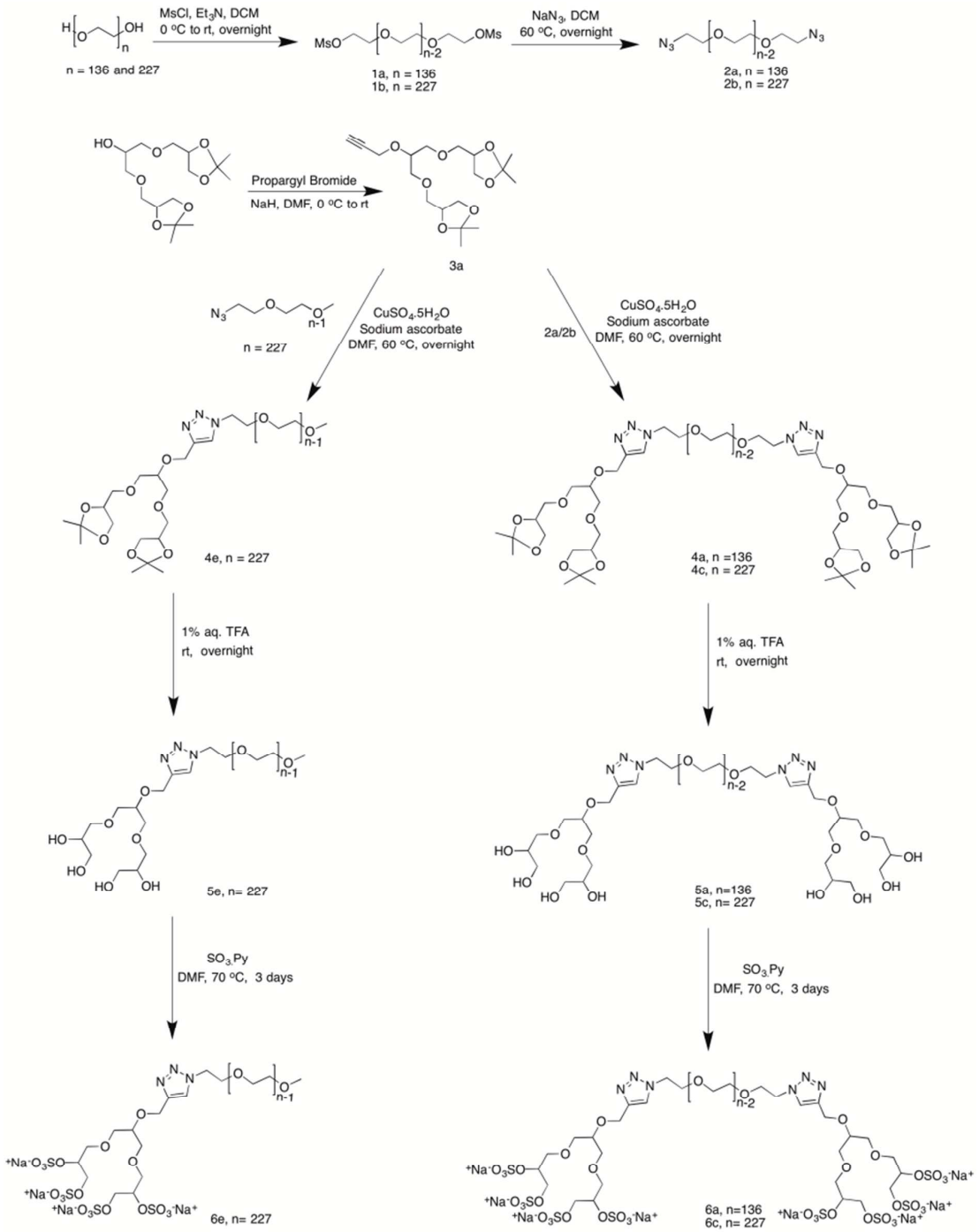


**Scheme 1.** Schematic representation for the synthesis of AB and ABA type sulfated dendronized PEG polymers. The synthesis is shown for generation 1 oligoglycerol dendrons. A similar synthetic procedure was followed for sulfated G2 dendronized polymers, synthetic scheme shown in SI.

**Table 1.** Characterization of synthesized polymers

| Polymers | Molecular weight[a] (kDa) | Experimental S content[b] (%) | Calculated S content[c] (%) | Size[d] (nm) | PDI[d] | Zeta potential | $K_D$[e] (nM) |
|---|---|---|---|---|---|---|---|
| 6a | 7 | 3.48 | 3.44 | 4.95±0.06 | 0.43 ± 0.24 | -11.1 ± 0.91 | 181 |
| 6b | 8 | 5.40 | 5.79 | 7.75±1.17 | 0.50 ± 0.13 | -14.3 ± 1.25 | 45.8 |
| 6c | 11 | 2.24 | 2.24 | 6.59±0.15 | 0.49 ± 0.01 | -12.6± 1.10 | 93.3 |
| 6d | 12 | 3.79 | 3.99 | 7.35±0.56 | 0.45 ± 0.12 | -15.0 ± 0.65 | 47.4 |
| 6e | 10 | 1.13 | 1.19 | 3.24±0.25 | 0.51 ± 0.06 | -7.00 ± 0.20 | No binding |
| 6f | 11 | 2.17 | 2.23 | 4.35±0.17 | 0.20±0.05 | -9.26 ± 0.59 | 2440 |

[a] obtained by $^1$HNMR

[b] obtained by elemental analysis (combustion analysis)

[c] calculated based on $^1$HNMR

[d] obtained by DLS (volume average)

[e] apparent binding affinities of soluble compounds to immobilized LOX-1 fusion (2CTLD-Fc) determined by SPR

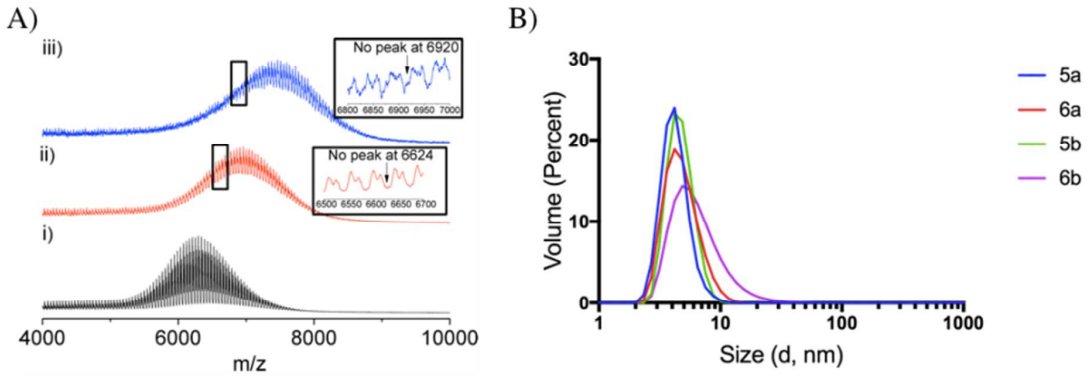


**Figure 3.** A) MALDI-TOF mass spectra of i) 6 kDa PEG-OH and bi-functionalization with ii) G1 and iii) G2 oligoglycerol dendrons, B) DLS plot by volume average

**Expression of LOX-1 tetramers**

Oligomerization of LOX-1 is an essential feature for the ligand-binding activity at the cell surface.[41] For the activity of recombinant soluble LOX-1 a multivalent protein is highly crucial.[42] Therefore, a tetrameric species of soluble LOX-1 was expressed following the recommendation reported by Cao *et al.*[42] to mimic receptor clustering. Details are given in the SI. In brief, constructs consisting of a duplicated C-type lectin domain (CTLD) of LOX-1 were successfully transiently expressed as either secreted Fc-fusion protein 2CTLD-Fc or full length LOX-1 (fl LOX-1) membrane bound receptor in the mammalian cell line HEK293. The soluble LOX-1 fusion protein was purified by affinity chromatography on a Protein A column and successfully analyzed by SDS-PAGE and Western blotting (Figure S26).

**Binding analysis by surface plasmon resonance**

Binding studies were performed by surface plasmon resonance (SPR), where the 2CTLD-Fc protein was coupled to the Protein A sensor chip to a density of (1500 RU). Compounds **6a-f** were used as analytes and flushed over the functionalized chip surface. From the resulting

sensorgrams, individual rate constants (Fig S28-S32) and the dissociation constant at equilibrium $K_D$ were calculated (Table 1). Across the whole series of molecules an enhancement in LOX-1 binding was observed as the number of sulfates increased. Obviously, the dendron generation is important and correlates with receptor binding affinities. While compound **6e** (G1 dendron with 4 sulfate groups) showed no binding, an affinity in the range of 2.44 μM was detected for compound 6f equipped with a G2 dendron (8 sulfate groups). A further affinity enhancement of about 50-fold was achieved by coupling two G2 dendrons to a bi-functional PEG linker. The finding that compounds **6b** and **6d** gave comparable $K_D$ values of 45.8 and 47.4 nM indicates that here the higher number of sulfate groups is important. Finally, it is interesting to note that the increase of binding affinity is only a factor of two when we compare molecules carrying two functional G1 moieties (**6a** and **6c**) versus those with G2 dendrons (**6b** and **6d**). Obviously, both bi-functionalized compounds **6b** and **6d** are well suited to target the "basic spine" of arginine residues displayed at the LOX-1 dimer surface via electrostatic interactions.[17,43] The charge density and hydrodynamic diameter seem to be absolutely important for an affine receptor recognition. Both the polymers **6b** and **6d** have similar hydrodynamic diameter of ~7 nm and the most negative zeta potentials (Table 1). On the other hand for **6c**, the hydrodynamic diameter is comparable but the charge density is not sufficient to have a similar binding affinity. This is in line with our previous results, where we addressed the flat surface of the adhesion receptor L-selectin with diverse polyanions.[44,45] So far, the accuracy of fit of compounds **6b** and **6d** to the LOX-1 surface cannot be finally answered and potential rebinding effects cannot be excluded.[46,47] Nevertheless, both multivalent compounds show a remarkable receptor affinity while possessing only a limited number of functionalities.

**Competitive binding studies**

LOX-1 acts as a scavenger receptor and is capable to bind different anionic molecules.[48] Clearance of aged red blood cells (aRBC) via LOX-1 expressing macrophages has been described.[34] Phosphatidylserine (PS) flips to the outer leaflet of aged/apoptotic RBC seems to be the dominant target for LOX-1 and initiates phagocytosis by macrophages.[49] Therefore competitive binding of the soluble receptor 2CTLD-Fc to aRBC as a model system was analyzed. A schematic overview of the assay is shown in the SI (Scheme S2). First, binding of the recombinant soluble LOX-1 fusion protein to aRBC was confirmed by co-incubation of receptor and ligand and subsequent visualization via a fluorescent probe; here the binding of FITC labelled Protein A to the Fc part of the fusion protein. The fluorescent image (Figure 4A, i) clearly proved targeting of aged red blood cells, whereas native freshly prepared red blood cells (nRBC) were not addressed (Figure 4A, ii). In a following experiment the addition of inhibitors i. e. mAB anti LOX-1 (Figure 4A, iii) and compound **6d** (Figure 4A, iv) at a concentration of 40 nM and 8 μM respectively, reduced the binding of 2CTLD-Fc to aRBC. The mAB served here as a positive control.[34] For quantification of fluorescent signals FACS analyses were performed (Figure 4B) and the normalized results depicted in Figure 3C. Binding of 2CTLD-Fc to aRBC was set to 100%, the negative control gave less than 0.5 % of the fluorescence, and as a positive control the inhibitory antibody reduced the fluorescent signal to 20%. A dose-dependent inhibition was observed for compound **6d.** at the highest concentration of 8 μM the signal intensity was reduced to 40 %.

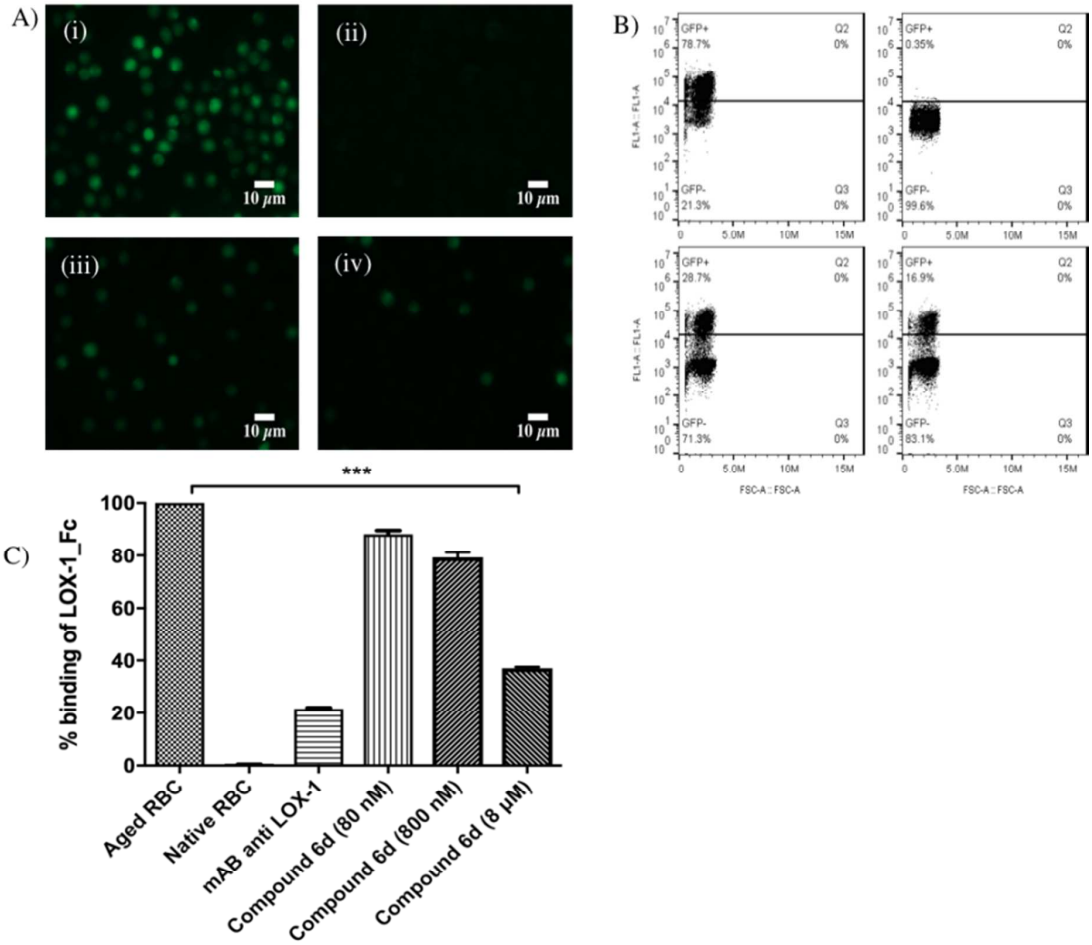


**Figure 4.** Competitive binding of soluble LOX-1 (FITC labeled 2CTLD-Fc) to aged red blood cells. **A)** Fluorescence microscopy images: i) aRBC (positive control); ii) nRBC (negative control), iii) aRBC + mAB anti LOX-1; iv) aRBC + compound 6d. **B)** Corresponding FACS analyses. **C)** Dose-dependent inhibition of compound 6d. Values for each bar are the average mean from 3 separate experiments, ***P<0.05

In a second in vitro model, binding of the pathogen *E.coli* (DH5α) to HEK293 cells expressing the membrane bound LOX-1 was analyzed. Interaction of Gram-positive as well as Gram-negative bacteria with LOX-1 has been described and again point to the versatility of this scavenger receptor.[35] From the fluorescent images (Figure S34) it is obvious that the membrane bound LOX-1 is functionally expressed in transformed HEK293 cells and therefore competent for *E. coli* binding. Protein expression was confirmed by a Western-blot

analysis (SI, Figure S27). At a concentration of 100 μg/mL compound **6d** reduced the bacterial adhesion to approximately 50% (Figure S34, B) and Poly(I) nearly to background level.

**Dil-oxLDL binding study**

Binding and uptake of oxLDLwas investigated after a 3 hours incubation with LOX-1 expressing HEK293 cells for and subsequent washing with culture medium. Confocal imaging (Figure 5) reveals that the cells expressing LOX-1 were able to bind and internalize Dil-oxLDL, whereas cells lacking LOX-1 did not show of Dil-oxLDL binding. Pre-exposition of the cells expressing LOX-1 with the compound **6d** (8 μM) caused a reduction in fluorescence intensity as showed in Figure 5A. FACS analyses (Figure 5B) and normalized fluorescence from trypsin treated cells (Figure 5C) indicate a 50% reduction of Dil-oxLDL uptake in the presence of 8 μM compound **6d.**

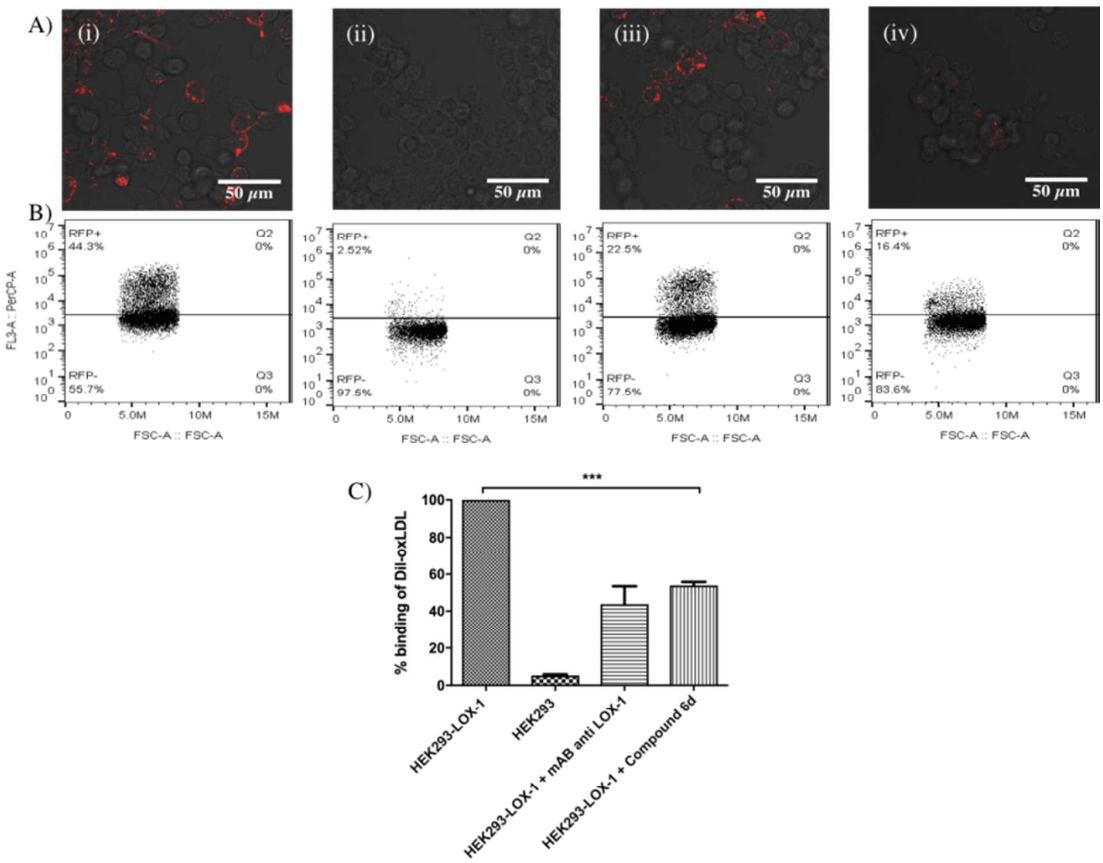


**Figure 5.** Competitive binding of soluble Dil-oxLDL to LOX-1 expressing cells. **A**, confocal merged images of brightfield and red fluorescent Dil-oxLDL **B**, FACS analyses. **C**, quantification of fluorescent signals. (i) Dil-oxLDL with LOX-1 expressing cells (positive control); (ii) Dil-oxLDL with cells without LOX-1 (negative control); Dil-oxLDL with LOX-1 expressing cells pre-incubated with (iii) compound 6d (8 μM); (iv) mAB anti LOX-1 (40 nM). Values for each bar are average mean from 3 separate experiments, ***P<0.05

**Cytotoxicity evaluation**

The most active molecules were analyzed for cytotoxicity. Cell membrane integrity was analyzed by the release of cytosolic lactate dehydrogenase (LDH) release assay, from HEK293 cells. Here, **6b, 6d** showed no harmful effect up to a concentration of 25 μM as shown in Figure S35. Hence, these molecules seems to be safe and applicable for further *in*

*vivo* studies to investigate their potential as LOX-1 inhibitors in in model systems of atherosclerosis.

## CONCLUSION

A series of sulfated dendronized multivalent ligands with PEG (6 and 10 kDa) as spacers were designed to target the lectin-like oxidized low-density lipoprotein receptor-1 (LOX-1). For ligand binding experiments soluble LOX-1 was successfully expressed and purified as a tetravalent Fc-fusion protein containing 2 tandem CTLD domains per heavy chain (2CTLD-Fc). In cell based assays full length LOX-1 was expressed as membrane anchored protein. As a result from SPR based binding assays it turned out that G2 dendrons carrying 8 sulfate groups were the more effective binders compared to G1 dendrons. Compounds carrying two G2 dendrons and bridged via a PEG spacer (**6b**, **6d**) gave binding affinities in the low nM range (~50 nM) irrespective of the linker length. As a further proof of function competitive binding studies of compound **6d** was demonstrated by inhibition of LOX-1 binding of aged red blood cells and a Gram-negative *E. coli* strain. Finally, compound **6d** significantly reduced binding of the ligand oxLDL. Regarding its prominent role in atherosclerosis, our results might pave the way for a specific ligand design to develop an efficient strategy to block oxLDL uptake via targeting LOX-1.

**Supporting Information**. Detailed synthetic procedure and characterization details, protocol for oxLDL preparation and FITC labeling of *E. coli*, $^{1}$HNMR spectra of synthesized compounds, SDS-PAGE and Western blot image for protein characterization, SPR data, fluorescence and bright field image for inhibition assay of LOX-1 with aRBC binding, fluorescence image and quantification graph for inhibition assay of LOX-1 with *E. coli*, graph for cytotoxicity evaluation.

## ACKNOWLEDGEMENTS

The authors thank the MULTI-APP ITN and Deutsche Forschungsgemeinschaft (SFB 765) for funding of this work and also acknowledge Katharina Goltsche for G1 and G2 dendron synthesis as well as Koichi Yamamoto MD, PhD (The department of geriatric and general medicine Osaka university graduate school of medicine) and Prof. Tatsuya Sawamura (Department of Physiology, Shinshu University School of Medicine) for providing full length LOX-1 plasmid.

## REFERENCES

1. Brown, M. S.; Goldstein, J. L., Receptor-mediated endocytosis: insights from the lipoprotein receptor system. *Proc. Natl. Acad. Sci. U. S. A.* **1979,** *76* (7), 3330-7.
2. Zani, I. A.; Stephen, S. L.; Mughal, N. A.; Russell, D.; Homer-Vanniasinkam, S.; Wheatcroft, S. B.; Ponnambalam, S., Scavenger receptor structure and function in health and disease. *Cells* **2015,** *4* (2), 178-201.
3. Canton, J.; Neculai, D.; Grinstein, S., Scavenger receptors in homeostasis and immunity. *Nat. Rev. Immunol.* **2013,** *13* (9), 621-34.
4. Sawamura, T.; Kume, N.; Aoyama, T.; Moriwaki, H.; Hoshikawa, H.; Aiba, Y.; Tanaka, T.; Miwa, S.; Katsura, Y.; Kita, T.; Masaki, T., An endothelial receptor for oxidized low-density lipoprotein. *Nature* **1997,** *386*, 73.
5. Chen, M.; Kakutani, M.; Naruko, T.; Ueda, M.; Narumiya, S.; Masaki, T.; Sawamura, T., Activation-dependent surface expression of LOX-1 in human platelets. *Biochem. Biophys. Res. Commun.* **2001,** *282* (1), 153-8.
6. Yoshida, H.; Kondratenko, N.; Green, S.; Steinberg, D.; Quehenberger, O., Identification of the lectin-like receptor for oxidized low-density lipoprotein in human macrophages and its potential role as a scavenger receptor. *Biochem. J.* **1998,** *334* (1), 9.
7. Mehta, J. L.; Chen, J.; Hermonat, P. L.; Romeo, F.; Novelli, G., Lectin-like, oxidized low-density lipoprotein receptor-1 (LOX-1): a critical player in the development of atherosclerosis and related disorders. *Cardiovasc. Res.* **2006,** *69* (1), 36-45.
8. Chen, M.; Masaki, T.; Sawamura, T., LOX-1, the receptor for oxidized low-density lipoprotein identified from endothelial cells: implications in endothelial dysfunction and atherosclerosis. *Pharmacol. Ther.* **2002,** *95* (1), 89-100.
9. Lusis, A. J., Atherosclerosis. *Nature* **2000,** *407* (6801), 233-41.
10. Glass, C. K.; Witztum, J. L., Atherosclerosis. *Cell* **2001,** *104* (4), 503-516.
11. Steinbrecher, U. P., Receptors for oxidized low density lipoprotein. *Biochim. Biophys. Acta* **1999,** *1436* (3), 279-98.
12. Brown, M. S.; Goldstein, J. L., Heart attacks: gone with the century? *Science* **1996,** *272* (5262), 629.

13. Organization, W. H., The top 10 causes of death. Jnuary 2017 ed.; 2017.
14. Tabas, I.; García-Cardeña, G.; Owens, G. K., Recent insights into the cellular biology of atherosclerosis. *The Journal of Cell Biology* **2015,** *209* (1), 13.
15. Braunwald, E., Cardiovascular Medicine at the Turn of the Millennium: Triumphs, Concerns, and Opportunities. *N. Engl. J. Med.* **1997,** *337* (19), 1360-1369.
16. Xie, Q.; Matsunaga, S.; Niimi, S.; Ogawa, S.; Tokuyasu, K.; Sakakibara, Y.; Machida, S., Human lectin-like oxidized low-density lipoprotein receptor-1 functions as a dimer in living cells. *DNA Cell Biol.* **2004,** *23* (2), 111-7.
17. Ohki, I.; Ishigaki, T.; Oyama, T.; Matsunaga, S.; Xie, Q.; Ohnishi-Kameyama, M.; Murata, T.; Tsuchiya, D.; Machida, S.; Morikawa, K.; Tate, S., Crystal structure of human lectin-like, oxidized low-density lipoprotein receptor 1 ligand binding domain and its ligand recognition mode to OxLDL. *Structure* **2005,** *13* (6), 905-17.
18. Wang, X.; Khaidakov, M.; Ding, Z.; Mitra, S.; Lu, J.; Dai, Y.; Mehta, J. L., Lectin-like oxidized low-density lipoprotein receptor-1 (LOX-1) and cardiac fibroblast growth. *Hypertension* **2012,** *60* (6), 1437-42.
19. HaJeung Park, F. G. A., and Jeffrey C. Boyington‡, The 1.4 Å Crystal Structure of the Human Oxidized Low Density Lipoprotein Receptor Lox-1*. *THE JOURNAL OF BIOLOGICAL CHEMISTRY* **2005,** *280* (14), 13593-13599.
20. Falconi, M.; Ciccone, S.; D'Arrigo, P.; Viani, F.; Sorge, R.; Novelli, G.; Patrizi, P.; Desideri, A.; Biocca, S., Design of a novel LOX-1 receptor antagonist mimicking the natural substrate. *Biochem. Biophys. Res. Commun.* **2013,** *438* (2), 340-5.
21. Thakkar, S.; Wang, X.; Khaidakov, M.; Dai, Y.; Gokulan, K.; Mehta, J. L.; Varughese, K. I., Structure-based Design Targeted at LOX-1, a Receptor for Oxidized Low-Density Lipoprotein. *Sci. Rep.* **2015,** *5*, 16740.
22. Papp, I.; Dernedde, J.; Enders, S.; Riese, S. B.; Shiao, T. C.; Roy, R.; Haag, R., Multivalent presentation of mannose on hyperbranched polyglycerol and their interaction with concanavalin A lectin. *ChemBioChem* **2011,** *12* (7), 1075-83.
23. Papp, I.; Sieben, C.; Sisson, A. L.; Kostka, J.; Bottcher, C.; Ludwig, K.; Herrmann, A.; Haag, R., Inhibition of influenza virus activity by multivalent glycoarchitectures with matched sizes. *ChemBioChem* **2011,** *12* (6), 887-95.
24. Dernedde, J.; Rausch, A.; Weinhart, M.; Enders, S.; Tauber, R.; Licha, K.; Schirner, M.; Zügel, U.; von Bonin, A.; Haag, R., Dendritic polyglycerol sulfates as multivalent inhibitors of inflammation. *Proc. Natl. Acad. Sci. U. S. A.* **2010,** *107* (46), 19679.
25. Bhatia, S.; Lauster, D.; Bardua, M.; Ludwig, K.; Angioletti-Uberti, S.; Popp, N.; Hoffmann, U.; Paulus, F.; Budt, M.; Stadtmuller, M.; Wolff, T.; Hamann, A.; Bottcher, C.; Herrmann, A.; Haag, R., Linear polysialoside outperforms dendritic analogs for inhibition of influenza virus infection in vitro and in vivo. *Biomaterials* **2017,** *138*, 22-34.
26. Dey, P.; Bergmann, T.; Cuellar-Camacho, J. L.; Ehrmann, S.; Chowdhury, M. S.; Zhang, M.; Dahmani, I.; Haag, R.; Azab, W., Multivalent Flexible Nanogels Exhibit Broad-Spectrum Antiviral Activity by Blocking Virus Entry. *ACS nano* **2018,** *12* (7), 6429-6442.
27. Ziem, B.; Azab, W.; Gholami, M. F.; Rabe, J. P.; Osterrieder, N.; Haag, R., Size-dependent inhibition of herpesvirus cellular entry by polyvalent nanoarchitectures. *Nanoscale* **2017,** *9* (11), 3774-3783.
28. Bhatia, S.; Camacho, L. C.; Haag, R., Pathogen Inhibition by Multivalent Ligand Architectures. *J. Am. Chem. Soc.* **2016,** *138* (28), 8654-66.

29. Chen, M.; Narumiya, S.; Masaki, T.; Sawamura, T., Conserved C-terminal residues within the lectin-like domain of LOX-1 are essential for oxidized low-density-lipoprotein binding. *Biochem. J.* **2001,** *355* (Pt 2), 289-96.
30. Hodgson, S. M.; McNelles, S. A.; Abdullahu, L.; Marozas, I. A.; Anseth, K. S.; Adronov, A., Reproducible Dendronized PEG Hydrogels via SPAAC Cross-Linking. *Biomacromolecules* **2017,** *18* (12), 4054-4059.
31. Lin, C. C.; Anseth, K. S., PEG hydrogels for the controlled release of biomolecules in regenerative medicine. *Pharm. Res.* **2009,** *26* (3), 631-43.
32. Sontjens, S. H.; Nettles, D. L.; Carnahan, M. A.; Setton, L. A.; Grinstaff, M. W., Biodendrimer-based hydrogel scaffolds for cartilage tissue repair. *Biomacromolecules* **2006,** *7* (1), 310-6.
33. Thakkar, S.; Wang, X.; Khaidakov, M.; Dai, Y.; Gokulan, K.; Mehta, J. L.; Varughese, K. I., Structure-based Design Targeted at LOX-1, a Receptor for Oxidized Low-Density Lipoprotein. *Sci Rep* **2015,** *5*, 16740.
34. Oka, K.; Sawamura, T.; Kikuta, K.; Itokawa, S.; Kume, N.; Kita, T.; Masaki, T., Lectin-like oxidized low-density lipoprotein receptor 1 mediates phagocytosis of aged/apoptotic cells in endothelial cells. *Proc. Natl. Acad. Sci. U. S. A.* **1998,** *95* (16), 9535-40.
35. Shimaoka, T.; Kume, N.; Minami, M.; Hayashida, K.; Sawamura, T.; Kita, T.; Yonehara, S., LOX-1 supports adhesion of Gram-positive and Gram-negative bacteria. *J. Immunol.* **2001,** *166* (8), 5108-14.
36. Weingart, C. L.; Broitman-Maduro, G.; Dean, G.; Newman, S.; Peppler, M.; Weiss, A. A., Fluorescent labels influence phagocytosis of Bordetella pertussis by human neutrophils. *Infect Immun.* **1999,** *67* (8), 4264-7.
37. Sawamura, T.; Kume, N.; Aoyama, T.; Moriwaki, H.; Hoshikawa, H.; Aiba, Y.; Tanaka, T.; Miwa, S.; Katsura, Y.; Kita, T.; Masaki, T., An endothelial receptor for oxidized low-density lipoprotein. *Nature* **1997,** *386* (6620), 73-7.
38. Kolb, H. C.; Finn, M. G.; Sharpless, K. B., Click Chemistry: Diverse Chemical Function from a Few Good Reactions. *Angew. Chem. Int. Ed. Engl.* **2001,** *40* (11), 2004-2021.
39. Wyszogrodzka, M., Haag, Rainer, A Convergent Approach to Biocompatible Polyglycerol "Click" Dendrons for the Synthesis of Modular Core–Shell Architectures and Their Transport Behavior. *Chem. - Eur. J.* **2008,** *14*, 9202-9214.
40. Dey, P.; Hemmati-Sadeghi, S.; Haag, R., Hydrolytically degradable, dendritic polyglycerol sulfate based injectable hydrogels using strain promoted azide–alkyne cycloaddition reaction. *Polym. Chem.* **2016,** *7* (2), 375-383.
41. Matsunaga, S.; Xie, Q.; Kumano, M.; Niimi, S.; Sekizawa, K.; Sakakibara, Y.; Komba, S.; Machida, S., Lectin-like oxidized low-density lipoprotein receptor (LOX-1) functions as an oligomer and oligomerization is dependent on receptor density. *Exp. Cell. Res.* **2007,** *313* (6), 1203-14.
42. Cao, W.; Calabro, V.; Root, A.; Yan, G.; Lam, K.; Olland, S.; Sanford, J.; Robak, A.; Zollner, R.; Lu, Z. J.; Ait-Zahra, M.; Agostinelli, R.; Tchistiakova, L.; Gill, D.; Harnish, D.; Paulsen, J.; Shih, H. H., Oligomerization is required for the activity of recombinant soluble LOX-1. *FEBS J.* **2009,** *276* (17), 4909-4920.
43. Park, H.; Adsit, F. G.; Boyington, J. C., The 1.4 Å Crystal Structure of the Human Oxidized Low Density Lipoprotein Receptor Lox-1. *J. Biol. Chem.* **2005,** *280* (14), 13593-13599.

44. Weinhart, M.; Groger, D.; Enders, S.; Dernedde, J.; Haag, R., Synthesis of dendritic polyglycerol anions and their efficiency toward L-selectin inhibition. *Biomacromolecules* **2011,** *12* (7), 2502-11.
45. Weinhart, M.; Groger, D.; Enders, S.; Riese, S. B.; Dernedde, J.; Kainthan, R. K.; Brooks, D. E.; Haag, R., The role of dimension in multivalent binding events: structure-activity relationship of dendritic polyglycerol sulfate binding to L-selectin in correlation with size and surface charge density. *Macromol. Biosci.* **2011,** *11* (8), 1088-98.
46. Fasting, C.; Schalley, C. A.; Weber, M.; Seitz, O.; Hecht, S.; Koksch, B.; Dernedde, J.; Graf, C.; Knapp, E.-W.; Haag, R., Multivalency as a Chemical Organization and Action Principle. *Angewandte Chemie International Edition* **2012,** *51* (42), 10472-10498.
47. Krishnamurthy, V. M.; Estroff, L. A.; Whitesides, G. M., Multivalency in Ligand Design. *Fragment-based Approaches in Drug Discovery* **2006**.
48. Yoshimoto, R.; Fujita, Y.; Kakino, A.; Iwamoto, S.; Takaya, T.; Sawamura, T., The discovery of LOX-1, its ligands and clinical significance. *Cardiovasc. Drugs Ther.* **2011,** *25* (5), 379-91.
49. Savill, J.; Fadok, V.; Henson, P.; Haslett, C., Phagocyte recognition of cells undergoing apoptosis. *Immunol. Today* **1993,** *14* (3), 131-6.

**Table of Contents (TOC)**

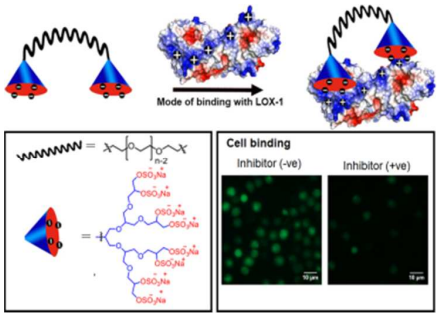

# Supplementary Information

# Design and Synthesis of PEG-Oligoglycerol Sulfates as Multivalent Inhibitors for the Scavenger Receptor LOX-1

*Shalini Kumari,*[a] *Katharina Achazi,*[a] *Pradip Dey,*[a] *Rainer Haag,*[a] *Jens Dernedde*[b*]

[a] Institute for Chemistry and Biochemistry, Freie Universität Berlin, Takustr. 3, 14195 Berlin, Germany.

[b] Charité-Universitätsmedizin Berlin, Institute of Laboratory Medicine, Clinical Chemistry and Pathobiochemistry, CVK Augustenburger Platz 1, 13353 Berlin, Germany

**List of content:**

**10. Compound toxicity**

## 1. Synthesis and characterization

### 1.1 Materials

All the reagents and solvents were purchased commercially and used without further purification. PEG of 6 kDa and 10 kDa were purchased from Roth chemicals. Oligoglycerol dendrons of generation 1 and 2 (G1 and G2) were synthesized according to a previously reported procedure[1]. $SO_3$-pyridine complex was used as received from Fluka GmbH. NMR Spectra were recorded on JEOL ECX400, JEOL ECP500, BRUKER AV500 and Bruker AV700 spectrometers at 500 and 700 MHz for $^1$H NMR spectra and 100 MHz, 125 MHz and 175 MHz for $^{13}$C NMR spectra. Chemical shifts are reported in parts per million (ppm) in relation to deuterated solvent peak calibration. IR spectra were recorded with a Nicolet AVATAR 320 FT-IR 5 SXC (Thermo Fischer Scientific, Waltham, MA, USA) with a DTGS detector from 4000 to 650 $cm^{-1}$ by dropping a solution of the compound and letting it dry for few seconds.

**i) Synthesis of polyethyleneglycol-dimesylate (Compounds 1a, 1b)**

PEG 6 kDa (5 g, 0.83 mmol, 1eq.) was dried overnight in high vacuum (HV) at 60 $^oC$ to remove traces of moisture. After cooling to room temperature the PEG was dissolved in 100 mL of anhydrous dichloromethane under argon atmosphere. Dry triethylamine (0.346 mL, 2.49 mmol, 3 eq.) was added with stirring and the mixture was cooled in an ice bath, followed by the dropwise addition of mesyl chloride (0.192 mL, 2.49 mmol, 3 eq.). After stirring the reaction mixture for overnight at room temperature under argon it was added to a separating funnel containing dichloromethane (300 mL) and brine (50 mL). The organic layer was washed

twice with brine (2 x 50 mL), combined, dried over $MgSO_4$ and concentrated in vacuum. The residue was precipitated in diethyl ether (250 mL) and stirred vigorously for 2 hours, filtered and washed again with diethyl ether to remove traces of triethylamine and methylsulfonyl chloride. Drying in high pressure yielded the desired product as nearly colourless solid.

Polyethyleneglycol-dimesylate with molecular weight of 10 kDa was prepared analogously starting from PEG 10 kDa (5.10 g, 0.51 mmol, 1eq) whereas the equivalents of trimethylamine (0.42 mL, 3.06 mmol, 6 eq.) and methylsulfonyl chloride (0.23 mL, 3.06 mmol, 6eq) were increased due to higher sterical hindrance of the PEG chains.

**Compound 1a**

(4.11 g, yield: 80 %).

$^1$HNMR (500 MHz; DMSO-d6): ∂ 4.31-4.30 (m, 4 H, $SO_2O\underline{CH_2}CH_2O$), 3.63–3.33 (m, 590 H, PEG-backbone), 3.18 (s, 6H, $\underline{CH_3}SO_2$) ppm.

**Compound 1b**

(3.83 g, yield: 74 %).

$^1$HNMR (500 MHz; DMSO-d6): ∂ 4.31-4.30 (m, 4 H, $SO_2O\underline{CH_2}CH_2O$), 3.68–3.35 (m, 995 H, PEG-backbone), 3.18 (s, 6H, $\underline{CH_3}SO_2$) ppm.

**ii) Synthesis of polyethyleneglycol-diazide (Compounds 2a, 2b)**

Compound **1a** (3 g, 0.48 mmol, 1 eq.) was dissolved in 30 mL of DMF, sodium azide (93 mg, 1.44 mmol, 3 eq.) was added and the mixture was stirred overnight at 60 °C. After removal of solvent the residue was dissolved in a mixture of dichloromethane (600 mL) and was washed twice with water (2 x 40 mL), and dried over anhydrous $MgSO_4$. After evaporation of solvent, the residue was dissolved in water and was dialyzed against deionised water (MWCO: 2 kDa). Freeze-drying yielded the product as nearly colourless solid.

Polyethyleneglycol-diazide with molecular weights of 10 kDa were prepared analogously

starting with Compound **1b** (3 g, 0.29 mmol, 1 eq.) whereas the equivalents of sodium azide (94 mg, 1.45 mmol, 5eq.) were increased due to similar reason as stated above.

**Compound 2a**

(2.17 g, yield: 74 %).

$^1$HNMR (500 MHz; DMSO-d6): ∂ 3.68–3.38 (m, 578 H, PEG-backbone), 3.29-3.27 (t, 4H, $OCH_2\underline{CH_2}N_3$) ppm.

**Compound 2b**

(2.22 g, yield: 76 %).

$^1$HNMR (500 MHz; DMSO-d6): ∂ 3.65–3.39 (m, 902 H, PEG-backbone), 3.37-3.35 (t, 4H, $OCH_2\underline{CH_2}N_3$) ppm.

### iii) Synthesis of propargyl ethers of oligoglycerol dendron (Compounds 3a, 3b)

To a solution of protected generation one of oligoglycerol dendron [G1] (5 g, 15.60 mmol, 1 eq.) in THF, sodium hydride (1.12 g, 46.80 mmol, 3 eq.) was added and stirred at 50 °C for 1h. To the above reaction mixture propargyl bromide (4.43 mL, 46.80 mmol, 3 eq.) was added slowly and stirred at room temperature overnight. The progress of the reaction was followed by TLC, after the completion of reaction excess of NaH was quenched by the drop wise addition of water while keeping the reaction flask in an ice bath. The reaction mixture was concentrated under reduced pressure and diluted with water. The compound was extracted with DCM and the organic layer was combined and dried over anhydrous $MgSO_4$. The reaction mixture was concentrated and purified by column chromatography to obtain a pale yellow liquid.

Similar procedure was opted for the synthesis of Compound **3b**, starting with protected generation two of oligoglycerol dendron [G2] (5 g, 7.17 mmol, 1 eq.).

**Compound 3a**

(3.91 g, yield: 70 %)

$^1$HNMR (500 MHz; $CDCl_3$): δ 4.33-4.14 (m, 4H, -CH$\underline{CH_2}$OC$(CH_3)_2$), 4.06-3.97 (m, 2H, -$\underline{CH}CH_2OC(CH_3)_2$), 3.83-3.45 (m, 11H, dendron), 2.96-2.90 (m, 1H, $\underline{CH}CCH_2$-), 1.32 (s, 6H, -C$\underline{CH3}$), 1.27 (s, 6H, -C$\underline{CH_3}$).

MS (ESI) m/z = calculated for $[C_{18}H_{30}O_7Na]^+$: 381.1884; found: 381.2093.

**Compound 3b**

(3.79 g, yield: 72 %)

$^1$HNMR (500 MHz; $CDCl_3$): δ 4.32-4.22 (m, 6H, -CH$\underline{CH_2}$OC$(CH_3)_2$), 4.05-4.02 (m, 4H, -$\underline{CH}CH_2OC(CH_3)_2$), 3.73-3.46 (m, 27H, dendron), 2.42-2.41 (m, 1H, $\underline{CH}CCH_2$-), 1.40 (s, 12H, -C$\underline{CH_3}$), 1.34 (s, 12H, -C$\underline{CH_3}$).

MS (ESI) m/z = calculated for $[C_{36}H_{62}O_{15}Na]^+$: 757.3981; found: 757.3964.

### iv) Protocol for click reactions (Compounds 4a, 4b, 4c, 4d, 4e, 4f)

To a mixture of the PEG-bisazide (1 eq.) and propargylated dendron (3 eq.) in DMF, copper sulfate solution (0.5 eq., aq. 0.1M) and sodium ascorbate (2 eq., 0.2M) were added. The reaction mixture was stirred at room temperature overnight. After complete consumption of azide, checked by IR spectroscopy, stirring was stopped and solvent was removed under reduced pressure and diluted with water. Organic compound was extracted from the aqueous phase using DCM. The combined organic phase was washed with satd. EDTA solution and water and dried over anhydrous $Na_2SO4$. After evaporation of solvent, the residue was dissolved in water/methanol and was dialyzed against water/methanol (50:50 v/v) followed by water (MWCO: 2 kDa). Freeze-drying yielded the product as nearly colourless solid.

**Compound 4a**

(0.84 g, yield: 77 %)

$^1$HNMR (500 MHz; $CDCl_3$): δ 7.77 (m, 2H, triazole), 4.78-4.63 (m, 4H, -$\underline{CH}CH_2OC(CH_3)_2$), 4.54-4.51 (m, 4H, O$\underline{CH_2}$-triazole), 4.23-4.20 (m, 4H, $OCH_2\underline{CH_2}$-triazole), 4.02-4.01 (m, 4H,

O$\underline{CH_2}CH_2$-triazole), 3.86-3.85 (m, 4H, -CH$\underline{CH_2}OC(CH_3)_2$), 3.72-3.54 (m, 915H, PEG-backbone & dendron), 1.39-1.37 (s, 12H, -C$\underline{CH_3}$), 1.33-1.31 (s, 12H, -C$\underline{CH_3}$).

**Compound 4b**

(0.96 g, yield: 78 %)

$^1$HNMR (500 MHz; $CDCl_3$): δ 7.71 (m, 2H, triazole), 4.76-4.49 (m, 12H, -$\underline{CH}CH_2OC(CH_3)_2$ and O$\underline{CH_2}$-triazole), 4.23-4.20 (m, 8H, $OCH_2\underline{CH_2}$-triazole), 4.02-3.85 (m, 16H, -CH$\underline{CH_2}OC(CH_3)_2$ and O$\underline{CH_2}CH_2$-triazole), 3.70-3.50 (m, 1168H, PEG-backbone & dendron), 1.38 (s, 24H, -C$\underline{CH_3}$), 1.32 (s, 24H, -C$\underline{CH_3}$).

**Compound 4c**

(0.80 g, yield: 75 %)

$^1$HNMR (500 MHz; DMSO-d6): δ 8.03 (m, 2H, triazole), 4.65-4.63 (m, 4H, -$\underline{CH}CH_2OC(CH_3)_2$), 4.52-4.49 (m, 4H, O$\underline{CH_2}$-triazole), 4.17-4.11 (m, 4H, $OCH_2\underline{CH_2}$-triazole), 3.99-3.94 (m, 4H, O$\underline{CH_2}CH_2$-triazole), 3.82-3.80 (t, 4H, -CH$\underline{CH_2}OC(CH_3)_2$), 3.55-3.45 (m, 1680H, PEG-backbone & dendron), 1.31 (s, 12H, -C$\underline{CH_3}$), 1.26 (s, 12H, -C$\underline{CH_3}$).

**Compound 4d**

(0.88 g, yield: 78 %)

$^1$HNMR (500 MHz; $D_2O$): δ 8.14 (s, 2H, triazole), 5.75-5.73 (m, 4H, -$\underline{CH}CH_2OC(CH_3)_2$), 5.58-5.56 (m, 4H, O$\underline{CH_2}$-triazole), 5.26-5.22 (m, 4H, $OCH_2\underline{CH_2}$-triazole), 4.68-4.66 (m, 16H, -CH$\underline{CH_2}OC(CH_3)_2$), 4.16-4.13 (m, 4H, O$\underline{CH_2}CH_2$-triazole), (4.00-3.57 (m, 2199H, PEG-backbone & dendron), 1.46 (s, 24H, -C$\underline{CH_3}$), 1.40 (s, 24H, -C$\underline{CH_3}$).

**Compound 4e**

(0.36 g, yield: 70 %)

$^1$HNMR (500 MHz; $CDCl_3$): δ 8.07 (s, 1H, triazole), 4.81-4.75 (m, 2H, -$\underline{CH}CH_2OC(CH_3)_2$), 4.62-4.57 (m, 2H, O$\underline{CH_2}$-triazole), 4.52-4.50 (m, 4H, $OCH_2\underline{CH_2}$-triazole), 4.23-3.40 (m, 1782H, PEG-backbone & dendron), 1.37 (s, 6H, -C$\underline{CH_3}$), 1.32 (s, 6H, -C$\underline{CH_3}$).

**Compound 4f**

(0.38 g, yield:71 %)

$^1$HNMR (500 MHz; $D_2O$): δ 8.15 (s, 1H, triazole), 4.43-4.35 (m, 8H, -CHCH$_2$OC(CH$_3$)$_2$, OCH$_2$-triazole and OCH$_2$CH$_2$-triazole), 3.90-3.43 (m, 1891H, PEG-backbone & dendron), 1.49 (s, 12H, -CCH$_3$), 1.43 (s, 12H, -CCH$_3$).

**v) Deprotection of protected dendrons (Compounds 5a, 5b, 5c, 5d, 5e, 5f)**

PEG conjugated with protected dendron was dissolved in 1% aq. TFA (10 ml) and stirred at room temperature overnight. Deprotection reaction was monitored using NMR by analysing the disappearance of acetal protons. After complete deprotection the solvent was removed and the compound was dissolved in water and dialyzed against water (MWCO: 2 kDa). Freeze-drying yielded a nearly colourless solid product.

**Compound 5a**

(0.40 g, yield: 82 %)

$^1$HNMR (500 MHz; $D_2O$): δ 8.14 (s, 2H, triazole), 4.84 (s, 4H, -CHCH$_2$OH), 4.69-4.67 (m, 4H, OCH$_2$-triazole), 4.03-4.01 (m, 4H, OCH$_2$CH$_2$-triazole) 3.89-3.64 (m, 1255H, PEG-backbone & dendron).

**Compound 5b**

(0.38 g, yield: 80 %)

$^1$HNMR (500 MHz; $D_2O$): δ 8.14 (s, 2H, triazole), 4.84-4.83 (m, 8H, -CHCH$_2$OH), 4.69-4.67 (m, 4H, OCH$_2$-triazole), 4.02-4.00 (m, 4H, OCH$_2$CH$_2$-triazole 3.92-3.47 (m, 778H, PEG-backbone & dendron).

**Compound 5c**

(0.39 g, yield: 81 %)

$^1$HNMR (500 MHz; $D_2O$): δ 8.13 (s, 2H, triazole), 4.85-4.84 (m, 4H, -CHCH$_2$OH), 4.69-

4.67(m, 4H, O$\underline{CH_2}$-triazole), 4.31-4.27 (m, 4H, OCH$_2\underline{CH_2}$-triazole), 4.23-3.63 (m, 1166H, PEG-backbone & dendron)

**Compound 5d**

(0.37 g, yield: 77 %)

$^1$HNMR (500 MHz; $CD_3OD$): δ 8.13 (s, 2H, triazole), 4.65-4.58 (m, 12H, -$\underline{CH}CH_2OH$, O$\underline{CH_2}$-triazole), 3.96 (s, 4H, OCH$_2\underline{CH_2}$-triazole), 3.82-3.36 (m, 1764H, PEG-backbone & dendron).

**Compound 5e**

(0.17 g, yield: 71 %)

$^1$HNMR (500 MHz; $D_2O$): δ 8.10 (s, 1H, triazole), 5.15-5.13 (t, 2H, -$\underline{CH}CH_2OH$), 4.64-4.24(m, 4H, O$\underline{CH_2}$-triazole, OCH$_2\underline{CH_2}$-triazole), 3.97-3.36 (m, 1120H, PEG-backbone & dendron)

**Compound 5f**

(0.18 g, yield: 74 %)

$^1$HNMR (500 MHz; $D_2O$): δ 8.16 (s, 1H, triazole), 5.51 (s, 4H, -$\underline{CH}CH_2OH$), 4.79-4.69 (t, 2H, O$\underline{CH_2}$-triazole), 4.04-4.02 (t, 2H, OCH$_2\underline{CH_2}$-triazole), 3.80-3.40 (m, 1505H, PEG-backbone & dendron)

### vi) Sulfation of deprotected molecules (Compounds 6a, 6b, 6c, 6d, 6e, 6f)

After drying the molecules for 18 h under high vacuum at 60 °C, they were dissolved in dry DMF under inert conditions. The polymer solution was heated to 60 °C and sulfur trioxide pyridine complex (5 eq. per OH) dissolved in a minimum amount of dry DMF, added dropwise. The reaction mixture was stirred for 18 h at 60 °C and further for 48 h at room temperature and the reaction was quenched by adding 10 ml deionized water. To the aqueous solution 1 M NaOH was added immediately until a pH of 11 was reached. Solvent was removed under vacuum and was further purified by dialysis in saturated aqueous NaCl solution and water. Results achieved from elemental analysis:

**Compound 6a**

(0.19 g, yield: 70 %)

$^1$HNMR (500 MHz; $D_2O$): δ 8.18 (s, 2H, triazole), 4.75-4.74 (m, 4H, -CHCH$_2$OSO$_3^-$Na$^+$), 4.68-4.67 (m, 4H, OCH$_2$-triazole), 4.29-4.20 (m, 4H, OCH$_2$CH$_2$-triazole) 4.02-3.63 (m, 563H, PEG-backbone & dendron).

**Compound 6b**

(0.22 g, yield: 73 %)

$^1$HNMR (500 MHz; $D_2O$): δ 8.16 (s, 2H, triazole), 5.19-5.00 (m, 4H, -CHCH$_2$OSO$_3^-$Na$^+$), 4.70-4.66 (m, 8H, OCH$_2$-triazole, -CHCH$_2$OSO$_3^-$Na$^+$), 4.32-4.28 (m, 4H, OCH$_2$CH$_2$-triazole) 4.24-3.57 (m, 704H, PEG-backbone & dendron).

**Compound 6c**

(0.18 g, yield: 70 %)

$^1$HNMR (500 MHz; $CDCl_3$): δ 8.19 (s, 2H, triazole), 4.69-4.68 (m, 4H, -CHCH$_2$OSO$_3^-$Na$^+$), 4.30-4.27(m, 4H, OCH$_2$-triazole), 4.25-4.21 (m, 4H, OCH$_2$CH$_2$-triazole), 4.03-3.62 (m, 1049H, PEG-backbone & dendron)

**Compound 6d**

(0.20 g, yield: 71 %)

$^1$HNMR (500 MHz; $D_2O$): δ 8.18 (s, 2H, triazole), 4.75-4.69 (m, 8H, -CHCH$_2$OSO$_3^-$Na$^+$), 4.33-4.30 (m, 4H, OCH$_2$-triazole), 4.26-4.23(m, 4H, OCH$_2$CH$_2$-triazole), 3.98-3.54 (m, 1114H, PEG-backbone & dendron).

**Compound 6e**

(90 mg, yield: 62 %)

$^1$HNMR (500 MHz; $D_2O$): δ 8.19 (s, 1H, triazole), 4.76-4.68 (m, 2H, -CHCH$_2$OSO$_3^-$Na$^+$), 4.29-4.21(m, 4H, OCH$_2$-triazole, OCH$_2$CH$_2$-triazole), 3.87-3.62 (m, 1431H, PEG-backbone & dendron)

**Compound 6f**

(0.10 g, yield: 66 %)

$^{1}$HNMR (500 MHz; $D_2O$): δ 8.14 (s, 1H, triazole), 4.30-4.14 (m, 8H, -$\underline{CH}CH_2OSO_3^-Na^+$, O$\underline{CH_2}$-triazole, $OCH_2\underline{CH_2}$-triazole), 3.90-3.37 (m, 1072H, PEG-backbone & dendron)

**2. Protocol for LDL particle isolation and oxidation.**

Native LDL was isolated according to previously reported protocol.[2] Briefly, native LDL was isolated from human blood plasma by sequential ultracentrifugation (1.006 to 1.34 g/mL). Native LDL was oxidised by using $CuSO_4$(5 μmol/L) in PBS at 37 $^{o}$C for 24 hours. The oxLDL was purified by dialysis against PBS at 4 $^{o}$C for 48 hours.

**3. Protocol for FITC labeling of *E. coli***

FITC labeling of *E. coli* was done as described in previously reported protocol. [3] *E. coli* bacteria were cultured in a volume of 5 mL and harvested by centrifugation at 10000 rpm speed for 10 min at 4 $^{o}$C. 10 mg of FITC (Sigma) was freshly dissolved in DMSO (1 mL). The bacterial pellet was re-suspended in 0.1 M sodium bicarbonate buffer at pH 9.0 and diluted to $10^{10}$ cells/mL in a total of 1 mL of sodium bicarbonate buffer. To this bacterial suspension 0.2 μL of FITC stock solution was added and resuspended. The cells were incubated in the dark with shaking for 30 min at room temperature. The cells were washed 3 times with PBS to remove unbound dye and resuspended to a concentration of $10^7$ cells/mL.

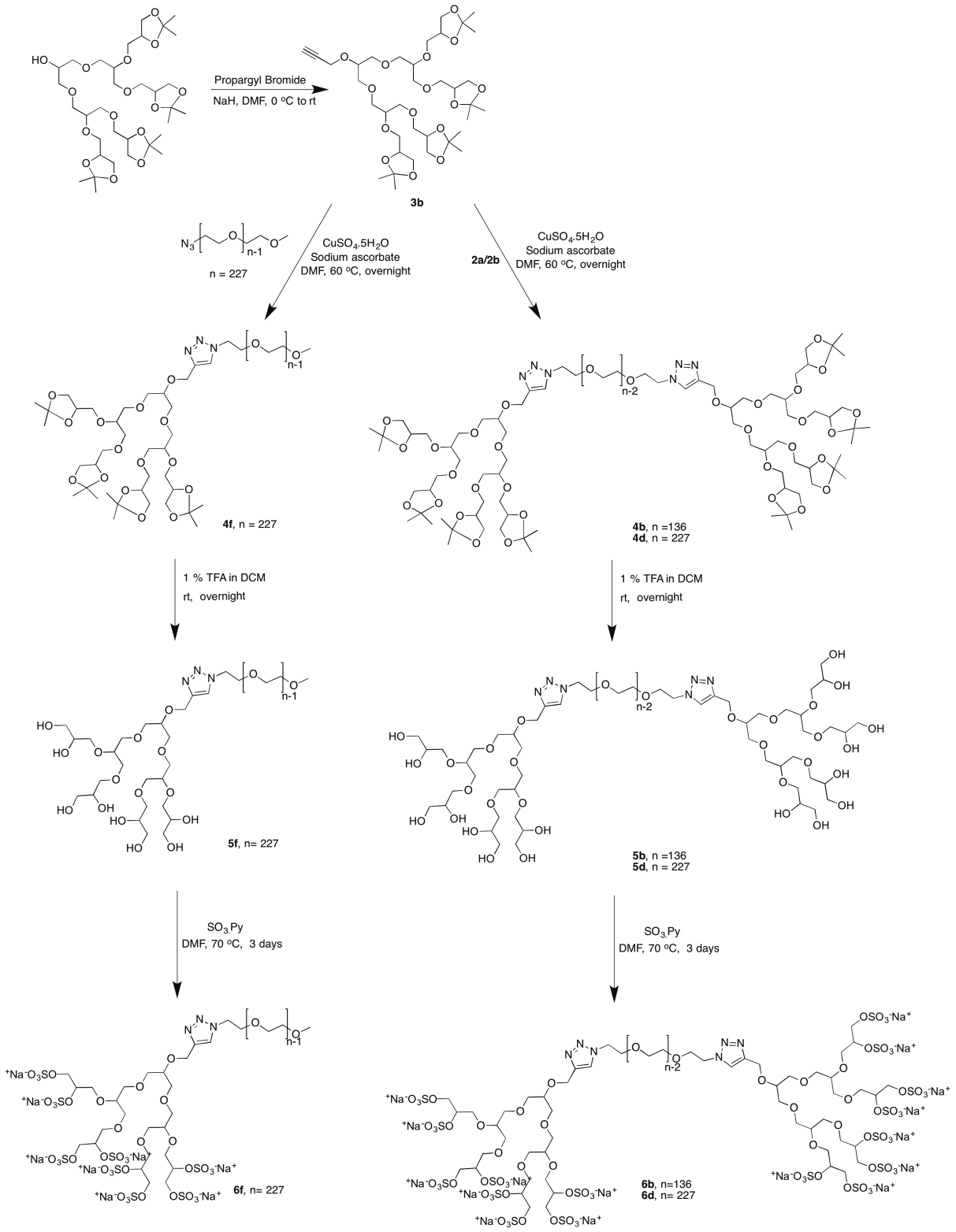
Propargyl Bromide
NaH, DMF, 0 °C to rt
3b
n = 227
CuSO4.5H2O
Sodium ascorbate
DMF, 60 °C, overnight
2a/2b
CuSO4.5H2O
Sodium ascorbate
DMF, 60 °C, overnight
4f, n = 227
4b, n =136
4d, n = 227
1 % TFA in DCM
rt, overnight
1 % TFA in DCM
rt, overnight
5f, n= 227
5b, n =136
5d, n = 227
SO3.Py
DMF, 70 °C, 3 days
SO3.Py
DMF, 70 °C, 3 days
6f, n= 227
6b, n=136
6d, n= 227

4. **Scheme S1.** Schematic representation for the synthesis of AB and ABA type sulfated dendronized PEG polymers. The synthesis is shown for generation 2 oligoglycerol dendrons.

## 5. Spectra:

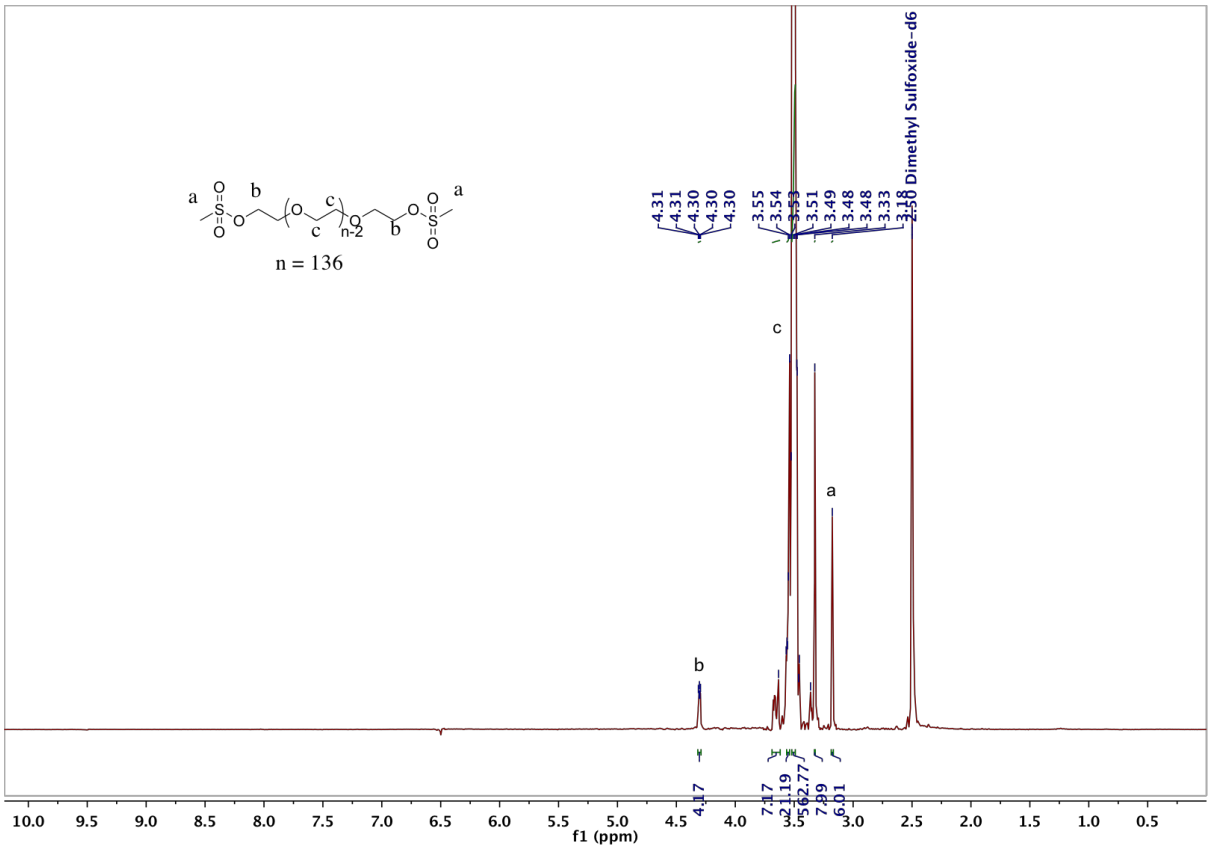


**Figure S1.** 1H NMR of compound **1a**

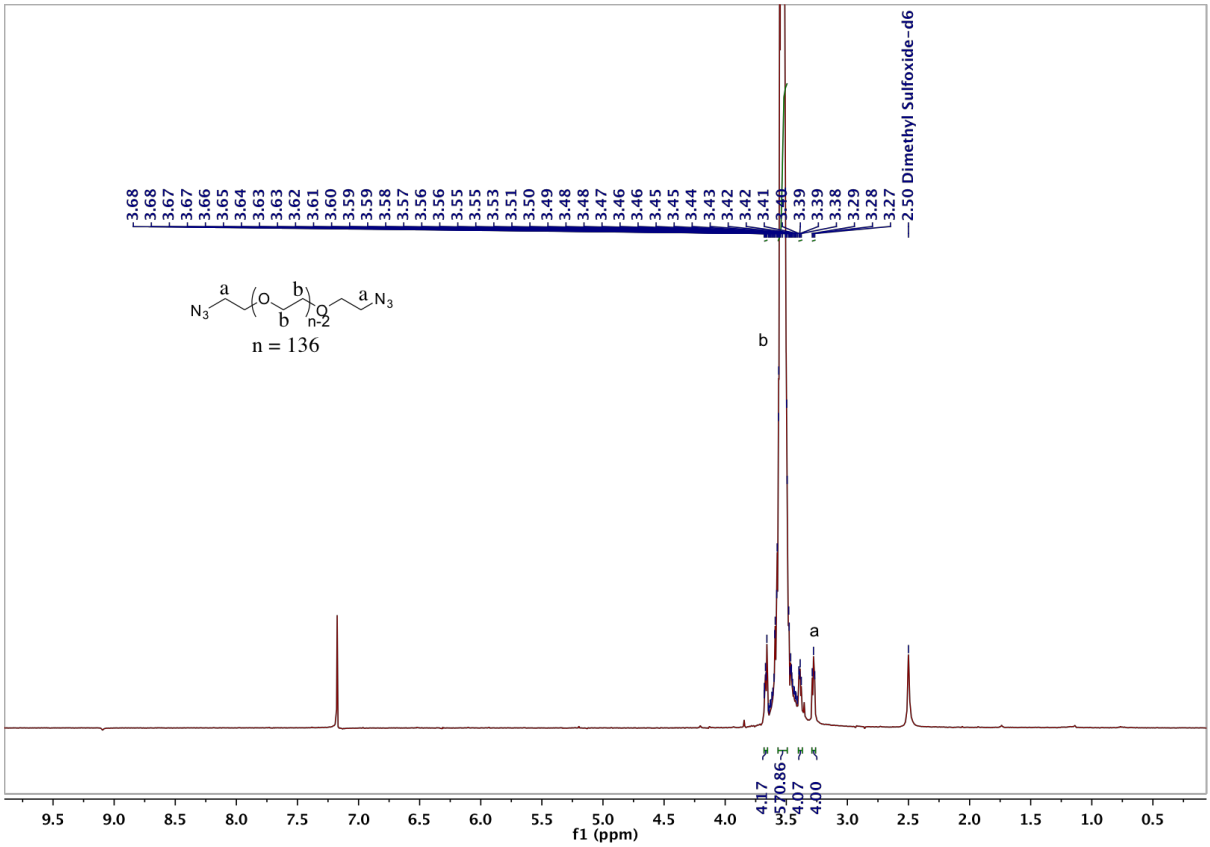


**Figure S2.** 1H NMR of compound **1b**

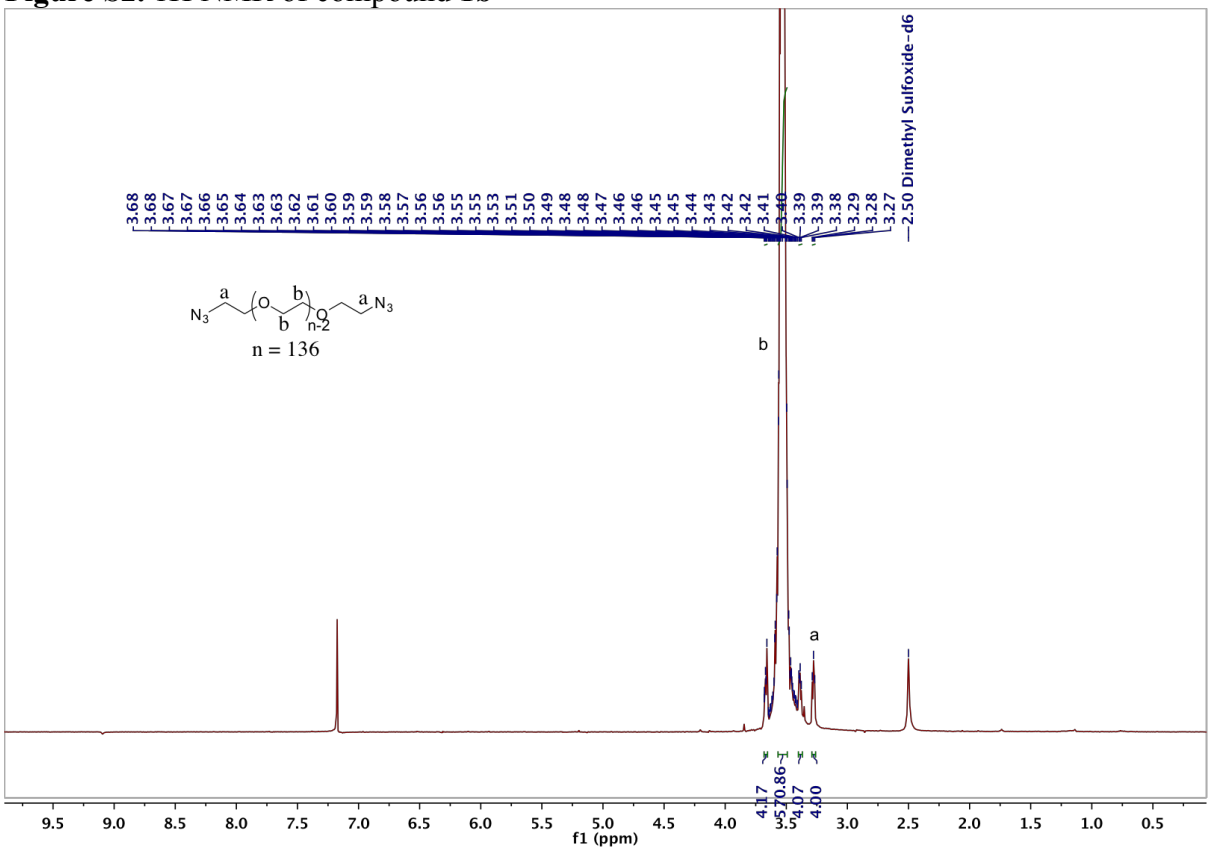


**Figure S3.** 1H NMR of compound **2a**

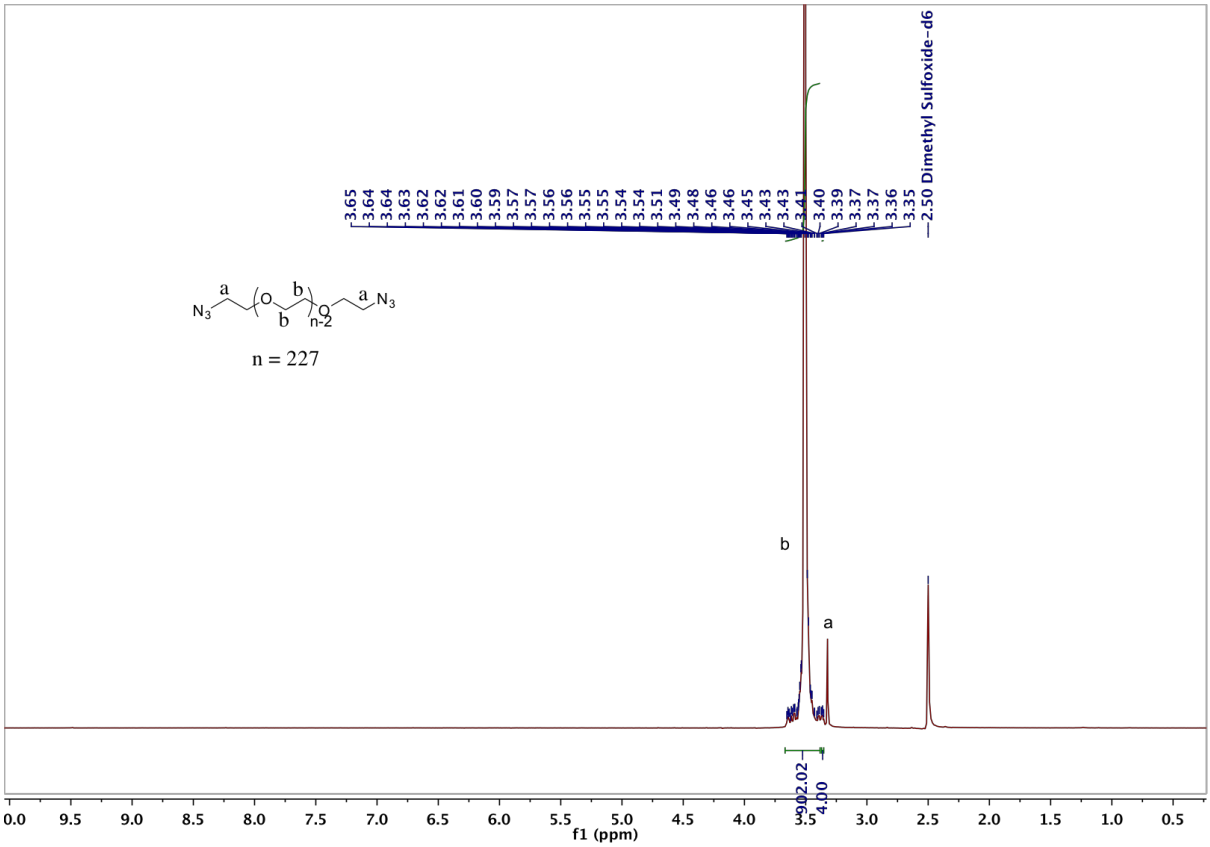


**Figure S4.** 1H NMR of compound **2b**

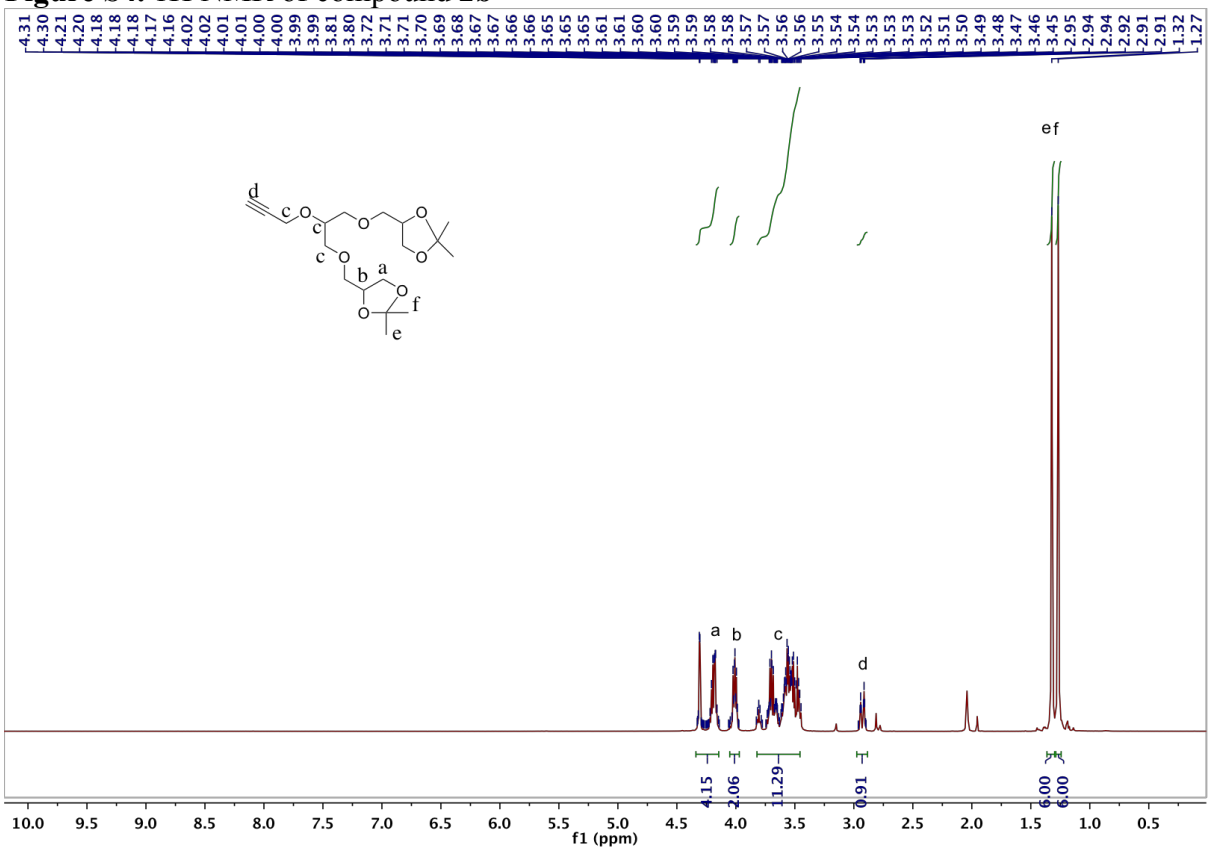


**Figure S5.** 1H NMR of compound **3a**

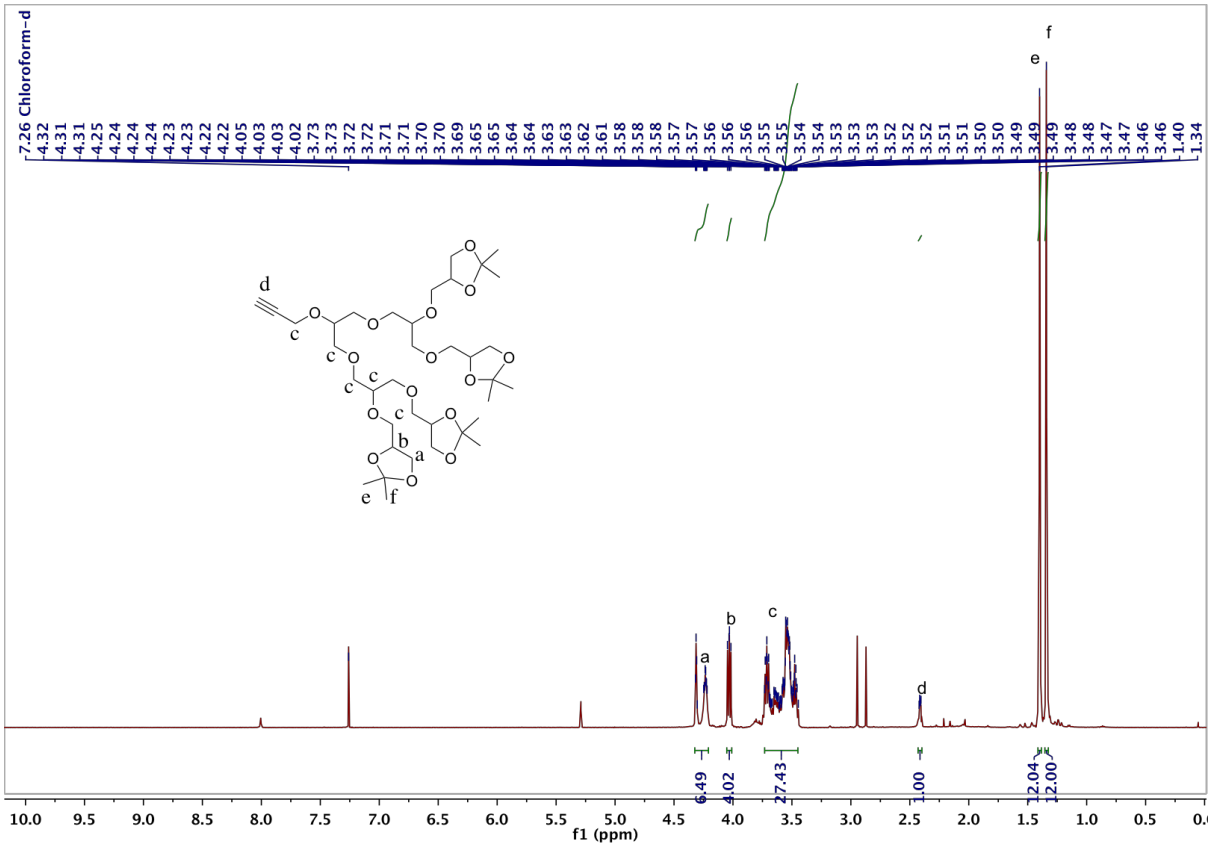


**Figure S6.** 1H NMR of compound **3b**

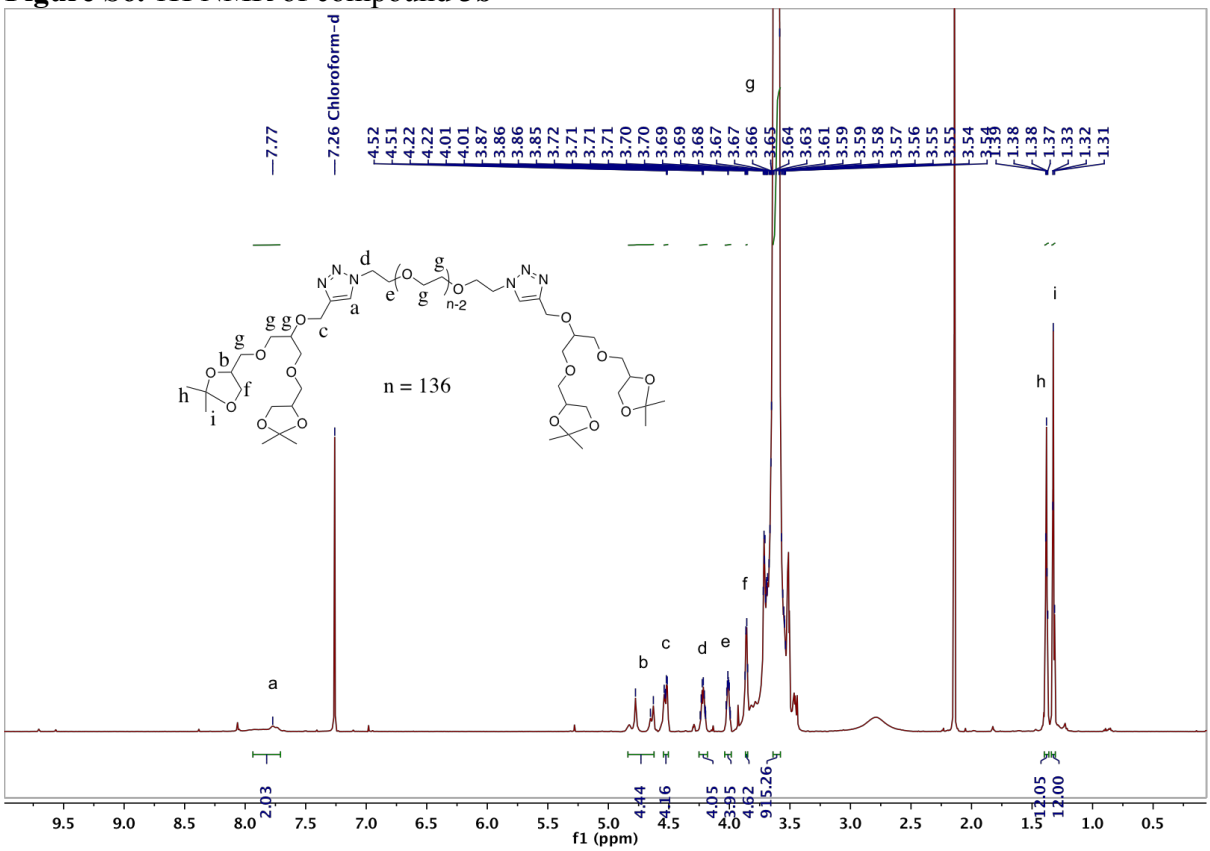


**Figure S7.** 1H NMR of compound **4a**

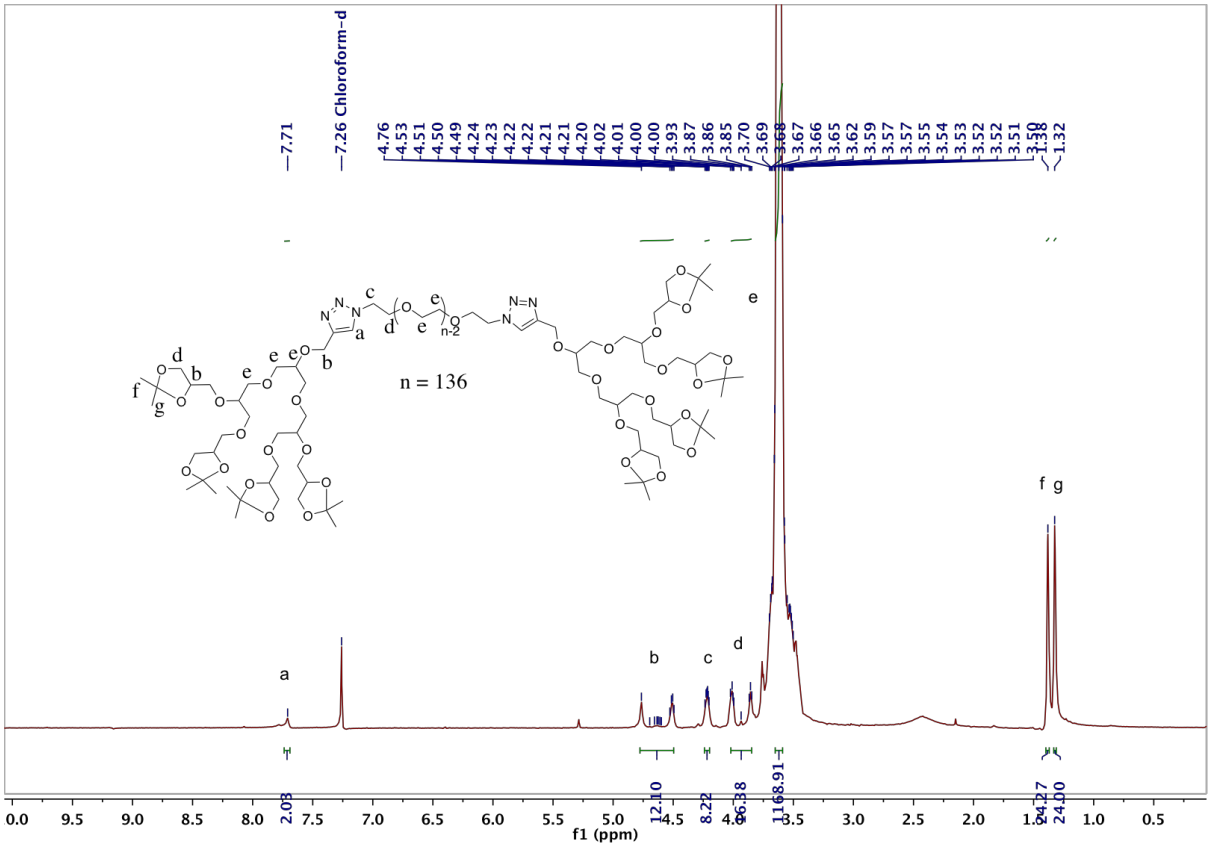


**Figure S8.** 1H NMR of compound **4b**

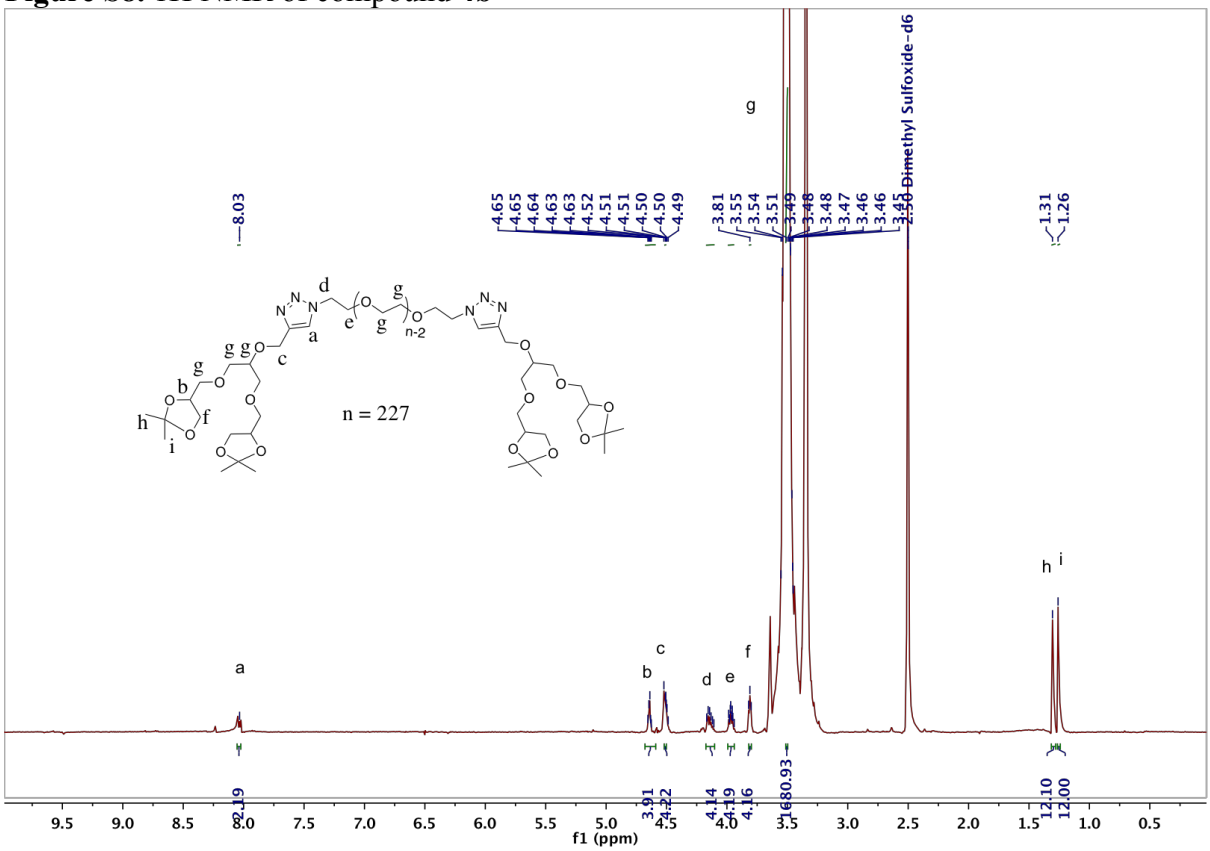


**Figure S9.** 1H NMR of compound **4c**

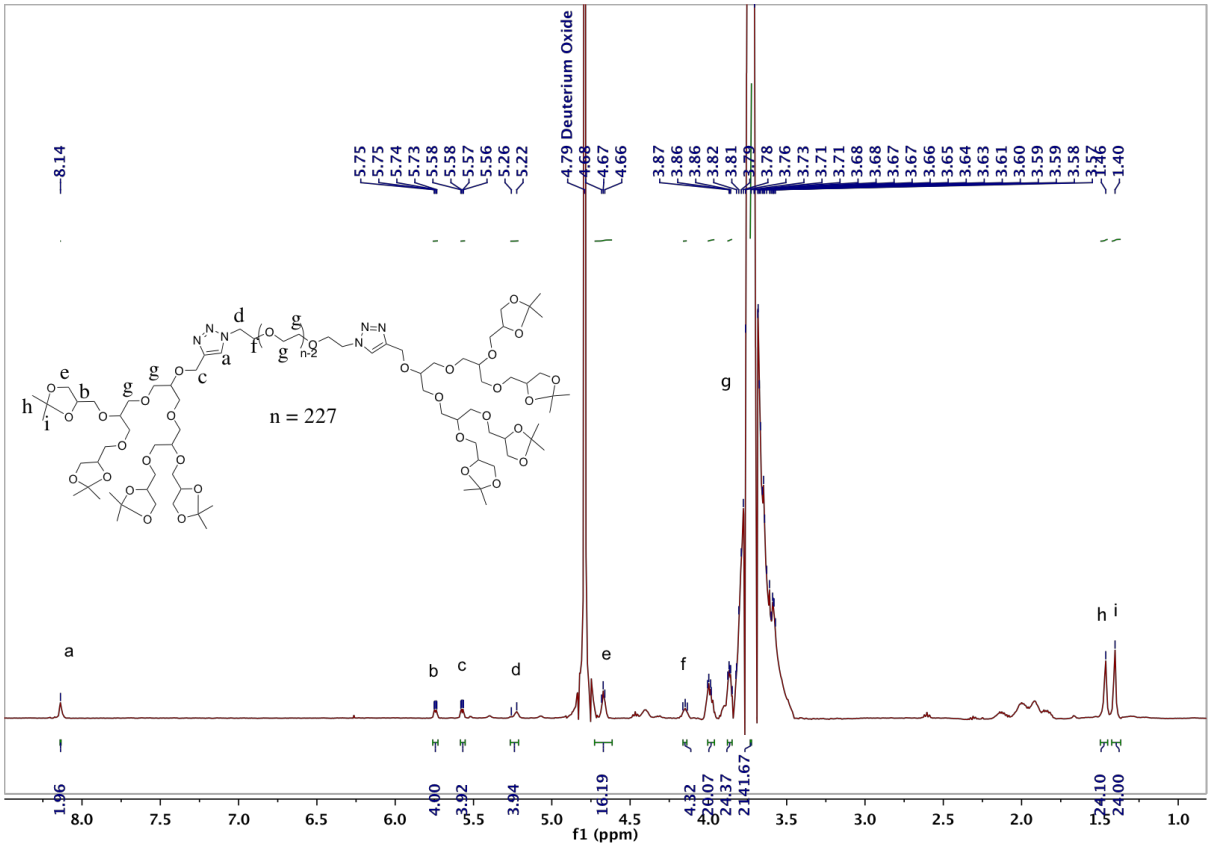


**Figure S10.** 1H NMR of compound **4d**

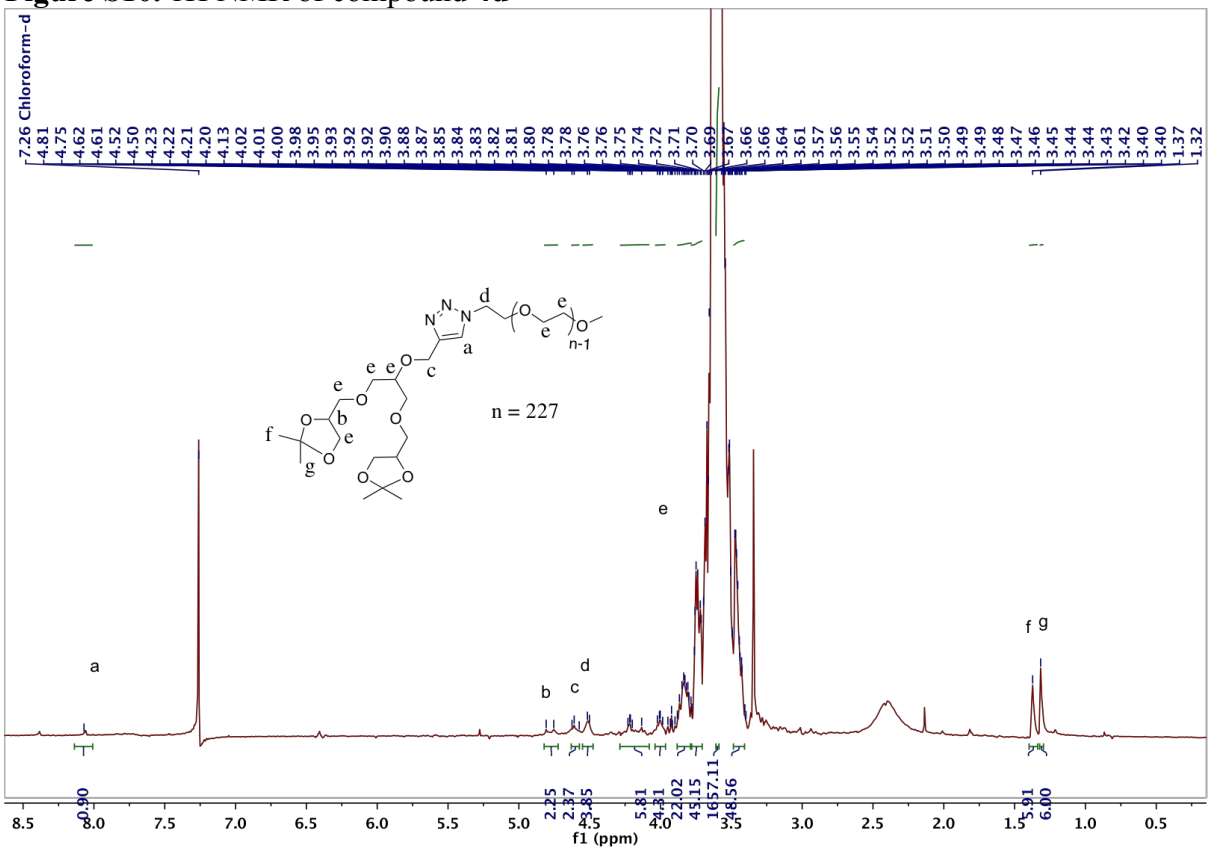


**Figure S11.** 1H NMR of compound **4e**

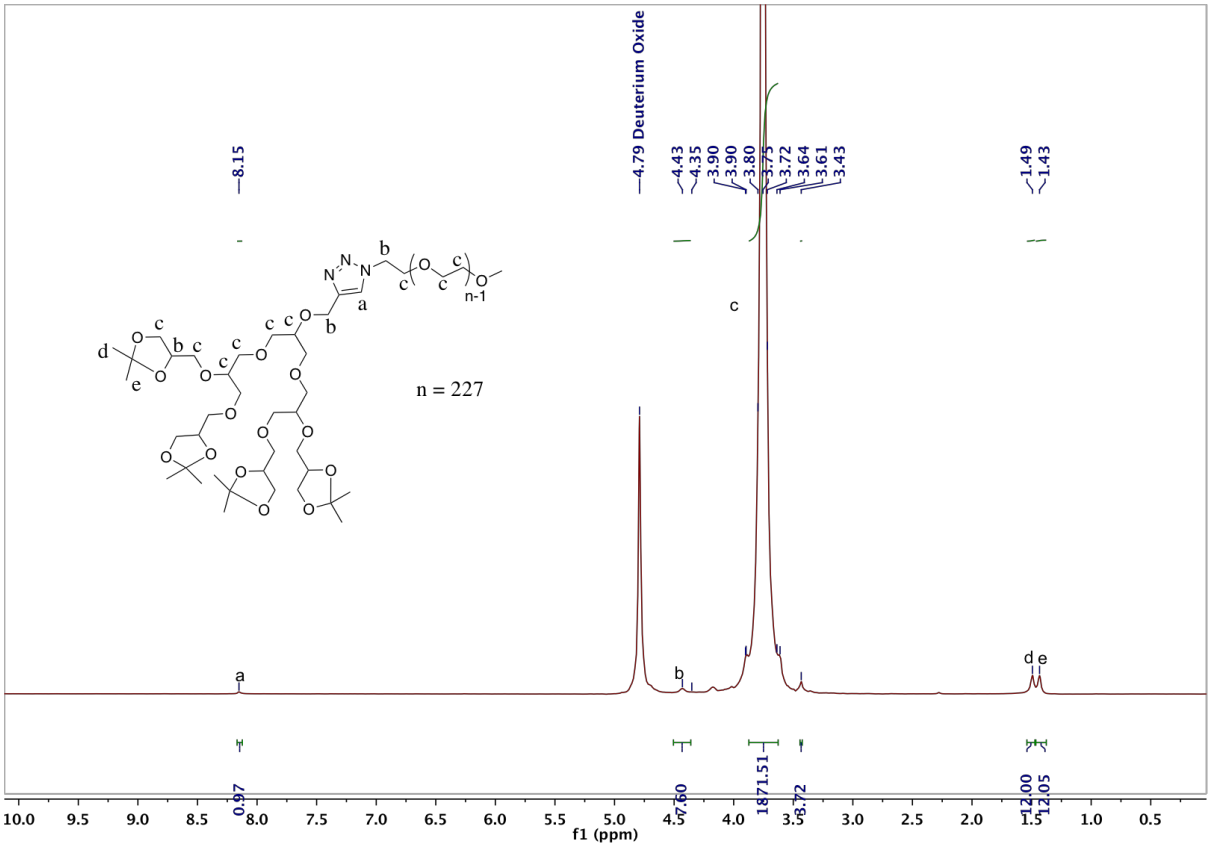


**Figure S12.** 1H NMR of compound **4f**

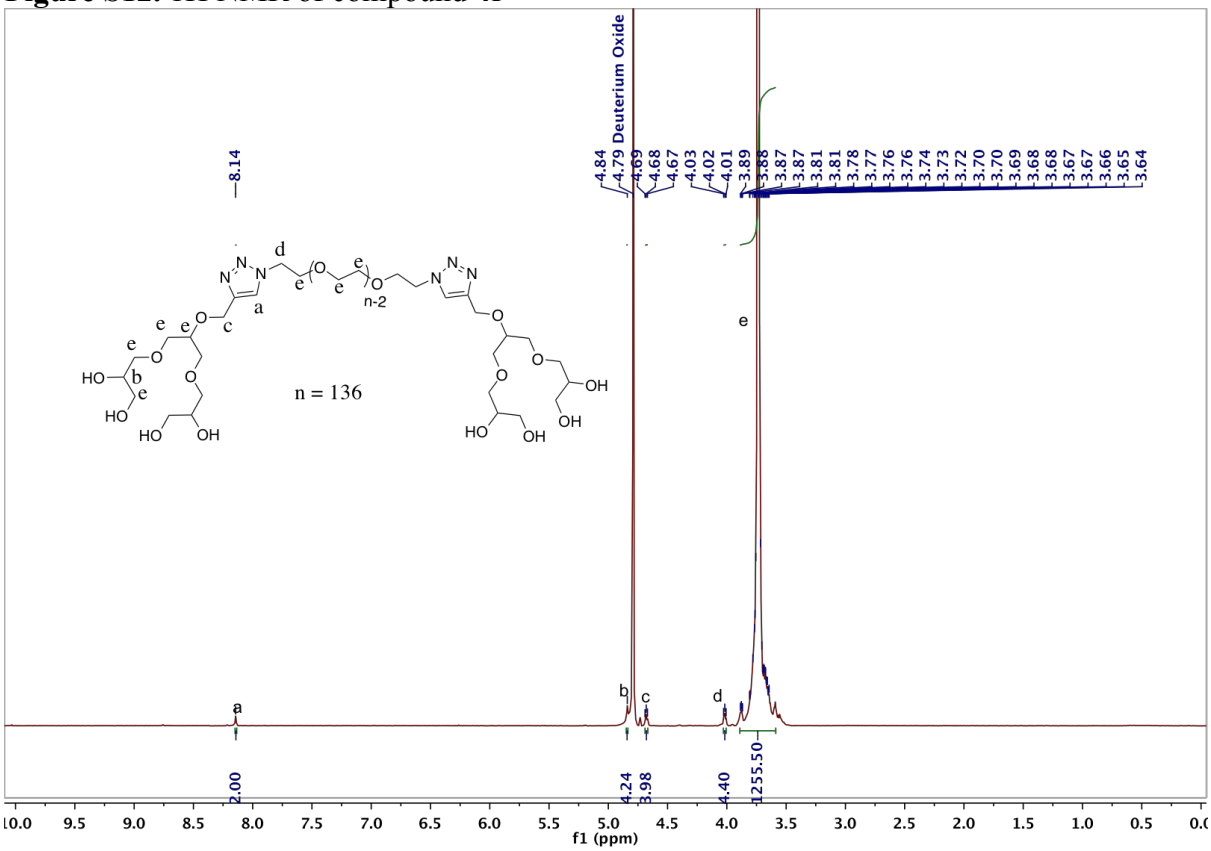


**Figure S13.** 1H NMR of compound **5a**

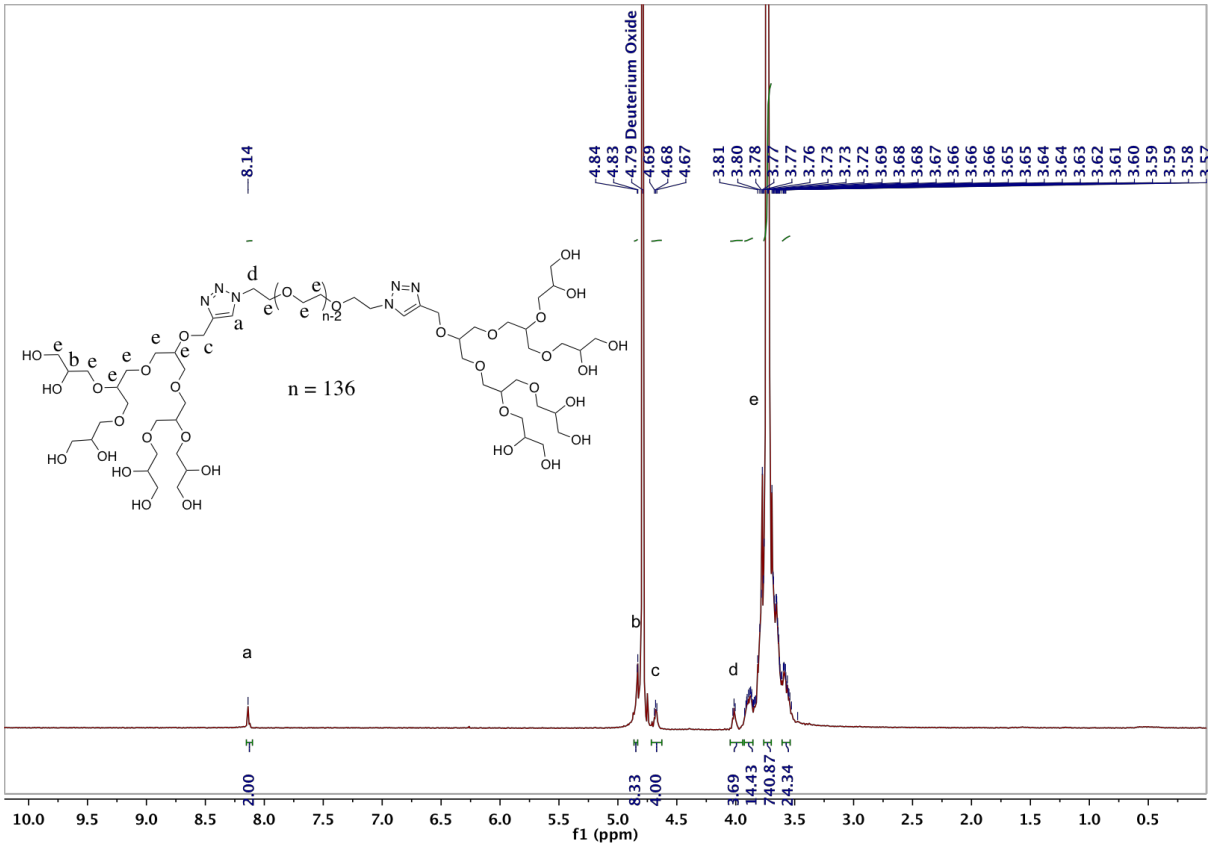


**Figure S14.** 1H NMR of compound **5b**

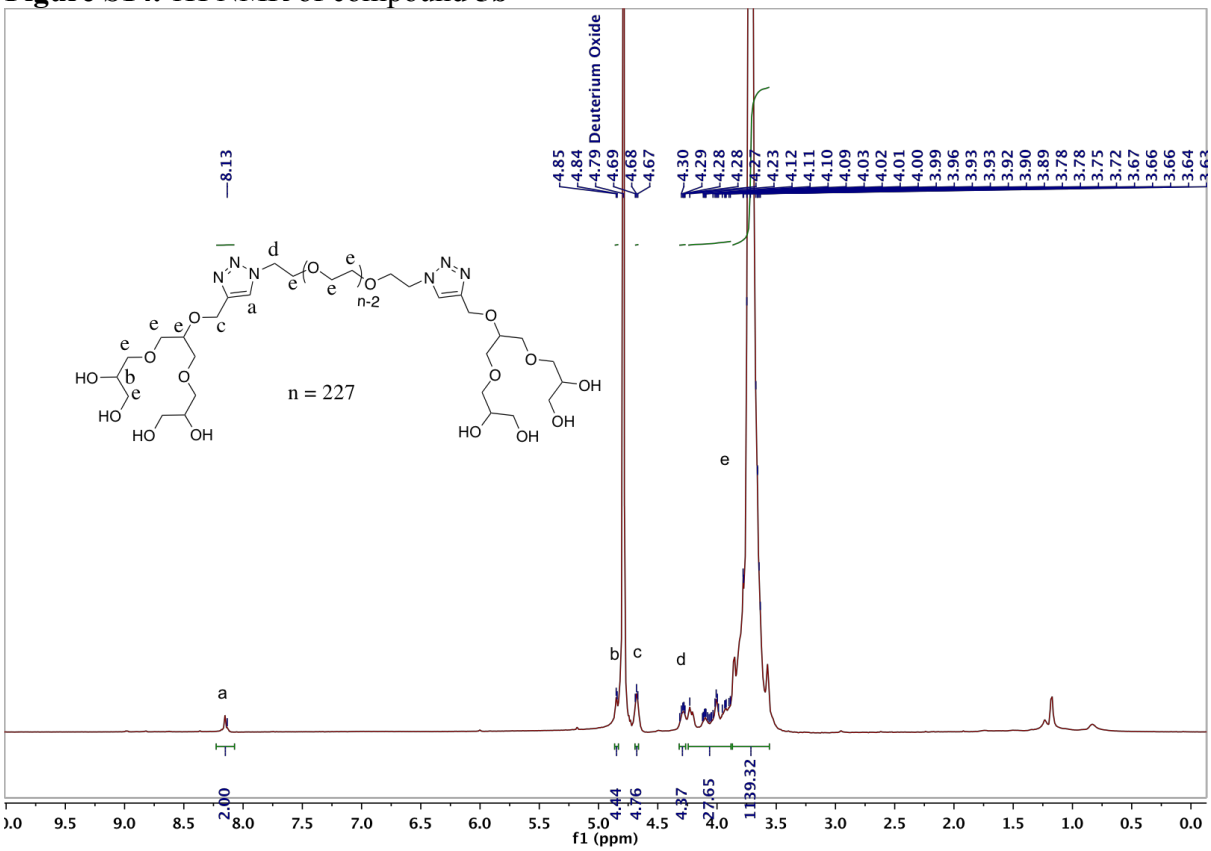


**Figure S15.** 1H NMR of compound **5c**

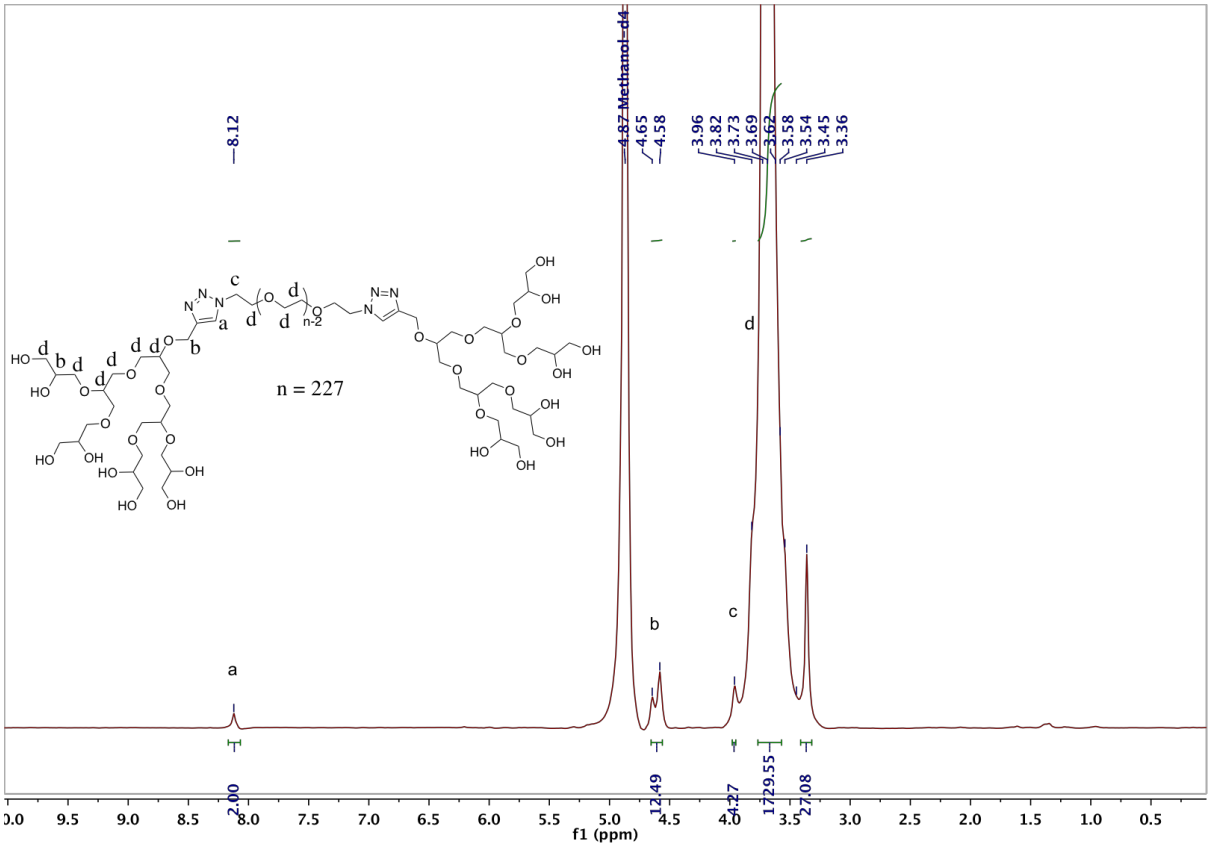


**Figure S16.** 1H NMR of compound **5d**

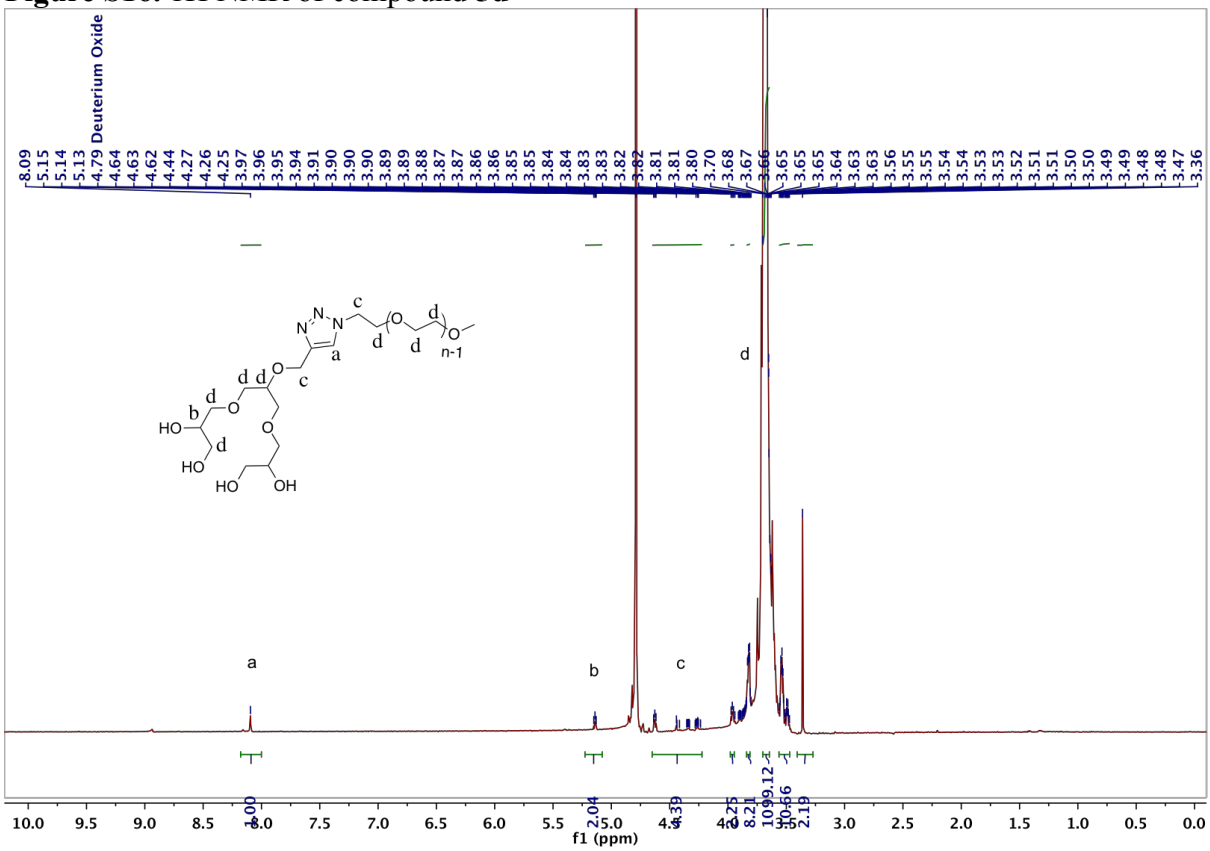


**Figure S17.** 1H NMR of compound **5e**

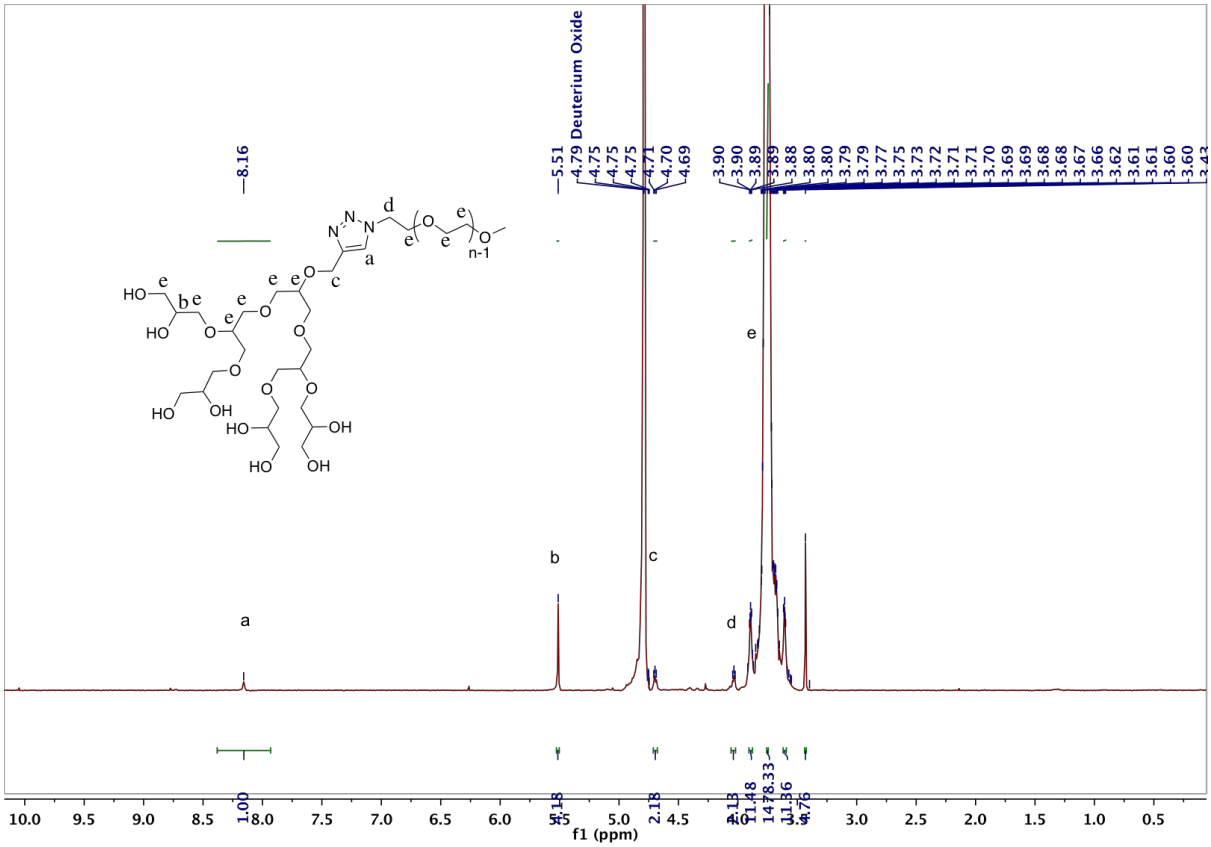


**Figure S18.** 1H NMR of compound **5f**

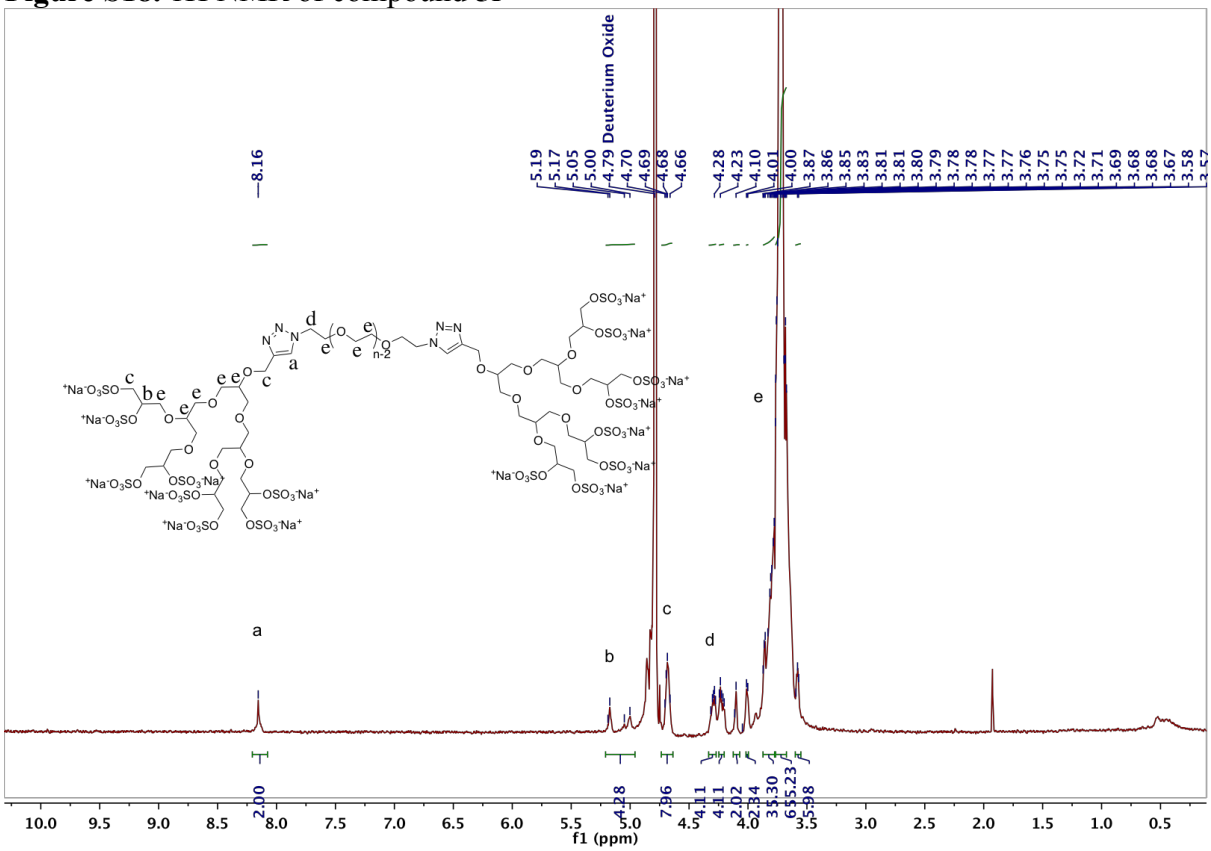


**Figure S19.** 1H NMR of compound **6a**

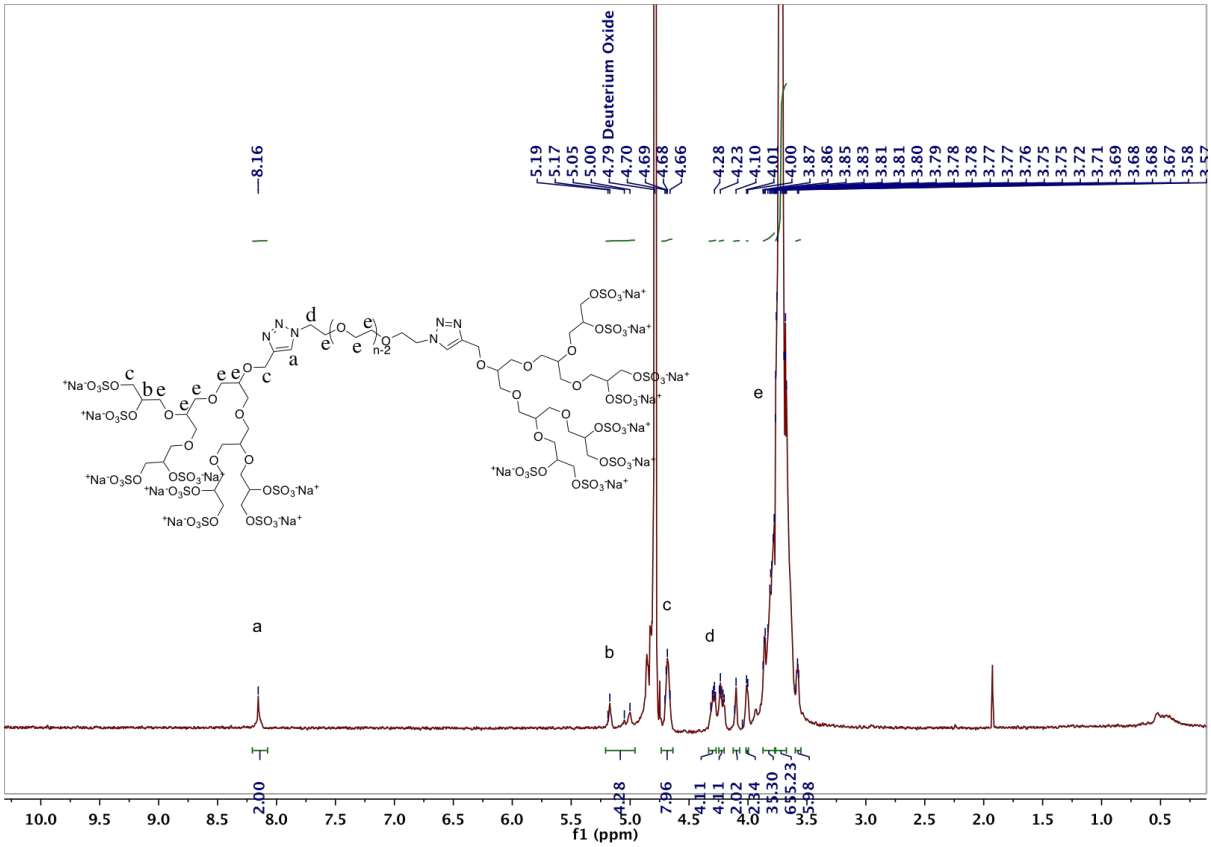


**Figure S20.** 1H NMR of compound **6b**

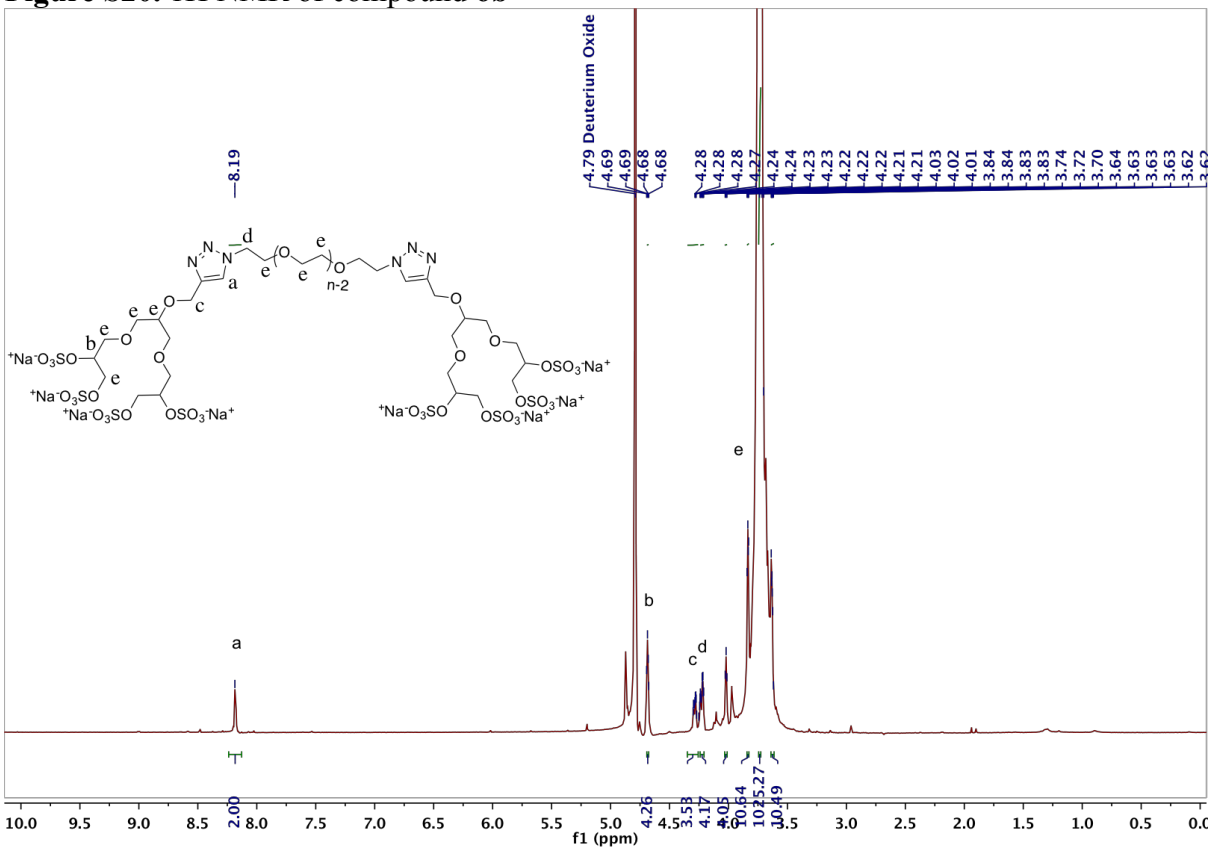


**Figure S21.** 1H NMR of compound **6c**

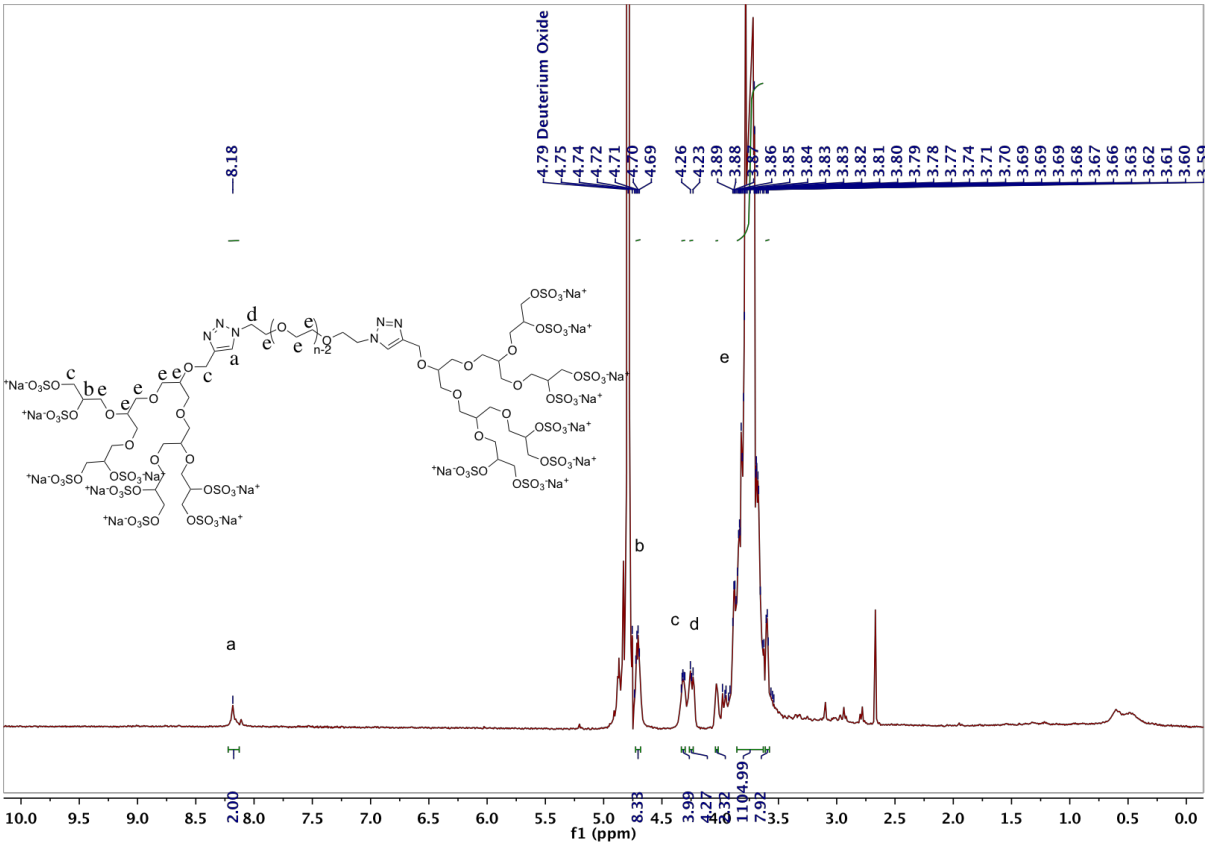


**Figure S22.** 1H NMR of compound **6d**

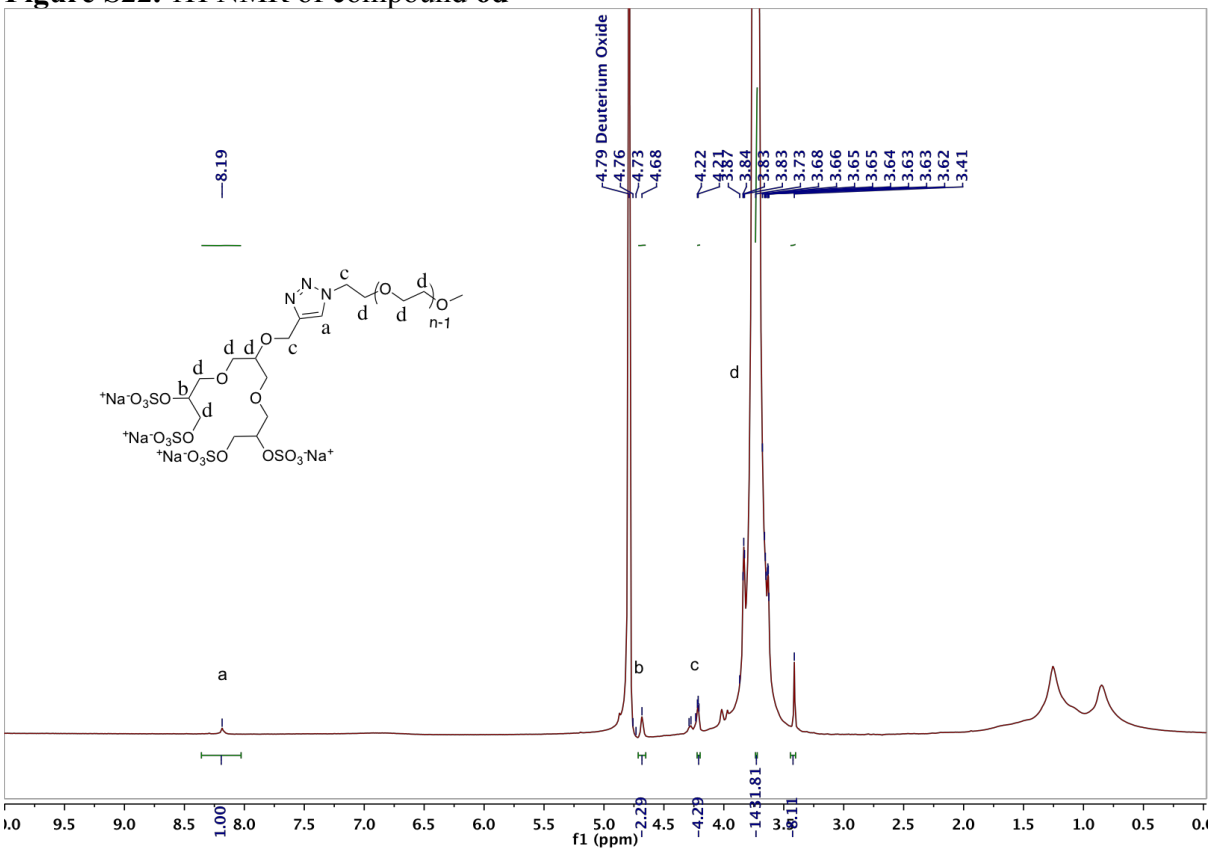


**Figure S23.** 1H NMR of compound **6e**

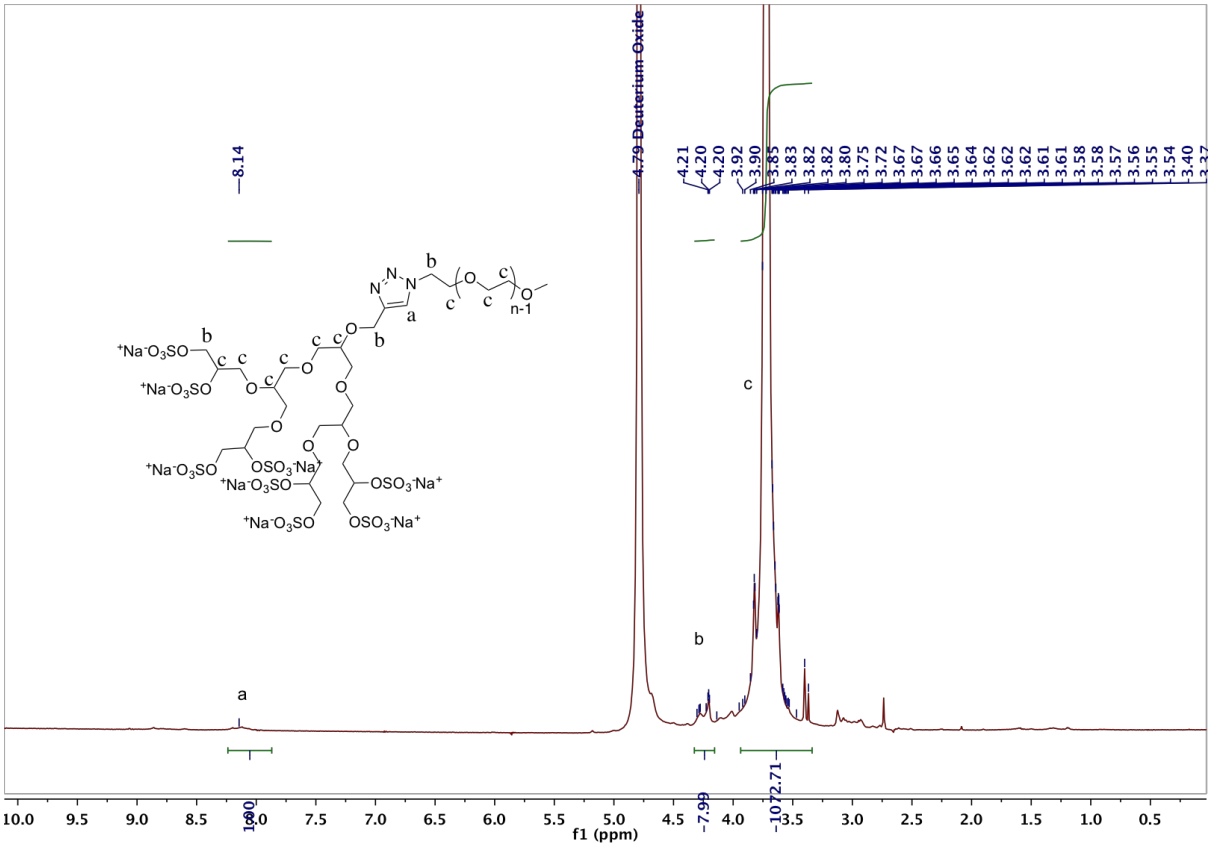


**Figure S24.** 1H NMR of compound **6f**

**Table S1.** Elemental analysis data of sulfated compounds.

| Compound | C | S | N | H |
|---|---|---|---|---|
| 6a | 52.04 | 3.48 | 1.65 | 8.84 |
| 6b | 44.60 | 5.40 | 1.24 | 6.62 |
| 6c | 48.70 | 2.24 | 1.07 | 8.55 |
| 6d | 49.39 | 3.79 | 0.63 | 7.98 |
| 6e | 19.47 | 1.03 | 0.41 | 4.09 |
| 6f | 20.57 | 2.17 | 0.56 | 4.17 |

**Table S2.** Molecular weight of polymers

| Sample name | Molecular weight peak (Mp)[a] (g/mol) | Expected molecular weight[b] (kDa) |
|---|---|---|
| 6 kDa PEG-OH | 6298 | 6 |
| 6 kDa PEG-G1OH | 6955 | 7 |

| | | |
|---|---|---|
| 6 kDa PEG-G2OH | 7417 | 8 |

[a] obtained by MALDI TOF

[b] calculated from $^{1}$H NMR and FTIR considering 100% conversion of starting molecular weights of 6 kDa as provided by manufacturer

**Table S3**. Molecular weight of single oligoglycerol dendron conjugated PEG polymers

| Formula | mol wt $m(n)$: $nm_{monomer}$ + $m_{end\ groups}$ + $m_{cation}$ | mass (g/mol) |
|---|---|---|
| $HO\text{-}(CH_2CH_2O)_n\text{-}H$ | 44.0 × n + 18 + 23 | 6298 |
| $N_3\text{-}CH_2CH_2\text{-}(O\text{-}CH_2CH_2)_{n-1}\text{-}[G1\text{-}OH]$ | [(n-1) × 44.05+84+28+278+23 | 6624 |
| $N_3\text{-}CH_2CH_2\text{-}(O\text{-}CH_2CH_2)_{n-1}\text{-}[G2\text{-}OH]$ | [(n-1) × 44.05+84+28+574+23 | 6920 |

n = 142

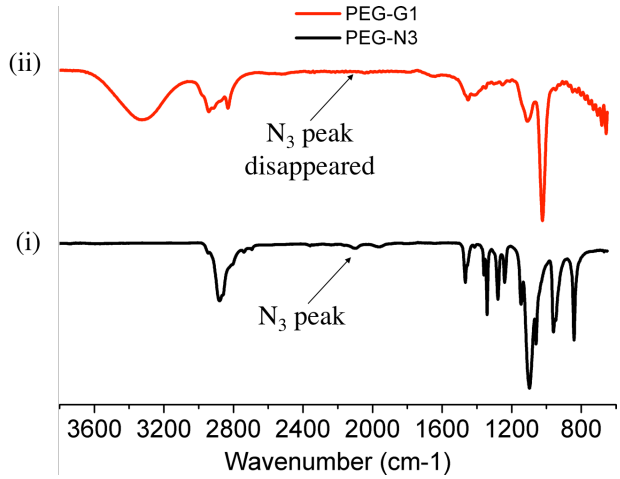


**Figure S25.** FTIR spectra of i) PEG-bisazide and ii) PEG-G1conjugate (G1OH-PEG10k-G1OH)

## 6. Proof of protein expression

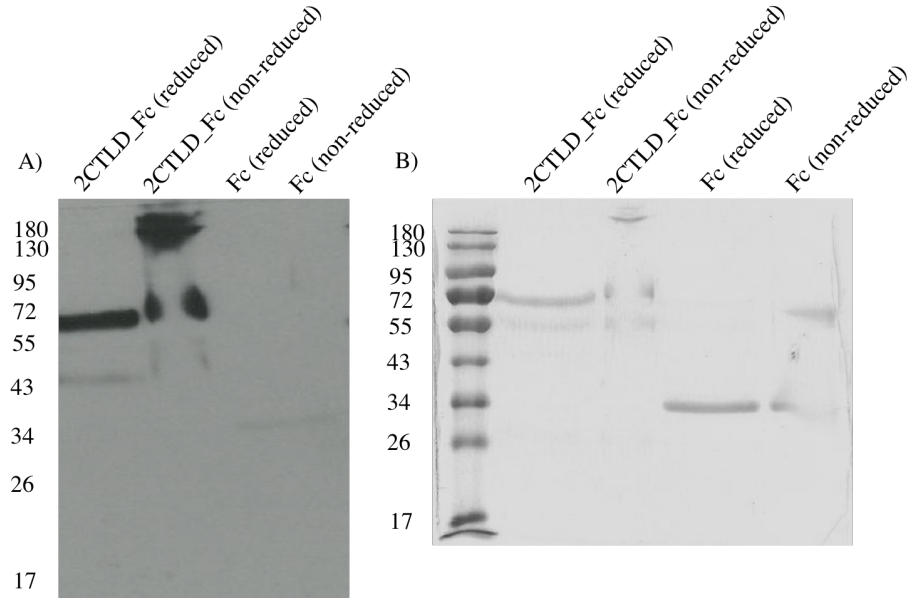


**Figure S26.** Expressed and purified proteins (2CTLD-Fc and Fc control) separated on a SDS-PAGE **A)** Western blot analysis and **B)** stained with Coomassie blue under reducing and non-reducing conditions.

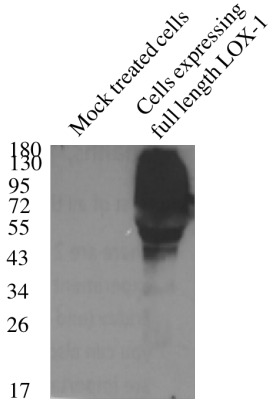


**Figure S27.** Expressed full length LOX-1 protein run on SDS-PAGE, analysed by Western blot under reducing condition.

### 7. SPR sensorgrams derived binding isotherms to calculate binding affinities

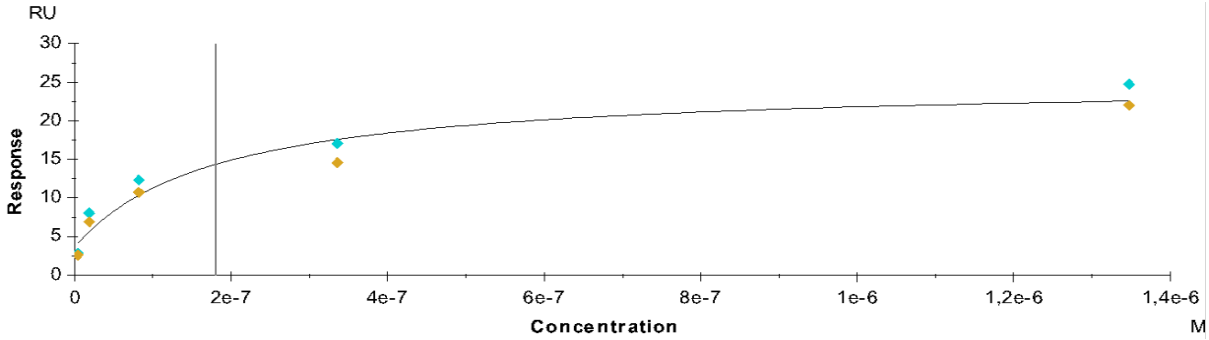


**Figure S28.** Isotherm for compound 6a.

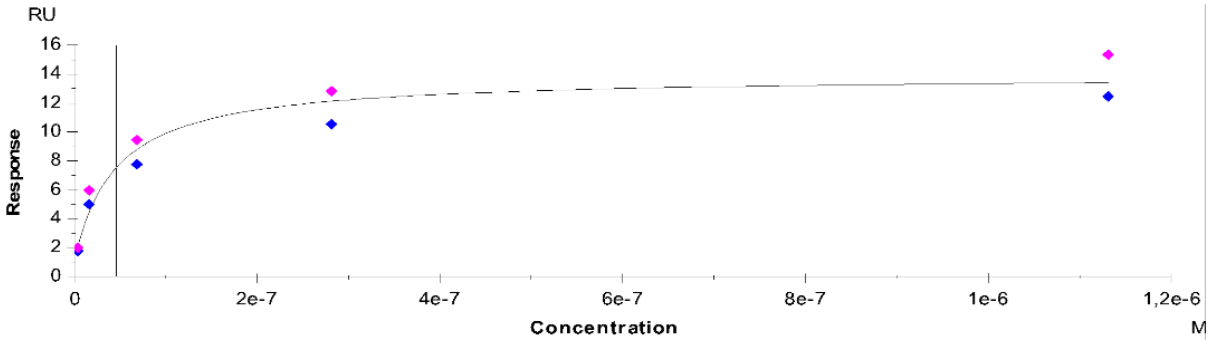


**Figure S29.** Isotherm for compound 6b.

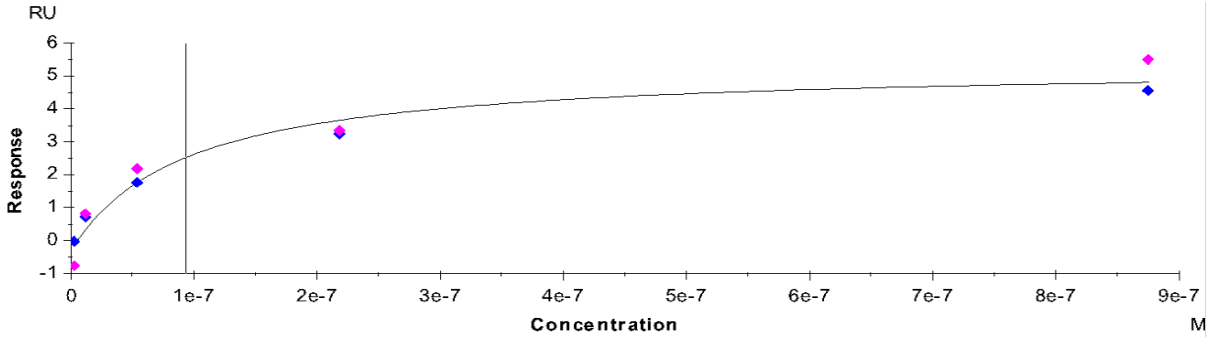


**Figure S30.** Isotherm for compound 6c.

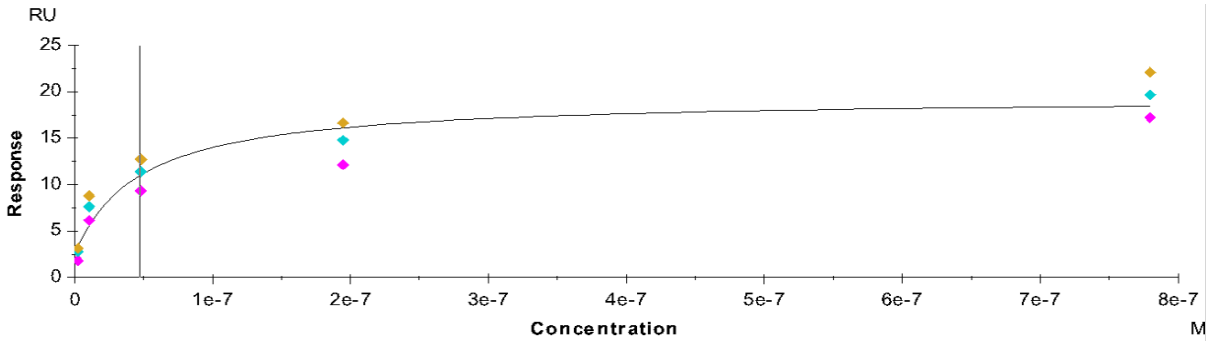


**Figure S31.** Isotherm for compound 6d.

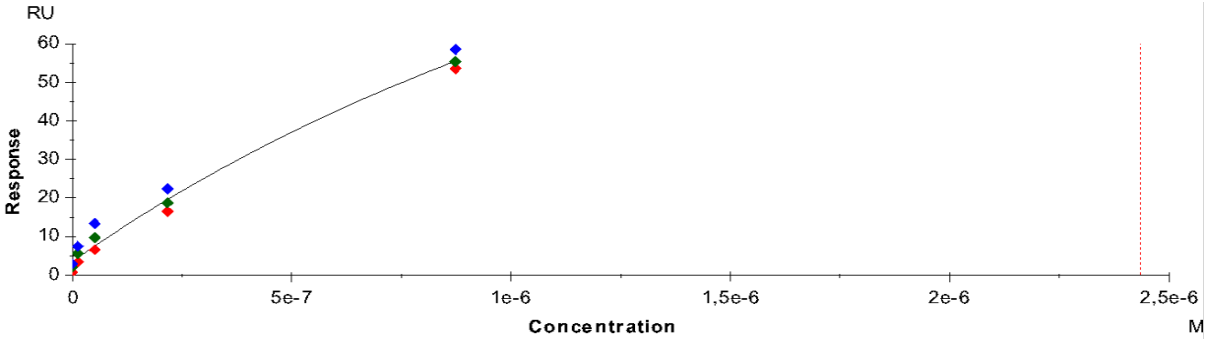


**Figure S32.** Isotherm for compound 6f.

## 5. LOX-1 mediated binding to aRBC

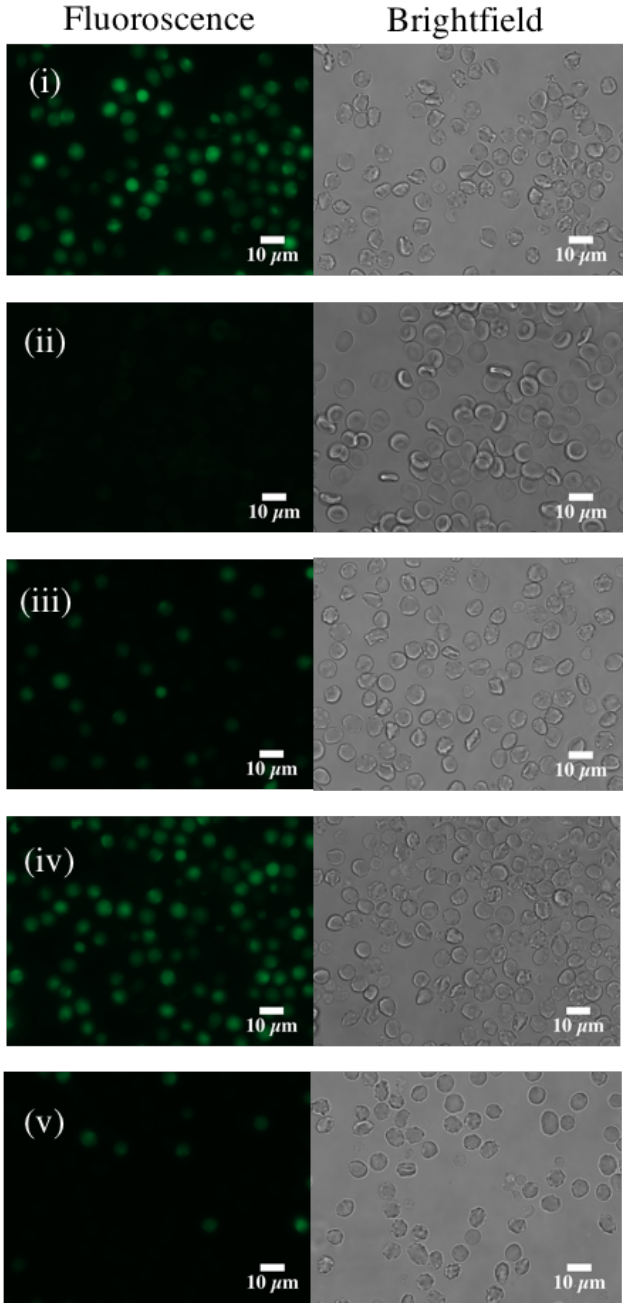

**Figure S33.** 2CTLD-Fc binding to RBC. Fluorescence and brightfield image of (i) aRBC; (ii), nRBC ; (iii), aRBC preincubated with compound **6d;** (iv), aRBC preincubated with compound **6f**; (v) aRBC preincubated with mAB.

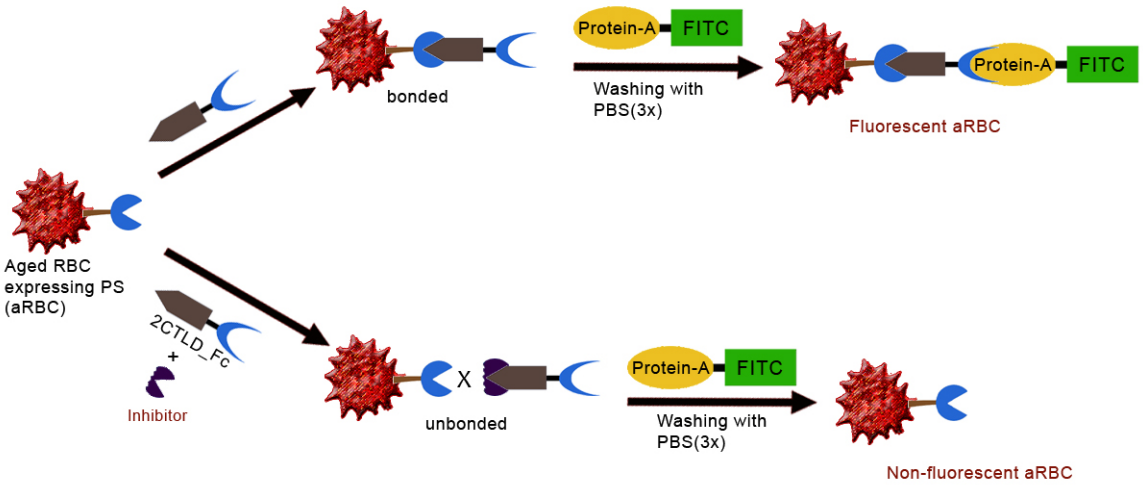


**Scheme S2.** Schematic illustration to monitor interaction of LOX-1 and aged RBC expressing phosphotidylserine (PS) in a competitive binding assay.

### 5. LOX-1 binding to *E. coli*

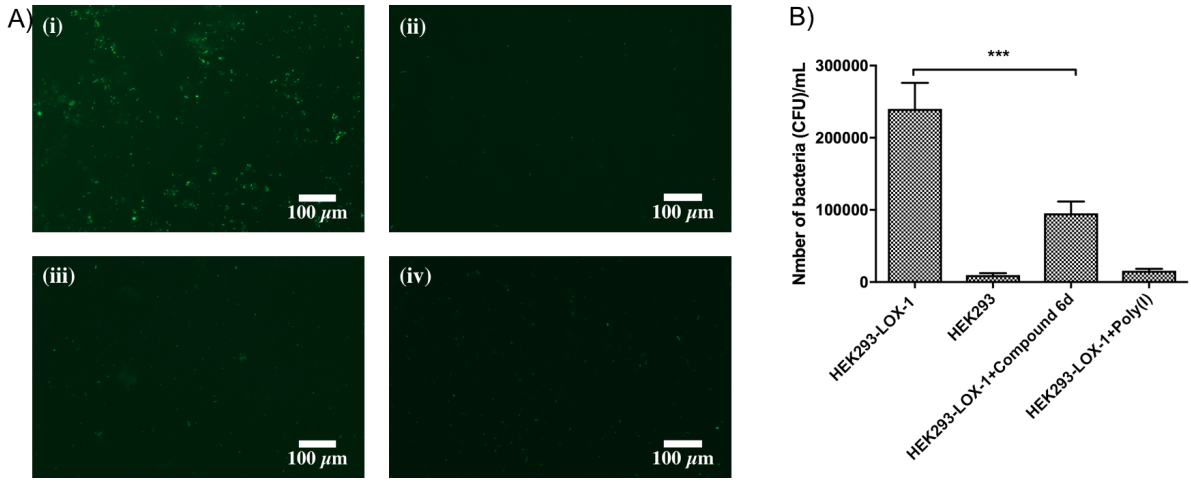


**Figure S34**. A) First row: fluorescence image, second row: overlap of fluorescence and bright field image; **i)** FITC- labeled *E. coli* bound to full length LOX-1 expressing cells **ii)** FITC-*E. coli* without LOX-1 expressing cells and FITC- labeled *E. coli* bound to membrane inserted full length LOX-1 expressing cells preincubated with **iii)** Poly(I) and **iv) Compound 6d** respectively. B) Quantification of *E. coli* (in terms of CFU counted) adhered to the LOX-1 positive cells in presence

and absence of Poly(I) (100 μg/mL) and compound 6d (100 μg/mL). Detached bacteria were harvested and dilutions transferred to agar plates. Colony forming units (CFU) were counted after cultivation. Values for each bar are average mean from 3 separate experiments, ***P<0.05 vs indicated bar.

**6. Compound toxicity**

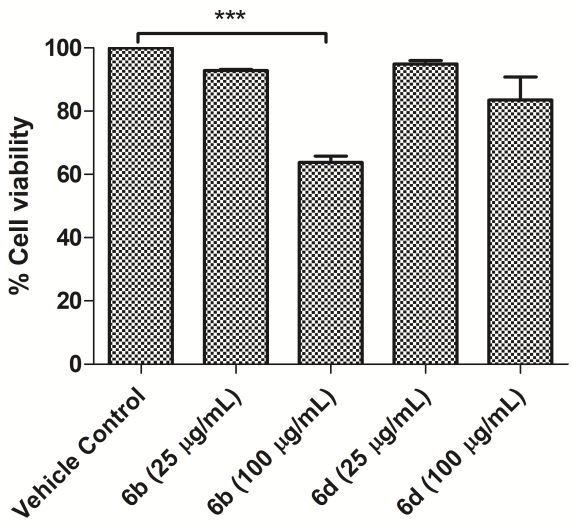


**Figure S35.** Cytotoxicity was measured using a LDH Cytotoxicity Assay Kit after exposing HEK293 cells to two different concentrations (25 μM and 100 μM) of compounds for 24 hours. Data are presented as mean ± SD; n = 3 (***P >0.05).

**References:**

1. Wyszogrodzka, M., Haag, Rainer, A Convergent Approach to Biocompatible Polyglycerol "Click" Dendrons for the Synthesis of Modular Core–Shell Architectures and Their Transport Behavior. *Chemistry – A European Journal* **2008**, *14*, 9202-14

2. Brousseau, T.; Clavey, V.; Bard, J. M.; Fruchart, J. C., Sequential ultracentrifugation micromethod for separation of serum lipoproteins and assays of lipids, apolipoproteins, and lipoprotein particles. *Clin Chem* **1993,** *39*, 960-4.

3. Weingart, C. L.; Broitman-Maduro, G.; Dean, G.; Newman, S.; Peppler, M.; Weiss, A. A., Fluorescent labels influence phagocytosis of Bordetella pertussis by human neutrophils. *Infect Immun* **1999,** *67*, 4264-7.

# 4 Summary and Conclusion

Based on the previous insight about polyanions and their interaction with various biologically relevant proteins, in this thesis the aim was to develop sulfated multivalent architectures targeting inflammation and cardiovascular diseases by inhibiting involved receptors i.e. L-selectin and LOX-1 respectively.

In the first part of thesis, a toolbox approach was developed with a possible variation of ligands and the subsequent ligand recognition was investigated. For the toolbox system, CDVs were functionalized non-covalently with different lectin recognizing ligands i.e. mannose containing ligands targeting ConA and sulfate bearing ligands targeting L-selectin. As discussed earlier L- selectin is an adhesion protein that supports the leukocyte attachment to endothelial cells leading to enhancement of inflammation process. PSGL-1 having an anionic sulphotyrosine residue is one of the physiological ligands which binds via electrostatic interaction to the positive charged region of L-, E-, and P- selectin. Targeting this electrostatic interaction, sulfated ligands having high negative charge density have been reported as potent binder to L-selectin which could block the interaction between leukocyte and endothelial cells. In order to have the multivalent supramolecular scaffold β-cyclodextrin vesicles were non-covalently functionalized with sulfated ligands. The ligands were designed is such a way that on one side the structural motif was conjugated with one or two adamantly residues allowing the ligand to complex with β-cyclodextrin at the surface of cyclodextrin vesicles. On the other side of ligand sulphate groups were introduced. Adamantane can form inclusion complex with β-CD with an affinity of $K_a \sim 10^4\ M^{-1}$ for 1:1 monovalent binding and two adamantane per ligand can lead to divalent binding with apparent affinity constant up to $K_a \sim 10^7\ M^{-1}$ and additional kinetic stablisation due to complexation. For the synthesis of the ligands glycerol based dendrons were synthesized according to published procedure and the focal hydroxyl group was converted to propargyl group using propargyl bromide. Propargylated glycerol based dendron was conjugated via copper catalyzed 1, 3 dipolar azide alkyne cycloaddition reaction to alkyne terminated adamantane having a linker of tetraethylene glycol. Further, the terminal acetal groups were cleaved off by using Dowex resin and the free hydroxyl group were sulfated using sulfur trioxide pyridine complex. For the synthesis of host part, the amphiphilic B-cyclodextrins were functionalized with alkyl and polyethylene glycol chains according previously reported protocol. The β-cyclodextrin vesicles were obtained by extrusion producing vesicles with a diameter in a range of 100-200 nm and the size and

morphology was investigated by dynamic light scattering (DLS) and cryogenic transmission electron microscopy (cryo-TEM). The non-covalent host-guest interaction of the complex was investigated between the adamantly ligands and β-CD using 1:1 ratio by isothermal titration calorimetry (ITC). The sulfated and non-sulfated ligands were analyzed to observe the effect of sulfation on the thermodynamic parameters. A reasonable binding affinity ($K_a \sim 10^4\ M^{-1}$) was observed for all the ligands. The sulfated ligands and respective CDV were analyzed for the binding with L-selectin by microscale thermophoresis (MST). The sulfated adamantly ligands without CDVs yields randomly fluctuating values for the MST response for the ligand titration range. While in presence of vesicles sigmoidal binding curves were obtained yielding a $K_D$ value of 34 μM and 25 μM for 4 and 8 sulfate groups, respectively. In this part of the thesis an enhanced binding towards L-selectin was achieved by multivalent display of the sulfated ligands on the CDV surface.

In the second part of thesis, polysulfates was used to target LOX-1 a cell surface receptor involved in binding and internalization of oxLDL leading to plaque formation in arteries and initiation of atherosclerosis. Major ligand recognition/binding site is the hydrophobic tunnel in between the dimer of LOX-1 and the linearly aligned arginine residues stretched over the dimer known as “basic spine”. LOX-1 inhibition to antagonize oxLDL uptake could be potential therapeutic approach for cardiovascular disease and curtail the acute inflammatory response. Previously reported inhibitors for LOX-1 include small molecules screened by simulation, or the modified lipid-based molecules, for fitting to hydrophobic tunnel of the LOX-1. Till now there is no multivalent inhibitor available targeting LOX-1. In this part of thesis, a novel class of multivalent inhibitor based on AB type diblock and ABA type triblock dendron-polymer conjugates were developed for the inhibition of LOX-1. The designing of polymer was done in such a way that it can bind to the basic amino acids in the ligands binding site which is a stretch of approximately 7 nm. For complete shielding and expansion over the dimeric surface a flexible linker was required, which can cover a distance of 7 nm. For the inhibitor design the block A of the polymer was sulfated glycerol based dendron with varying number of sulfates based on the generation of the dendron and the block B was linear polyethylene glycol of 6 and 10 kDa. The synthesized polymers were analyzed in binding assay with LOX-1 by surface plasmon resonance (SPR). For the binding study LOX-1 was expressed as tetramers as oligomerization of recombinant soluble LOX-1 is highly crucial for the activity and high binding affinity with the ligands. From the analysis of binding affinities of the synthesized polymers we came to know that bifunctional molecules well suited to target the basic spine of arginine residues on the

dimer of LOX-1 and high number of sulfate is important for strong binding. Hence, charge density and hydrodynamic diameter plays an important role to recognize a potential inhibitor for LOX-1. The major ligand of LOX-1 includes oxLDL, bacteria, aged red blood cells. Phosphatidylserine expressed on aged RBC happens to be the dominant target for LOX-1 binding. A competitive binding of soluble LOX-1 to aged RBC was analyzed as a model system. The bound LOX-1 was visualized by FITC labelled protein A and pre-incubation of LOX-1 with the polymers caused a reduction in binding to aged RBC. In another *in vitro* assay LOX-1 expressing on cell surface showed binding to Dil-oxLDL and the binding was reduced on pre-incubation of the cells with the sulfated polymers. Similarly, an assay was set-up to visualize the inhibition of binding of LOX-1 with FITC labelled *E. coli* in presence of sulfated architectures. As a conclusion we can say that the molecules with two G2 dendrons carrying 8 sulfates on each end of the PEG linker showed high affinity in low nanomolar (~50 nM) concentration. Further as a proof of function these polymers were able to inhibit the binding of LOX-1 to aged RBC, a Gram-negative *E. coli* strain and finally the major ligand oxLDL.

In conclusion, sulfated multivalent architectures are potential choice while addressing inflammation or cardiovascular disease through targeting L-selectin to inhibit leukocyte adhesion to endothelial cells or by targeting LOX-1 to inhibit binding and uptake of oxLDL. Nonetheless, binding affinities are highly dependent on the number of the sulfate group, structure and stability of the scaffold and also on linker length. Still a lot of open questions needs to be answered regarding the specificity of these polymers and interaction with various other biological proteins.

# 5 Outlook

The development of sulfated multivalent dendrons for inhibition of two different receptors has substantiated that the compounds can be used for receptor inhibition at low concentrations. However, the efficacy and target specificity must be improved. Non-covalent supramolecular assemblies e. g. CD-Adamantane as scaffold for multivalent ligand presentation, due to their propensity of disintegration at micromolar concentration. Considering an application *in vivo* a robust, high affinity compound is wanted that outcompetes additional potential binding partners. Therefore, electrostatic interactions that perfectly fit the given receptor architecture might not be sufficient to provide specificity. In the case of L-selectin binding, a sulfated dendron could be linked to a carbohydrate moiety that targets the sugar-binding site. For LOX-1, the intrinsic hydrophobic tunnel of the dimer should be addressed in addition to the basic spine at the receptor surface. A sulfated dendron equipped with a short hydrophobic part should be evaluated. A detailed look to the available crystal structures of both proteins may guide a computer-aided drug design.

# 6 Abstract and Kurzzusammenfassung

## 6.1 Abstract

Within the scope of this thesis, multivalent sulfated polymers were synthesized and investigated concerning their targeting properties towards two proteins: L-selectin, a cell adhesion molecule expressed on leukocytes and LOX-1, a scavenger receptor from macrophages. Whereas L-selectin plays a dominant role in chronic diseases, LOX-1 can contribute to atherosclerosis. In both cases, a targeted intervention is desired.

In the first part, β-cyclodextrin vesicles were non-covalently functionalized with oligosulfate-adamantyl conjugates as guest molecules. The supramolecular assemblies were evaluated for L-selectin binding in solution by microscale thermophoresis. An increase in binding affinity was observed with respect to the sulfate valency of the ligands. The adamantly conjugates with 4 and 8 sulfate groups revealed $K_D$ values of 34 and 25 μM, respectively. Unfunctionalized vesicles and sulfate-adamantly conjugates alone did not show any effect. However, the complex stability was limited.

In the second part, sulfated oligoglycerol dendrons were conjugated to polyethylene linkers yielding mono- and bi-functionalized compounds. For binding studies, a soluble recombinant fusion protein was expressed that carries two LOX-1 dimers. Targeting of the positively charged, linearly aligned arginine residue on the dimer surface was evaluates for all polymeric architectures by surface plasmon resonance and two of the molecules gave binding affinities in the low nM range (~50 nM). In cell-based assays the sulfated polymers were able to reduce the binding of soluble LOX-1 to target cells. Recognition of a physiological ligand, oxidized low density lipoprotein particle (oxLDL) by LOX-1 expressing cells was reduced upon preincubation with the sulfated polymers.

As a result, the work demonstrates that multivalent compounds enhance binding affinity and therefore, multivalency is a useful concept to interfere with planar biological surfaces.

## 6.2 Kurzzusammenfassung

Ziel der Doktorarbeit war die Synthese multivalenter sulfatierter Polymere und Untersuchungen der Bindung an zwei Zielproteine: L-Selektin, einem Zell-Adhäsionsmolekül, das auf Leukozyten exprimiert wird und LOX-1, ein Scavenger-Rezeptor der auf Makrophagen vorkommt. Während L-Selektin eine wichtige Rolle bei chronischen Erkrankungen spielt, kommt LOX-1 eine zentrale Rolle bei der Entwicklung der Atherosklerose zu. In beiden Krankheitsbildern ist eine zielgerichtete medizinische Intervention wünschenswert.

Im ersten Teil der Arbeit wurden β-Cyclodextrinvesikel mit Oligosulfat-Adamantylkonjugaten als Gast-Moleküle nicht-kovalent funktionalisiert. Diese supramolekularen Systeme wurden in Lösung mittels mikroskalarer Thermophorese hinsichtlich ihrer L-Selektinbindung untersucht. Dabei wurde eine Steigerung der Bindungsaffinität in Abhängigkeit von der Anzahl an Sulfatgruppen nachgewiesen. Die Adamantylkonjugate mit 4 bzw. 8 Sulfatgruppen ergaben $K_D$-Werte von 34 und 25 µM. Nicht funktionalisierte Vesikel und die sulfatierten Adamantylkonjugate allein zeigten keine Bindung. Auffällig war, dass die Stabilität der Komplexe begrenzt war.

Im zweiten Teil der Arbeit wurden sulfatierte Oligoglyceroldendrone an mono- und bi-funktionelle Polyethylenlinker konjugiert. Zur Untersuchung der Funktionalität der Konjugate wurde ein lösliches Fusionsprotein exprimiert, dass aus zwei LOX-1 Dimeren besteht. Die Bindung an eine positiv geladene, lineare Poly-Argininsequenz auf der Oberfläche des LOX-1 Proteins wurde mit allen synthetisierten Konjugaten mittels Oberflächenplasmonresonanz-Spektroskopie bestimmt. Zwei Konjugate zeigten dabei Bindungsaffinitäten im unteren nM Bereich (~50 nM). In zellbasierten Experimenten reduzierten die sulfatierten Polymere die Bindung des rekombinanten löslichen LOX-1 an Zielzellen. Durch Vorinkubation eines physiologischen Liganden, dem oxidierten Lipoprotein Partikel (oxLDL) mit den sulfatierten Polymeren konnte die Bindung des Liganden an membranständiges LOX-1 auf Zielzellen reduziert werden.

Als Ergebnis zeigt die Arbeit, dass multivalente Systeme geeignet sind Bindungsaffinität zu erhöhen und Multivalenz ein geeignetes Konzept ist, um planare biologische Oberflächen zu adressieren.

# 7 References


[1] D. Bobo, K. J. Robinson, J. Islam, K. J. Thurecht, S. R. Corrie, *Pharm Res* **2016**, *33*, 2373-2387.

[2] M. A. Karimi, Pourhakkak, Pouran, Adabi, Mahdi, Firoozi, Saman, Adabi, Mohsen, Naghibzadeh, Majid, *e-polymers* **2015**, *15*; in *Regenerative Medicine, Artificial Cells and Nanomedicine, Vol. Volume 3*, WORLD SCIENTIFIC, **2013**, p. 600; Y.-Y. S. Jiu-Ju Feng, Xiao-Miao Feng, Nabeen Kumar Shrestha, and Nattawadee Wisitruangsakul, *Journal of Nanomaterials* **2013**.

[3] E. A. J. Bleeker, W. H. de Jong, R. E. Geertsma, M. Groenewold, E. H. W. Heugens, M. Koers-Jacquemijns, D. van de Meent, J. R. Popma, A. G. Rietveld, S. W. P. Wijnhoven, F. R. Cassee, A. G. Oomen, *Regulatory Toxicology and Pharmacology* **2013**, *65*, 119-125.

[4] M. A. Naghibzadeh, *Fibers and Polymers* **2014**, *15*, 767-777; M. Adabi, M. Naghibzadeh, M. Adabi, M. A. Zarrinfard, S. S. Esnaashari, A. M. Seifalian, R. Faridi-Majidi, H. Tanimowo Aiyelabegan, H. Ghanbari, *Artif Cells Nanomed Biotechnol* **2017**, *45*, 833-842.

[5] S. K. Murthy, *Int J Nanomedicine* **2007**, *2*, 129-141; N. Ketabchi, Naghibzadeh, M., Adabi, M., Esnaashari, S.S., & Faridi-Majidi, R. , *Neural Computing and Applications* **2016**, *28*, 3131-3143.

[6] G. V. Dubacheva, T. Curk, B. M. Mognetti, R. Auzély-Velty, D. Frenkel, R. P. Richter, *Journal of the American Chemical Society* **2014**, *136*, 1722-1725.

[7] M. A. van Dongen, C. A. Dougherty, M. M. Banaszak Holl, *Biomacromolecules* **2014**, *15*, 3215-3234.

[8] K. P. Johnson, B. R. Brooks, J. A. Cohen, C. C. Ford, J. Goldstein, R. P. Lisak, L. W. Myers, H. S. Panitch, J. W. Rose, R. B. Schiffer, T. Vollmer, L. P. Weiner, J. S. Wolinsky, *Neurology* **1998**, *50*, 701-708; J. Crawford, *Semin Oncol* **2003**, *30*, 24-30.

[9] J. Shi, A. R. Votruba, O. C. Farokhzad, R. Langer, *Nano Lett* **2010**, *10*, 3223-3230.

[10] M. Foldvari, M. Bagonluri, *Nanomedicine: Nanotechnology, Biology and Medicine* **2008**, *4*, 183-200; I. Bala, S. Hariharan, M. N. Kumar, *Crit Rev Ther Drug Carrier Syst* **2004**, *21*, 387-422.

[11] A. E. Nel, L. Mädler, D. Velegol, T. Xia, E. M. V. Hoek, P. Somasundaran, F. Klaessig, V. Castranova, M. Thompson, *Nature Materials* **2009**, *8*, 543.

[12] M. A. Dobrovolskaia, S. E. McNeil, *Nature Nanotechnology* **2007**, *2*, 469.

[13] D. Leu, B. Manthey, J. Kreuter, P. Speiser, P. P. DeLuca, *J Pharm Sci* **1984**, *73*, 1433-1437.

[14] B. E. Rolfe, I. Blakey, O. Squires, H. Peng, N. R. Boase, C. Alexander, P. G. Parsons, G. M. Boyle, A. K. Whittaker, K. J. Thurecht, *J Am Chem Soc* **2014**, *136*, 2413-2419.

[15] F. E, *International Journal of Nanomedicine* **2012**.

[16] M. Mammen, S.-K. Choi, G. M. Whitesides, *Angewandte Chemie International Edition* **1998**, *37*, 2754-2794.

[17] C. Fasting, C. A. Schalley, M. Weber, O. Seitz, S. Hecht, B. Koksch, J. Dernedde, C. Graf, E.-W. Knapp, R. Haag, *Angewandte Chemie International Edition* **2012**, *51*, 10472-10498.

[18] V. M. Krishnamurthy, L. A. Estroff, G. M. Whitesides, **2006**.

[19] P. I. Kitov, D. R. Bundle, *J Am Chem Soc* **2003**, *125*, 16271-16284.

[20] J. J. Lundquist, E. J. Toone, *Chemical Reviews* **2002**, *102*, 555-578.

[21] J. D. Badjic, A. Nelson, S. J. Cantrill, W. B. Turnbull, J. F. Stoddart, *Acc Chem Res* **2005**, *38*, 723-732.
[22] M. C. T. Fyfe, J. F. Stoddart, *Accounts of Chemical Research* **1997**, *30*, 393-401.
[23] x. C. Y.-h. Huang Hao-zhi, 	Yu Wan-cheng,	Luo Kai-fu	. *Chinese Journal of Chemical Physics* **2016**, *29*, 564-570; J. Huskens, A. Mulder, T. Auletta, C. A. Nijhuis, M. J. Ludden, D. N. Reinhoudt, *J Am Chem Soc* **2004**, *126*, 6784-6797.
[24] V. M. Krishnamurthy, V. Semetey, P. J. Bracher, N. Shen, G. M. Whitesides, *J Am Chem Soc* **2007**, *129*, 1312-1320; J. D. Badjić, S. J. Cantrill, J. F. Stoddart, *Journal of the American Chemical Society* **2004**, *126*, 2288-2289.
[25] A. Schoen, E. Freire, *Biochemistry* **1989**, *28*, 5019-5024.
[26] W. J. Lees, A. Spaltenstein, J. E. Kingery-Wood, G. M. Whitesides, *J Med Chem* **1994**, *37*, 3419-3433.
[27] M. Mammen, G. Dahmann, G. M. Whitesides, *Journal of Medicinal Chemistry* **1995**, *38*, 4179-4190.
[28] H. Connell, W. Agace, P. Klemm, M. Schembri, S. Marild, C. Svanborg, *Proceedings of the National Academy of Sciences of the United States of America* **1996**, *93*, 9827-9832.
[29] A. Varki, *The Journal of clinical investigation* **1997**, *99*, 158-162; J. B. Lowe, P. A. Ward, *The Journal of clinical investigation* **1997**, *99*, 822-826.
[30] R. Roy, D. Zanini, S. J. Meunier, A. Romanowska, *Journal of the Chemical Society, Chemical Communications* **1993**, 1869; L. V. Mochalova, A. B. Tuzikov, V. P. Marinina, A. S. Gambaryan, N. E. Byramova, N. V. Bovin, M. N. Matrosovich, *Antiviral Research* **1994**, *23*, 179-190.
[31] G. M. W. A. Spaltenstein, *J. Am. Chem. Soc.* **1991**; X. Gong, D. H. Dubois, D. J. Miller, B. D. Shur, *Science* **1995**, *269*, 1718-1721.
[32] D. J. Diestler, E. W. Knapp, *Phys Rev Lett* **2008**, *100*, 178101.
[33] L. L. Kiessling, J. E. Gestwicki, L. E. Strong, *Angew Chem Int Ed Engl* **2006**, *45*, 2348-2368.
[34] S. Bhatia, D. Lauster, M. Bardua, K. Ludwig, S. Angioletti-Uberti, N. Popp, U. Hoffmann, F. Paulus, M. Budt, M. Stadtmuller, T. Wolff, A. Hamann, C. Bottcher, A. Herrmann, R. Haag, *Biomaterials* **2017**, *138*, 22-34.
[35] H. A. B. W. Z. HASSID, *Journal of Biological Chemistry* **1940**.
[36] K. Koschek, V. Durmaz, O. Krylova, M. Wieczorek, S. Gupta, M. Richter, A. Bujotzek, C. Fischer, R. Haag, C. Freund, M. Weber, J. Rademann, *Beilstein journal of organic chemistry* **2015**, *11*, 837-847.
[37] S. Bhatia, L. C. Camacho, R. Haag, *J Am Chem Soc* **2016**, *138*, 8654-8666.
[38] F. Abendroth, A. Bujotzek, M. Shan, R. Haag, M. Weber, O. Seitz, *Angew Chem Int Ed Engl* **2011**, *50*, 8592-8596; C. Scheibe, A. Bujotzek, J. Dernedde, M. Weber, O. Seitz, *Chemical Science* **2011**, *2*, 770.
[39] F. Biedermann, H.-J. Schneider, *Chemical Reviews* **2016**, *116*, 5216-5300.
[40] P. I. Kitov, J. M. Sadowska, G. Mulvey, G. D. Armstrong, H. Ling, N. S. Pannu, R. J. Read, D. R. Bundle, *Nature* **2000**, *403*, 669-672; E. Fan, Z. Zhang, W. E. Minke, Z. Hou, C. L. M. J. Verlinde, W. G. J. Hol, *Journal of the American Chemical Society* **2000**, *122*, 2663-2664.
[41] J. Rao, J. Lahiri, L. Isaacs, R. M. Weis, G. M. Whitesides, *Science* **1998**, *280*, 708-711.
[42] A. Jain, G. M. Whitesides, R. S. Alexander, D. W. Christianson, *Journal of Medicinal Chemistry* **1994**, *37*, 2100-2105.
[43] V. M. Krishnamurthy, B. R. Bohall, V. Semetey, G. M. Whitesides, *J Am Chem Soc* **2006**, *128*, 5802-5812.

[44] G. Wang, A. D. Hamilton, *Chemistry – A European Journal* **2002**, *8*, 1954-1961.
[45] W. H. Chapman, R. Breslow, *Journal of the American Chemical Society* **1995**, *117*, 5462-5469.
[46] R. Schweitzer-Stenner, A. Licht, I. Luescher, I. Pecht, *Biochemistry* **1987**, *26*, 3602-3612; B. Schuler, E. A. Lipman, P. J. Steinbach, M. Kumke, W. A. Eaton, *Proc Natl Acad Sci U S A* **2005**, *102*, 2754-2759.
[47] J. M. Paar, N. T. Harris, D. Holowka, B. Baird, *J Immunol* **2002**, *169*, 856-864.
[48] D. M. Vincent Semetey, and George M. Whitesides*, *Angew. Chem. Int. Ed.* **2006**.
[49] X. Ma, Y. Zhao, *Chemical Reviews* **2015**, *115*, 7794-7839.
[50] M. Delbianco, P. Bharate, S. Varela-Aramburu, P. H. Seeberger, *Chemical Reviews* **2016**, *116*, 1693-1752; U. Kauscher, M. C. Stuart, P. Drucker, H. J. Galla, B. J. Ravoo, *Langmuir* **2013**, *29*, 7377-7383.
[51] H. Yoon, E. J. Dell, J. L. Freyer, L. M. Campos, W.-D. Jang, *Polymer* **2014**, *55*, 453-464.
[52] M. Rubinstein, G. A. Papoian, *Soft Matter* **2012**, *8*, 9265-9267.
[53] A. Agarwal, Y. Lvov, R. Sawant, V. Torchilin, *Journal of Controlled Release* **2008**, *128*, 255-260; N. Arnberg, A. H. Kidd, K. Edlund, J. Nilsson, P. Pring-Akerblom, G. Wadell, *Virology* **2002**, *302*, 33-43.
[54] J. Jacob, K. S. Sebastian, S. Devassy, L. Priyadarsini, M. F. Farook, A. Shameem, D. Mathew, S. Sreeja, R. V. Thampan, *Mol Cell Endocrinol* **2006**, *246*, 34-41; V. M. Krishnamurthy, L. A. Estroff, G. M. Whitesides, *Fragment-based Approaches in Drug Discovery* **2006**.
[55] J. H. a. B. N. W. Kunz, *Curr. Opin. Colloid Interface Sci.* **2004**, *9*, 19-37.
[56] J. B. Chaires, *Annu Rev Biophys* **2008**, *37*, 135-151.
[57] X. Xu, S. Angioletti-Uberti, Y. Lu, J. Dzubiella, M. Ballauff, *Langmuir* **2018**.
[58] Q. Ran, X. Xu, P. Dey, S. Yu, Y. Lu, J. Dzubiella, R. Haag, M. Ballauff, *The Journal of Chemical Physics* **2018**, *149*, 163324.
[59] P. A. Janmey, D. R. Slochower, Y.-H. Wang, Q. Wen, A. Cēbers, *Soft matter* **2014**, *10*, 1439-1449.
[60] J. Dernedde, A. Rausch, M. Weinhart, S. Enders, R. Tauber, K. Licha, M. Schirner, U. Zügel, A. von Bonin, R. Haag, *Proceedings of the National Academy of Sciences* **2010**, *107*, 19679.
[61] N. Shitan, K. Yazaki, in *International Review of Cell and Molecular Biology, Vol. 305* (Ed.: K. W. Jeon), Academic Press, **2013**, pp. 383-433.
[62] P. Abimbola O. Adebowale, Donna S. Cox, MS, Zhongming Liang, MS, Natalie D. Eddington, PhD,*, *The FASEB Journal* **2003**, *3*; S. Sakai, E. Otake, T. Toida, Y. Goda, *Chem Pharm Bull (Tokyo)* **2007**, *55*, 299-303.
[63] M. A. Nugent, *Proc Natl Acad Sci U S A* **2000**, *97*, 10301-10303.
[64] S. Alban, *Hamostaseologie* **2008**, *28*, 400-420.
[65] I. Bjork, U. Lindahl, *Mol Cell Biochem* **1982**, *48*, 161-182.
[66] J. W. E. a. G. J. Hankey, *MJA* **2002**, *177*.
[67] R. J. Linhardt, N. S. Gunay, *Semin Thromb Hemost* **1999**, *25 Suppl 3*, 5-16.
[68] R. J. G. Peters, Joyner, Campbell, Bassand, Jean-Pierre, Afzal, Rizwan, Chrolavicius, Susan, S. R. Mehta, Oldgren, Jonas, Wallentin, Lars, Budaj, Andrzej, Fox, Keith A., Yusuf, Salim, *European Heart Journal* **2008**.
[69] J. T. Gallagher, A. Walker, *Biochemical Journal* **1985**, *230*, 665.
[70] A. Ori, M. C. Wilkinson, D. G. Fernig, *J Biol Chem* **2011**, *286*, 19892-19904.
[71] J. R. Fromm, R. E. Hileman, E. E. Caldwell, J. M. Weiler, R. J. Linhardt, *Arch Biochem Biophys* **1995**, *323*, 279-287; M. C. Meneghetti, A. J. Hughes, T. R. Rudd, H. B. Nader, A. K. Powell, E. A. Yates, M. A. Lima, *J R Soc Interface* **2015**, *12*, 0589.

[72] M. Bernfield, M. Gotte, P. W. Park, O. Reizes, M. L. Fitzgerald, J. Lincecum, M. Zako, *Annu Rev Biochem* **1999**, *68*, 729-777; A. K. Powell, E. A. Yates, D. G. Fernig, J. E. Turnbull, *Glycobiology* **2004**, *14*, 17r-30r.
[73] P. Libby, *Nutr Rev* **2007**, *65*, S140-146.
[74] R. Medzhitov, *Nature* **2008**, *454*, 428-435.
[75] U. Weiss, *Nature* **2008**, *454*, 427.
[76] G. M. Barton, *The Journal of clinical investigation* **2008**, *118*, 413-420.
[77] J. S. Pober, W. C. Sessa, *Nat Rev Immunol* **2007**, *7*, 803-815.
[78] R. Medzhitov, C. A. Janeway, Jr., *Cell* **1997**, *91*, 295-298.
[79] C. N. Serhan, J. Savill, *Nat Immunol* **2005**, *6*, 1191-1197.
[80] A. U. Ahmed, *Frontiers in Biology* **2011**, *6*, 274.
[81] T. A. Springer, *Cell* **1994**, *76*, 301-314.
[82] S. D. Rosen, C. R. Bertozzi, *Curr Biol* **1996**, *6*, 261-264; K. Drickamer, *Ciba Found Symp* **1989**, *145*, 45-58, discussion 58-61.
[83] W. S. Somers, J. Tang, G. D. Shaw, R. T. Camphausen, *Cell* **2000**, *103*, 467-479.
[84] D. Vestweber, J. E. Blanks, *Physiol Rev* **1999**, *79*, 181-213.
[85] T. Pouyani, B. Seed, *Cell* **1995**, *83*, 333-343.
[86] D. M. Lewinsohn, R. F. Bargatze, E. C. Butcher, *The Journal of Immunology* **1987**, *138*, 4313; P. Mehta, R. D. Cummings, R. P. McEver, *J Biol Chem* **1998**, *273*, 32506-32513.
[87] P. P. Wilkins, K. L. Moore, R. P. McEver, R. D. Cummings, *Journal of Biological Chemistry* **1995**, *270*, 22677-22680.
[88] D. J. Lefer, *Annual Review of Pharmacology and Toxicology* **2000**, *40*, 283-294.
[89] D. J. Lefer, D. M. Flynn, M. L. Phillips, M. Ratcliffe, A. J. Buda, *Circulation* **1994**, *90*, 2390-2401; M. J. Murohara T, Phillips LM,, D. S. Paulson JC, et al., *Cardiovasc. Res* **1995**.
[90] O. Renkonen, S. Toppila, L. Penttila, H. Salminen, J. Helin, H. Maaheimo, C. E. Costello, J. P. Turunen, R. Renkonen, *Glycobiology* **1997**, *7*, 453-461; S. M. Game, P. K. Rajapurohit, M. Clifford, M. I. Bird, R. Priest, N. V. Bovin, N. E. Nifant'ev, G. O'Beirne, N. D. Cook, *Anal Biochem* **1998**, *258*, 127-135.
[91] R. M. Nelson, O. Cecconi, W. G. Roberts, A. Aruffo, R. J. Linhardt, M. P. Bevilacqua, *Blood* **1993**, *82*, 3253-3258.
[92] L. S. Ted Wun, Laura DeCastro, Marilyn J. Telen, Frans Kuypers, Anthony Cheung,, H. F. William Kramer, Seungshin Rhee, John L. Magnani, Helen Thackray, *PLOS ONE* **2014**.
[93] H. Türk, R. Haag, S. Alban, *Bioconjugate Chemistry* **2004**, *15*, 162-167.
[94] M. Weinhart, D. Groger, S. Enders, S. B. Riese, J. Dernedde, R. K. Kainthan, D. E. Brooks, R. Haag, *Macromol Biosci* **2011**, *11*, 1088-1098.
[95] A. J. Lusis, *Nature* **2000**, *407*, 233-241.
[96] M. S. Brown, J. L. Goldstein, *Science* **1996**, *272*, 629.
[97] W. H. Organization, Jnuary 2017 ed., **2017**.
[98] R. Ross, *Nature* **1993**, *362*, 801-809.
[99] A. Ghattas, H. R. Griffiths, A. Devitt, G. Y. Lip, E. Shantsila, *J Am Coll Cardiol* **2013**, *62*, 1541-1551.
[100] E. V. Ratchford, N. S. Evans, *Vasc Med* **2014**, *19*, 512-515.
[101] F. G. Fowkes, V. Aboyans, F. J. Fowkes, M. M. McDermott, U. K. Sampson, M. H. Criqui, *Nat Rev Cardiol* **2017**, *14*, 156-170.
[102] R. O. Mathew, S. Bangalore, M. P. Lavelle, P. A. Pellikka, M. S. Sidhu, W. E. Boden, A. Asif, *Kidney Int* **2017**, *91*, 797-807.
[103] V. M. Pak, M. A. Grandner, A. I. Pack, *Sleep Medicine Reviews* **2014**, *18*, 25-34; S. Blankenberg, S. Barbaux, L. Tiret, *Atherosclerosis* **2003**, *170*, 191-203.

[104] B. Osterud, E. Bjorklid, *Physiol Rev* **2003**, *83*, 1069-1112.
[105] F. Montecucco, F. Mach, *Semin Immunopathol* **2009**, *31*, 1-3; E. Galkina, K. Ley, *Annu Rev Immunol* **2009**, *27*, 165-197.
[106] E. Braunwald, *New England Journal of Medicine* **1997**, *337*, 1360-1369.
[107] I. Tabas, G. García-Cardeña, G. K. Owens, *The Journal of Cell Biology* **2015**, *209*, 13.
[108] J. L. Mehta, J. Chen, P. L. Hermonat, F. Romeo, G. Novelli, *Cardiovasc Res* **2006**, *69*, 36-45.
[109] Z. Ding, S. Liu, X. Wang, Y. Dai, M. Khaidakov, F. Romeo, J. L. Mehta, *Can J Physiol Pharmacol* **2014**, *92*, 524-530.
[110] J. Frostegard, *BMC Med* **2013**, *11*, 117; C. K. Glass, J. L. Witztum, *Cell* **2001**, *104*, 503-516.
[111] M. S. Brown, J. L. Goldstein, *Proc Natl Acad Sci U S A* **1979**, *76*, 3330-3337.
[112] D. R. Greaves, S. Gordon, *J Lipid Res* **2009**, *50 Suppl*, S282-286; J. Kzhyshkowska, C. Neyen, S. Gordon, *Immunobiology* **2012**, *217*, 492-502; M. Prabhudas, D. Bowdish, K. Drickamer, M. Febbraio, J. Herz, L. Kobzik, M. Krieger, J. Loike, T. K. Means, S. K. Moestrup, S. Post, T. Sawamura, S. Silverstein, X. Y. Wang, J. El Khoury, *J Immunol* **2014**, *192*, 1997-2006.
[113] J. Canton, D. Neculai, S. Grinstein, *Nat Rev Immunol* **2013**, *13*, 621-634.
[114] K. J. Moore, M. W. Freeman, *Arterioscler Thromb Vasc Biol* **2006**, *26*, 1702-1711.
[115] I. A. Zani, S. L. Stephen, N. A. Mughal, D. Russell, S. Homer-Vanniasinkam, S. B. Wheatcroft, S. Ponnambalam, *Cells* **2015**, *4*, 178-201.
[116] R. Yoshimoto, Y. Fujita, A. Kakino, S. Iwamoto, T. Takaya, T. Sawamura, *Cardiovasc Drugs Ther* **2011**, *25*, 379-391.
[117] S. Mitra, T. Goyal, J. L. Mehta, *Cardiovasc Drugs Ther* **2011**, *25*, 419-429.
[118] T. Sawamura, N. Kume, T. Aoyama, H. Moriwaki, H. Hoshikawa, Y. Aiba, T. Tanaka, S. Miwa, Y. Katsura, T. Kita, T. Masaki, *Nature* **1997**, *386*, 73.
[119] Q. Xie, S. Matsunaga, S. Niimi, S. Ogawa, K. Tokuyasu, Y. Sakakibara, S. Machida, *DNA Cell Biol* **2004**, *23*, 111-117.
[120] I. Ohki, T. Ishigaki, T. Oyama, S. Matsunaga, Q. Xie, M. Ohnishi-Kameyama, T. Murata, D. Tsuchiya, S. Machida, K. Morikawa, S. Tate, *Structure* **2005**, *13*, 905-917.
[121] H. Park, F. G. Adsit, J. C. Boyington, *Journal of Biological Chemistry* **2005**, *280*, 13593-13599.
[122] S. Matsunaga, Q. Xie, M. Kumano, S. Niimi, K. Sekizawa, Y. Sakakibara, S. Komba, S. Machida, *Exp Cell Res* **2007**, *313*, 1203-1214.
[123] M. Chen, S. Narumiya, T. Masaki, T. Sawamura, *Biochem J* **2001**, *355*, 289-296.
[124] T. Sawamura, N. Kume, T. Aoyama, H. Moriwaki, H. Hoshikawa, Y. Aiba, T. Tanaka, S. Miwa, Y. Katsura, T. Kita, T. Masaki, *Nature* **1997**, *386*, 73-77.
[125] D. Y. Li, Y. C. Zhang, M. I. Philips, T. Sawamura, J. L. Mehta, *Circ Res* **1999**, *84*, 1043-1049.
[126] D. Li, J. L. Mehta, *Circ Res* **2009**, *104*, 566-568.
[127] S. Xu, S. Ogura, J. Chen, P. J. Little, J. Moss, P. Liu, *Cell Mol Life Sci* **2013**, *70*, 2859-2872.
[128] D. Li, J. L. Mehta, *Circulation* **2000**, *101*, 2889-2895.
[129] M. Nagase, S. Hirose, T. Sawamura, T. Masaki, T. Fujita, *Biochem Biophys Res Commun* **1997**, *237*, 496-498.
[130] J. L. Mehta, D. Li, *J Am Coll Cardiol* **2002**, *39*, 1429-1435.
[131] T. Shimaoka, N. Kume, M. Minami, K. Hayashida, T. Sawamura, T. Kita, S. Yonehara, *J Immunol* **2001**, *166*, 5108-5114.

[132] H. Kataoka, N. Kume, S. Miyamoto, M. Minami, M. Morimoto, K. Hayashida, N. Hashimoto, T. Kita, *Arteriosclerosis, Thrombosis, and Vascular Biology* **2001**, *21*, 955-960.
[133] D. Li, V. Williams, L. Liu, H. Chen, T. Sawamura, F. Romeo, J. L. Mehta, *J Am Coll Cardiol* **2003**, *41*, 1048-1055.
[134] N. V. K. Pothineni, S. K. Karathanasis, Z. Ding, A. Arulandu, K. I. Varughese, J. L. Mehta, *J Am Coll Cardiol* **2017**, *69*, 2759-2768.
[135] A. Arjuman, N. C. Chandra, *Diab Vasc Dis Res* **2013**, *10*, 442-451.
[136] A. L. True, A. Rahman, A. B. Malik, *Am J Physiol Lung Cell Mol Physiol* **2000**, *279*, L302-311.
[137] A. Pirillo, G. D. Norata, A. L. Catapano, *Mediators Inflamm* **2013**, *2013*, 152786.
[138] H. Moriwaki, N. Kume, T. Sawamura, T. Aoyama, H. Hoshikawa, H. Ochi, E. Nishi, T. Masaki, T. Kita, *Arterioscler Thromb Vasc Biol* **1998**, *18*, 1541-1547.
[139] G. Marsche, S. Levak-Frank, O. Quehenberger, R. Heller, W. Sattler, E. Malle, *Faseb j* **2001**, *15*, 1095-1097.
[140] K. Oka, T. Sawamura, K. Kikuta, S. Itokawa, N. Kume, T. Kita, T. Masaki, *Proc Natl Acad Sci U S A* **1998**, *95*, 9535-9540; M. Kakutani, T. Masaki, T. Sawamura, *Proceedings of the National Academy of Sciences* **2000**, *97*, 360.
[141] Y. Fujita, A. Kakino, M. Harada-Shiba, Y. Sato, K. Otsui, R. Yoshimoto, T. Sawamura, *Clin Chem* **2010**, *56*, 478-481.
[142] S. Xu, Z. Liu, Y. Huang, K. Le, F. Tang, H. Huang, S. Ogura, P. J. Little, X. Shen, P. Liu, *Transl Res* **2012**, *160*, 114-124.
[143] B. Y. Kang, J. A. Khan, S. Ryu, R. Shekhar, K. B. Seung, J. L. Mehta, *J Cardiovasc Pharmacol* **2010**, *55*, 417-424.
[144] S. Guan, B. Wang, W. Li, J. Guan, X. Fang, *Am J Chin Med* **2010**, *38*, 1161-1169; H. C. Ou, T. Y. Song, Y. C. Yeh, C. Y. Huang, S. F. Yang, T. H. Chiu, K. L. Tsai, K. L. Chen, Y. J. Wu, C. S. Tsai, L. Y. Chang, W. W. Kuo, S. D. Lee, *J Appl Physiol (1985)* **2010**, *108*, 1745-1756; H. C. Chang, T. G. Chen, Y. T. Tai, T. L. Chen, W. T. Chiu, R. M. Chen, *J Cereb Blood Flow Metab* **2011**, *31*, 842-854.
[145] O. L. Francone, M. Tu, L. J. Royer, J. Zhu, K. Stevens, J. J. Oleynek, Z. Lin, L. Shelley, T. Sand, Y. Luo, C. D. Kane, *J Lipid Res* **2009**, *50*, 546-555.
[146] M. Falconi, S. Ciccone, P. D'Arrigo, F. Viani, R. Sorge, G. Novelli, P. Patrizi, A. Desideri, S. Biocca, *Biochem Biophys Res Commun* **2013**, *438*, 340-345.
[147] M. S. Zhou, E. A. Jaimes, L. Raij, *Am J Hypertens* **2004**, *17*, 167-171; Y. Sun, X. Chen, *Fundam Clin Pharmacol* **2011**, *25*, 572-579.
[148] S. Biocca, F. Iacovelli, S. Matarazzo, G. Vindigni, F. Oteri, A. Desideri, M. Falconi, *Cell Cycle* **2015**, *14*, 1583-1595.
[149] J. L. Mehta, J. Chen, F. Yu, D. Y. Li, *Cardiovasc Res* **2004**, *64*, 243-249.
[150] T. Nishizuka, Y. Fujita, Y. Sato, A. Nakano, A. Kakino, S. Ohshima, T. Kanda, R. Yoshimoto, T. Sawamura, *Proc Jpn Acad Ser B Phys Biol Sci* **2011**, *87*, 104-113.
[151] S. Iwamoto, N. Nishimichi, Y. Tateishi, Y. Sato, H. Horiuchi, S. Furusawa, T. Sawamura, H. Matsuda, *mAbs* **2009**, *1*, 357-363.
[152] S. Thakkar, X. Wang, M. Khaidakov, Y. Dai, K. Gokulan, J. L. Mehta, K. I. Varughese, *Sci Rep* **2015**, *5*, 16740.

# 8 Appendix

## 8.1 Publications and Conference Contributions

### Publications

(1) S. Ehrmann[1], C.-W. Chu[1], **S. Kumari**[1], K. Silberreis, C. Böttcher, J. Dernedde, B. J. Ravoo, and R. Haag, *J. Mater. Chem. B*, **2018**, 6, 4216-4222. A Toolbox Approach for Multivalent Presentation of Ligand-Receptor Recognition on a Supramolecular Scaffold. *DOI: 10.1039/C8TB00922H,* [1] – Authors equally contributed.

(2) **Shalini Kumari**, Katharina Achazi, Pradip Dey, Rainer Haag, Jens Dernedde*, Design and Synthesis of PEG-Oligoglycerol Sulfates as Multivalent Inhibitors for the Scavenger Receptor LOX-1, *Submitted*

### Conference Contributions

### Poster Presentations

(1) European Winterschool on Physical Organic Chemistry, Bressenone, Italy (February 2016), *Synthesis of Multivalent Polymer Architecture Targeting Inflammation;* S. Kumari, J. Dernedde, and R. Haag

(2) Workshop by SFB765, Freie University Berlin, Germany (August 2016), *Synthesis of inhibitor for scavenger receptor LOX-1;* S. Kumari, J. Dernedde, and R. Haag

(3) Phd workshop by SFB765, Hannover, Germany (August 2016), *Synthesis of Multivalent Polymer Architecture Targeting Inflammation;* S. Kumari, J. Dernedde, and R. Haag

(4) SFB765 Doktorandentag at Freie University Berlin, Germany (February 2017), *Synthesis of inhibitor for scavenger receptor LOX-1;* S. Kumari, J. Dernedde, and R. Haag

(5) NanoBioMater 2017 Summer School & International Conference by University of Stutgart, Germany (June 2017), *Development of inhibitors for scavenger receptor-LOX-1;* S. Kumari, J. Dernedde, and R. Haag

(6) ICMS Outreach Symposium at Technical university of Eindhoven, Netherland (January 2018), *Multivalent Sialylated Polyglycerol Derivatives Inhibit Influenza Virus Propagation*; Pallavi Kiran[#], Shalini Kumari[#], Sumati Bhatia, Daniel Lauster, Kai Ludwig, Christoph Böttcher, Alf Hamann, Andreas Herrmann, Rainer Haag. # – contributed equally

(7) SFB765 Doktorandentag, Freie University Berlin, Germany (March 2018), *Multivalent Sialylated Polyglycerol Derivatives Inhibit Influenza Virus Propagation;* Pallavi Kiran[#], Shalini Kumari[#], Sumati Bhatia, Daniel Lauster, Kai Ludwig, Christoph Böttcher, Alf Hamann, Andreas Herrmann, Rainer Haag. # – contributed equally

(8) Workshop on Symposium on Cooperative Effects in Chemistry, Muenster, Germany (April 2018), *Multivalent Sialylated Polyglycerol Derivatives Inhibit Influenza Virus Propagation;* Pallavi Kiran[#], Shalini Kumari[#], Sumati Bhatia, Daniel Lauster, Kai Ludwig, Christoph Böttcher, Alf Hamann, Andreas Herrmann, Rainer Haag. # – contributed equally

## 8.2 List of abbreviations

| | |
|---|---|
| ApoB | Apolipoprotein B |
| Arg | Arginine |
| AT1 | Angiotensin 1 |
| Ang-II | Angiotensin II |
| CD | Cyclodextrin |
| CDV | Cyclodextrin Vesicle |
| ConA | Concavallin A |
| CTLD | C-type lectin like domain |
| CRP | C-reactive protein |
| Cryo-TEM | Cryo- Transmission electron microscopy |
| DF | Degree of functionalization |
| Dil-oxLDL | Dil labelled oxidised low density lipoprotein |
| DLS | Dynamic light scattering |
| DNA | Deoxy ribose nucleic acid |
| dPG | Dendritic polyglycerol |
| dPGS | Dendritic polyglycerol sulfate |
| ECM | Extracellular matrix |
| *E.Coli* | Escherichia Coli |
| eNOS | Endothelial nitric oxide synthase |
| FITC | Fluorescein isothiocyanate |
| FDA | US food and drug administration |
| GAG | glycosaminoglycan |
| ICAM-1 | Intracellular adhesion molecule-1 |
| IL | Interleukin |
| ITC | Isothermal titration calorimetry |
| Kd | Dissociation constant |
| LDL | Lox density lipoprotein |
| LPs | Lipoproteins |
| LOX-1 | Low density oxidized lipoprotein – 1 |
| lPG | Linear polyglycerol |
| MST | Microscale thermophoresis |
| mRNA | Messenger ribose nucleic acid |

| | |
|---|---|
| NF-Kb | Nuclear factor kappa-light-chain-enhancer of activated B cells |
| NMR | Nuclear magnetic resonance |
| OxLDL | Oxidised low density lipoprotein |
| PAMAM | Poly(amido-amine) |
| PEG | Polyethylene glycol |
| PSGL-1 | P-selectin glycoprotein ligand-1 |
| RBC | Red blood cell |
| RNA | Ribose nucleic acid |
| ROMP | Ring opening metathesis polymerization |
| siRNA | Small interfering RNA |
| sLea | Sialylated Lewisa |
| sLex | Sialylated LewisX |
| SPR | Surface plasmon resonance |
| SR | Scavenger receptor |
| TM | Transmembrane |
| TNFα | Tumor necrosis factor α |
| VCAM-1 | Vascular cell adhesion molecule-1 |
| 3D | Three-dimensional |

## 8.3 Curriculum vitae

For reasons of data protection, the curriculum vitae is not published in the electronic version.